KINETIC MECHANISM AND EQUILIBRIUM THERMODYNAMIC OF LIPASE-CATALYZED SYNTHESIS OF RUTIN FLAVONOID ESTER

NURUL NADIAH ABD RAZAK

FACULTY OF SCIENCE
UNIVERSITY OF MALAYA
KUALA LUMPUR

2015

KINETIC MECHANISM AND EQUILIBRIUM THERMODYNAMIC OF LIPASE-CATALYZED SYNTHESIS OF RUTIN FLAVONOID ESTER

NURUL NADIAH ABD RAZAK

DISSERTATION SUBMITTED IN FULFILLMENT OF
THE REQUIREMENT FOR THE DEGREE OF
MASTER OF SCIENCE

INSTITUTE OF BIOLOGICAL SCIENCES
FACULTY OF SCIENCE
UNIVERSITY OF MALAYA
KUALA LUMPUR

2015

UNIVERSITI MALAYA

ORIGINAL LITERARY WORK DECLARATION

Name	:	**NURUL NADIAH BINTI ABD RAZAK** :
I/C/Pasport No.	:	**SGR 120077**
Registration/Matric No.	:	**MASTER OF SCIENCE**
Name of Degree		

Title of Project Paper/Research Report/Dissertation/Thesis ("this Work") :

KINETIC MECHANISM AND EQUILIBRIUM THERMODYNAMIC OF LIPASE-CATALYZED SYNTHESIS OF RUTIN FLAVONOID ESTER

Field of Study	:	**BIOTECHNOLOGY**

I do solemnly and sincerely declare that :

(1) I am the sole author/writer of this Work,
(2) This Work is original,
(3) Any use of any work in which copyright exists was done by way of fair dealing and for permitted purposes and any excerpt or extract from, or reference to or reproduction of any copyright work has been disclosed expressly and sufficiently and the title of the Work and its authorship have been acknowledged in this Work,
(4) I do not have any actual knowledge nor do I ought reasonably to know that the making of this work constitutes an infringement of any copyright work,
(5) I hereby assign all and every rights in the copyright to this Work to the University of Malaya ("UM"), who henceforth shall be owner of the copyright in this Work and that any reproduction or use in any form or by any means whatsoever is prohibited without the written consent of UM having been first had and obtained,
(6) I am fully aware that if in the course of making this Work I have infringed any copyright whether intentionally or otherwise, I may be subject to legal action or any other action as may be determined by UM.

Candidate Signature : Date : 18 08 05 2015

Subscribed and solemnly declared before,

Witness's Signature : Date 18/8/2015

Name :

Designation :

ABSTRACT

Flavonoids are natural compounds in plant with wide spectrum of health-beneficial activities. They exhibit a variety of physico-chemical properties and biological activities but they are normally characterized by low solubility and stability. In order to improve upon these limitations, the enzymatic acylation of these molecules with fatty acids is seen as a selective, specific and mild route.

In this study, the synthesis of flavonoid esters catalyzed by lipase was investigated. Three different flavonoid structures from different classes were selected to be studied *viz.* rutin (flavonols), naringin (flavanones) and catechin (flavanols). The effects of these flavonoid structures on the esterification were investigated with lauric acid as an acyl donor. The results showed that rutin was the most reactive substrate. Conversion yields were at 56 % and 47 % for rutin and naringin, respectively. For an aglycone flavonoid, such as catechin, no glycoside ester formation was observed. Based on the conversion yield and solubility consideration, rutin was selected for further studies. For different chain length fatty acid (C12–C16), no significant difference was observed in terms of yield irrespective of fatty acids used.

Full factorial experimental design (FFD) was used to study the effects of different process parameters towards the synthesis of rutin laurate. The effects of three selected operating variables *viz.* lauric acid concentration (M), temperature (^oC) and enzyme loading (g) were significant in all cases ($P < 0.05$). The factors studied showed temperature has the strongest influence on the ester yield followed by lauric acid concentration and enzyme loading.

In thermo-kinetic investigation, analysis indicated that lipase-mediated esterification exhibited Ping-Pong Bi-Bi mechanism with no apparent inhibition by both substrates. The apparent kinetic of the esterification reaction followed a first-order

behavior. The magnitude of glycoside ester formation and the apparent first-order rate constant, k_1' value increased with temperature. Activation energy, E_a for the esterification was calculated at 37 kJ mol^{-1}. The esterification process was endothermic with the enthalpy, ΔH and entropy, ΔS values calculated at +51 kJ mol^{-1} and +113 J mol^{-1} K^{-1}, respectively. Based on the value of Gibbs free energy change, ΔG the esterification reaction under the conditions studied was predicted to be non-spontaneous below 175 °C but spontaneous at higher temperatures.

The study also confirmed, through ^{13}C-NMR analysis, the exact location of rutin esterification. The investigated process biochemistry highlighted important behavior concerning the biosynthesis of functionalized flavonoid with implication for reactor design.

ABSTRAK

Flavonoid adalah sebatian semula jadi dalam tumbuhan yang mempunyai spektrum yang luas untuk manfaat kesihatan. Flavonoid mempamerkan kepelbagaian ciri-ciri fizikal-kimia dan aktiviti biologi namun kelarutan dan kestabilannya adalah rendah. Dalam usaha untuk memperbaiki sifat-sifat flavonoid, pengasilan molekul flavonoid dengan asid lemak oleh enzim dilihat sebagai jalan yang selektif, spesifik dan mudah untuk meningkatkan limitasi ini.

Kajian ini memberi tumpuan kepada sintesis ester flavonoid yang dimangkinkan oleh enzim lipase. Tiga struktur flavonoid yang berbeza yang dari kelas yang berlainan telah dikaji; rutin (flavonol), naringin (flavanon) dan catechin (flavanol). Kesan struktur flavonoid kepada pengesteran telah dijalankan dengan asid laurik sebagai penderma acil. Hasil kajian menunjukkan bahawa rutin adalah substrat yang paling reaktif. Hasil penukaran adalah pada 56 dan 47% untuk rutin dan naringin. Flavonoid jenis aglikon seperti catechin tidak menunjukkan sebarang tindakbalas. Berdasarkan hasil penukaran dan pertimbangan kelarutan, rutin telah dipilih untuk kajian selanjutnya. Tiada perbezaan yang ketara dari segi hasil penukaran substrat untuk asid lemak yang berantai panjang (C12-C16).

Rangka experimen secara faktor lengkap (FFD) telah digunakan untuk mengkaji kesan perbezaan parameter ke atas sintesis rutin laurate. Kesan tiga faktor terpilih iaitu kepekatan asid laurik (M), suhu (ºC) dan kandungan enzim (g) adalah signifikan untuk kesemua pembolehubah ($P < 0.05$). Berdasarkan faktor-faktor yang dikaji, suhu (ºC) merupakan pengaruh terkuat diikuti dengan kepekatan asid laurik (M) dan kandungan enzim (g).

Dalam kajian termo-kinetik, analisis menunjukkan bahawa pengesteran menggunakan lipase sebagai pengantara menepati mekanisma Ping-Pong Bi-Bi tanpa

perencatan oleh kedua-dua substrat. Kinetik tindak balas pengesteran mengikuti kinetik tertiban pertama. Magnitud pembentukan produk dan kadar pemalar tertiban pertama, nilai k_1' meningkat dengan peningkatan suhu. Tenaga pengaktifan, E_a untuk pengesteran ialah 37 kJ mol^{-1}. Proses pengesteran yang berlaku adalah endotermik dengan nilai entalpi, ΔH dan entropi, ΔS masing-masing ialah +51 kJ mol^{-1} dan +113 J mol^{-1} K^{-1}. Berdasarkan nilai perubahan tenaga bebas Gibbs, tindak balas pengesteran ΔG di bawah syarat-syarat yang dikaji telah diramalkan untuk menjadi bukan spontan di bawah 175 ° C tetapi spontan pada suhu yang lebih tinggi.

Kajian ini juga mengesahkan, melalui analisis ^{13}C-NMR, lokasi sebenar pengesteran rutin. Kajian proses biokimia ini menekankan kepentingan perlakuan tindakbalas berkaitan biosintesis flavonoid berfungsi bagi tujuan reka bentuk reaktor.

ACKNOWLEDGEMENT

Praise to God for providing me with strength and perseverance to complete this research project, for blessing me with numerous opportunities and many wonderful individuals without whom the completion of this project would not be possible.

First and foremost, I would like to express my uttermost gratitude to my supervisor, Professor Dr. M. Suffian M. Annuar for always being available and guiding me throughout the entire process. Your encouragement and guidance are something that I truly value.

My deepest appreciation to the members of the Bioprocess and Enzyme Technology (B.E.T) Laboratory; Dr. Ahmad, Abang Naziz, Kak Syairah, Kak Aneen, Pey Ling, Chuck, Ana, Kak Faezah, Kak Suhayati, Haziqah, Haziq, Rafais and Chong Boon whose support and friendship made this time both successful and enjoyable.

I also would like to thank my parents, Salmiah Ismail and Abd Razak bin Munip and my siblings for getting me through the hard times. No words could express how grateful I am to be blessed with wonderful family members, who have been showing their love and motivation during this project.

I am also indebted and appreciative to Ministry of Education Malaysia for the MyBrain scholarship and University of Malaya for the short term PPP grant (PG033-2013A); which had helped me financially through my postgraduate study.

Last but not least, thanks to all my friends for any big or small contributions - truly cherish having each and every one of you in my life. Thank you.

TABLE OF CONTENT

LIST OF FIGURES

LIST OF TABLES

LIST OF ABBREVIATIONS

CAL-B	*Candida antartica* lipase B
Ser	Serine
His	Histidine
Asp	Aspartate
kDa	kilo Dalton
$d[A]/dt$	Rate of reaction
$d[P]/dt$	Rate of product formation
v	Velocity
k	Rate contant
k_{cat}	Catalytic rate constant
K_m	Michealis-Menten contant
V_{max}	Maximum velocity
ln	Natural logarithm
e	Exponential
T	Absolute temperature (K)
R	Gas constant (8.3145 J mol^{-1} K^{-1})
A	Frequency factor,
E_a	Energy of activation
K_{eq}	Equilibrium constant
ΔG	Gibbs free energy
ΔG^o	Gibbs free energy at standard state
ΔH	Enthalpy of reaction
ΔS	Entropy of reaction
*p*NPP	*para*-nitrophenol palmitate
NaOH	Sodium hydroxide
DMSO	Dimethylsulfoxide
Å	Angstrom
$\Delta A/\Delta t$	Absorbance changes per minute (min^{-1})
ξ	Molar extinction coefficient (M^{-1} cm^{-1})
l	Light path length (cm)
m/z	mass-to-charge ratio
t_R	Retention time
δ	Delta
Hz	Hertz
HPLC	High pressure liquid chromatography
LC/MS/MS	Liquid chromatography/mass spectrometry/mass spectrometry
NMR	Nuclear magnetic resonance
UV-Vis	Ultraviolet-visible
FFD	Full factorial design
ANOVA	Analysis of variance
DoF	Degree of freedom

SS	Sum of squares
MS	Mean on squares
Adj SS	Adjusted sum of squares
Adj MS	Adjusted mean of squares
F	*F*-statistic
P	*P*-statistic
T	*T*-statistic

CHAPTER 1

INTRODUCTION

There has been an increasing interest over the past few years in natural phenolic compounds, primarily due to their antioxidant capacity and potential health effects. Among them, flavonoids are an interesting group of secondary plant metabolites, polyhydroxylated diphenylpyrane derivatives that have recently received a lot of attention. They have been linked to a wide range of health benefits, from the prevention and treatment of cardiovascular and liver diseases to inhibitory effects on cancers (Stevenson & Hurst, 2007; Pandey & Rizvi, 2009; Ferrazzano *et al.*, 2011; Hollman *et al.*, 2011; Chiva-Blanch & Visioli, 2012). In fact, anti-allergenic, anti-viral, anti-microbial, anti-mutagenic and anti-inflammatory properties have all been documented for flavonoids (Arct & Pytkowska, 2008), yet it is their anti-oxidative related properties which have really generated the most biggest to date.

Due to the biological activities of flavonoids, researchers have embarked on a continuous search for natural antioxidants as alternatives to synthetic ones for application in food and cosmetic products (Havsteen, 2002). However, the use of these antioxidants is strongly limited due to their hydrophilic nature that reduces their solubility and stability in lipophilic environment. Therefore, the preparation of lipophilic flavonoid by acylation of hydroxyl functional with groups(s) aliphatic molecules is a promising method to modify these flavonoid compounds. It has been proposed that selectively modified flavonoids show improved properties in term of the physico-chemistry of these molecules and also introduce many beneficial properties to the original compound, such as penetration through the cell membrane and improve existing or provide novel

bioactivities (Mellou *et al.*, 2005; Katsoura *et al.*, 2006; Mellou *et al.*, 2006; Salem *et al.*, 2010; Viskupicova *et al.*, 2010).

There have been very few attempts to synthesize these promising molecules either chemically or enzymatically. To avoid the disadvantages of the conventional chemical process, enzymes-mediated catalysis in non-aqueous medium has opened new ways for obtaining products derived from natural antioxidants with high added value (Patti *et al.*, 2000; Riva, 2002; Passicos *et al.*, 2004; Viskupicova *et al.*, 2010). The use of enzymes for selective acylation of flavonoid provides a useful alternative to classical chemical methods. Lipase is preferred due to its high regioselectivity and mild reaction conditions that avoid substrate alteration. The use of enzymes made possible to develop a significantly simple approach to the preparation of flavonoid esters (Gao *et al.*, 2001; Ardhaoui *et al.*, 2004a; Almeida *et al.*, 2012; Bridson *et al.*, 2013).

While most of the lipase kinetic studies are related to soluble substrates reactions, the literature on esterification kinetics between immiscible substrates are clearly lacking. Most of these studies deal with the esterification of sugar with acids/esters (Acros *et al.*, 2001; Naoe *et al.*, 2001; Flores & Halling, 2002; Gumel *et al.*, 2011b). The only data available on flavonoid esterification by lipase was reported by Céliz *et al.* (2012). Even then, the salient feature of the reaction was inadvertently omitted.

Therefore, it is of great importance to investigate the prominent aspects of this ill-studied and difficult reaction. The present investigation will be focused on the kinetics of lipase-catalyzed esterification of flavonoids and acyl donors. The biggest challenge of this study is due to the reaction is being strongly limited by the solubility of the flavonoids. Generally, Michaelis-Menten kinetic describes well reaction that takes place in a homogenous phase. It is hypothesized that in heterogeneous system such as the one that will be employed in the proposed investigation, a different kinetic model would be

more appropriate. A working kinetic model plays an important part in the elucidation of the reaction mechanism. In addition, equilibrium thermodynamics of flavonoid esterification will also be studied. Understanding of these fundamental aspects has significant implication for a rational design of the synthesis reaction/reactor for flavonoid esters, which constitute important ingredients in the food, pharmaceutical and cosmetic industries.

The aims of the study are to determine the key factors that influence the efficiency of the reaction and to investigate the thermo-kinetic behaviour of the system. The objectives of the study are:

1) To study the effects of the flavonoids structure on the flavonoid acylation efficiency;
2) To study the effects of selected process parameters towards the synthesis of selected flavonoid ester;
3) To elucidate the kinetic mechanism of lipase-catalyzed esterification of flavonoids;
4) To investigate the equilibrium thermodynamics of lipase-catalyzed synthesis of selected flavonoid ester.

CHAPTER 2

LITERATURE REVIEW

2.1 POLYPHENOL

Phenolic compounds are widely distributed in plants, usually with a higher concentration in leaves and green steams. These compounds are considered natural defense substances, and their concentrations in each plant may be influenced by several factors including physiological variations, environmental condition, geographic variation, genetic factors and evolution (Pandey & Rizvi, 2009; Martins *et al.*, 2011). Several thousand molecules having a polyphenol structure have been identified in higher plants, and several hundred are found in edible plants (Scalbert *et al.*, 2005; Silva *et al.*, 2007). Over the past 10 years, researchers have become increasingly interested in polyphenols because of their antioxidant properties (Pietta, 2000; Scalbert *et al.*, 2005; Chiva-Blanch & Visioli, 2012), their great abundance and their role in the prevention of various diseases such as cancer and cardiovascular and neurodegenerative diseases (Manach *et al.*, 2004; Stevenson & Hurst, 2007; Pandey & Rizvi, 2009; Lambert & Elias, 2010). These compounds have been classified into different groups based on the number of phenol rings and the structural elements that bind these rings to one another (Tsao, 2010; Ferrazzano *et al.*, 2011). The classified groups are flavonoids, phenolic acids, stilbenes, and lignans (Fig. 2.1).

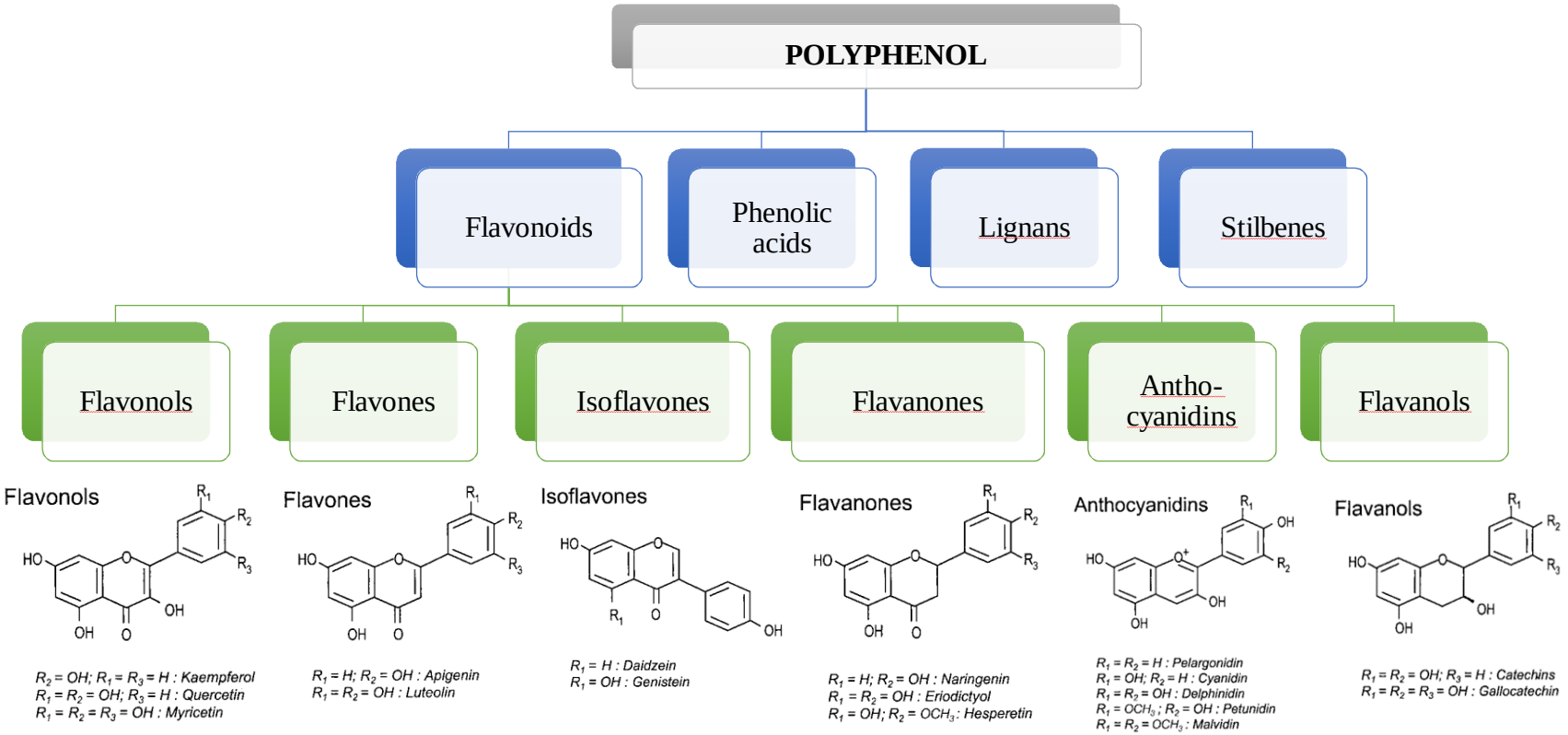

Figure 2.1 Polyphenol classifications.

2.2 FLAVONOIDS

Flavonoids are a diverse subset of polyphenols. Flavonoids share a common structure in which they are two aromatic rings (A and B) that are bound together by three carbon atoms that form an oxygenated heterocycle (ring C) (Fig. 2.2). They can be divided into six subclasses as a function of the type of heterocycle involved: flavonols, flavones, isoflavones, flavanones, anthocyanidins, and flavanols (catechins and proanthocyanidins) (Hollman & Katan, 1999; Aherne & O'Brien, 2002; Manach *et al.*, 2004). Flavonoid molecules that are not attached to sugar moieties are referred to as the aglycone form, whereas flavonoid molecules with sugar moieties are called flavonoid glycosides.

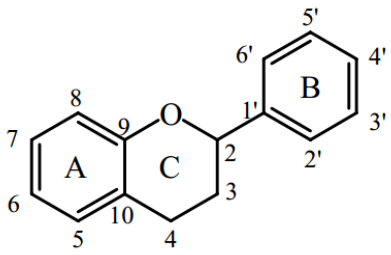

Figure 2.2 Basic structure of flavonoid.

2.2.1 Flavonols

Flavonols are a class of flavonoids that have the 3-hydroxyflavone backbone. Their diversity stems from the different positions the phenolic -OH groups. One of the most frequently studied flavonol is rutin.

Rutin (quercetin-3-rutinoside) comprises quercetin and the disaccharide rutinose (glucose and rhamnose) (Fig. 2.3). It is one of the medicinally important flavonoids which is identified as vitamin P and widely present in many plants (Hamad, 2012; Olennikov & Partilkhaev, 2012; Ashok & Saini, 2013) and fruits (Slimestad & Verheul, 2011; Wu *et al.*, 2015). Buckwheat (*Fagopyrum esculentum* Moench) from the family Polygonaceae

is reported as a major source of natural rutin (Kreft *et al.*, 2002; Kim *et al.*, 2005; Cui & Wang, 2012; Gupta *et al.*, 2012).

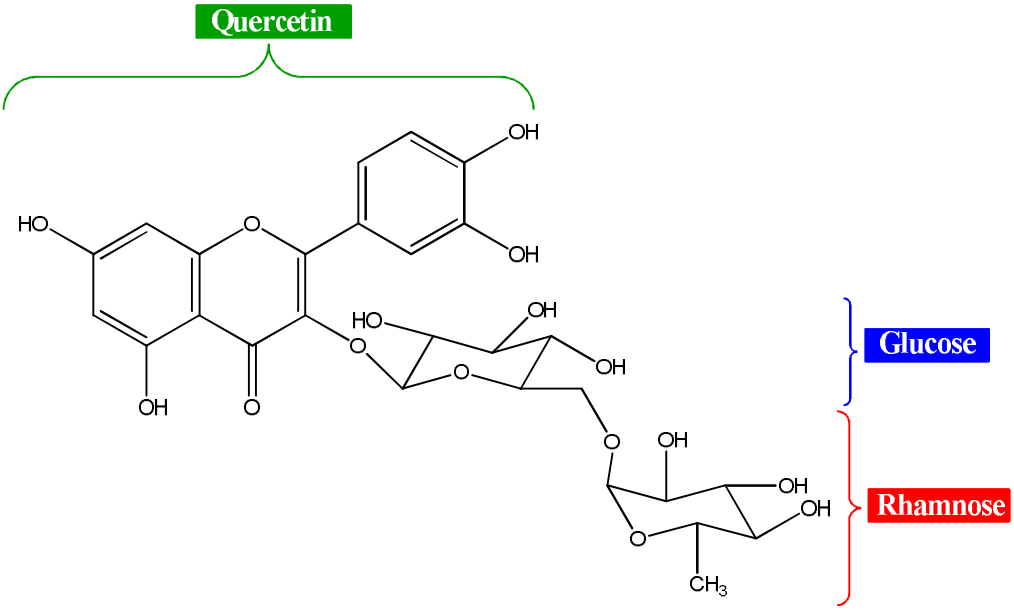

Figure 2.3 Chemical structure of rutin.

Rutin is a powerful antioxidant (Ahmed *et al.*, 2010; Gonçalves *et al.*, 2012; Mahmoud, 2012) with multiple pharmacological activities including anti-hypertensive (Yang *et al.*, 2008; Lee *et al.*, 2012), anti-inflammatory (Guardia *et al.*, 2001; Selloum *et al.*, 2003; Kazłowska *et al.*, 2010), anti-diabetic (Kamalakkannan & Prince, 2006; Ahmed *et al.*, 2010; Hassan *et al.*, 2010; Jadhav & Puchchakayala, 2012) and anti-leukemia (Bourogaa *et al.*, 2011; Lin *et al.*, 2012).

Rutin has been proven to be effective in reducing the risk of chronic diseases (Knekt *et al.*, 2002) and reducing oxidative stress in hepatocarcinoma Cells (Wu *et al.*, 2011). It has been reported to prevent cognitive impairments (Javed *et al.*, 2012), inhibits secretion and aggregation of platelets (Boligon *et al.*, 2014; Kim *et al.*, 2014), inhibits gastric mucosal ulceration in animal models (La Casa *et al.*, 2000; Dubey *et al.*, 2013; Liu *et al.*, 2013) and exhibits protection against paracetamol and liver injuries (Janbaz *et al.*, 2002).

2.2.2 Flavanones

Flavanones are generally glycosylated by a disaccharide at position seven to give flavanone glycoside. Naringin (naringenine-7-rhamnosidoglucoside) is a major and active flavanone glycoside found in grape fruits and other related citrus species (Bharti *et al.*, 2014) with bitter taste characteristic (Real *et al.*, 2007; Ribeiro & Ribeiro, 2008) and insoluble in water (Zhang *et al.*, 2015).

Naringin consists of naringenin, the aglycone part and linked by the two sugars (glucose and rhamnose) (Fig. 2.4). It has been experimentally documented to possess numerous biological properties such as antioxidant (Jeon *et al.*, 2001; Singh *et al.*, 2004), anti-hypercholesterolemic (Jeon *et al.*, 2004), anti-atherogenic (Lee *et al.*, 2001), anti-inflammatory (Amaro *et al.*, 2009; Nie *et al.*, 2012) and anti-apoptotic activities (Shaik *et al.*, 2012).

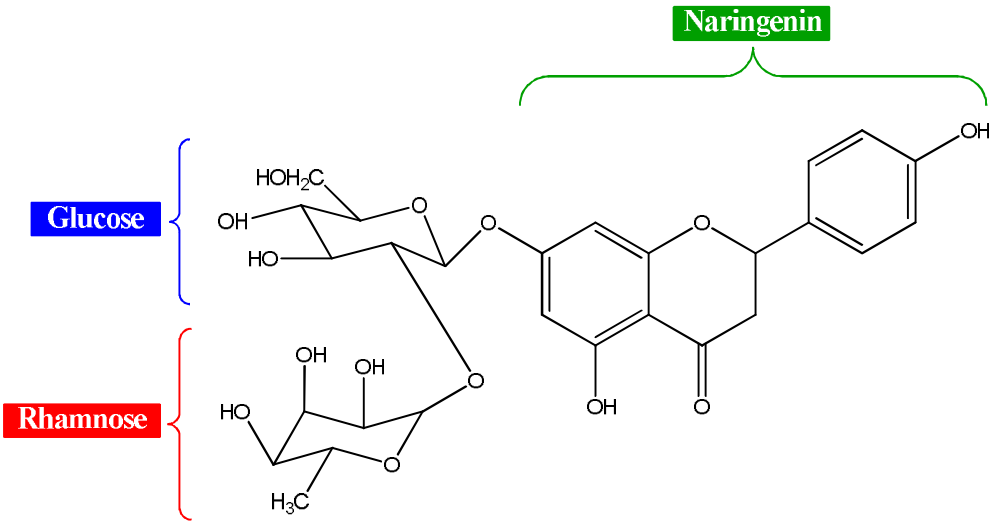

Figure 2.4 Chemical structure of naringin

Apart from this, naringin inhibited the retinoic acid-induced osteoporosis (Wei *et al.*, 2007; Wu *et al.*, 2008), tumor growth (Camargo *et al.*, 2012) and breast cancer (Zhang *et al.*, 2004) and showed potential application in the prevention and treatment of oral diseases (Yeum & Choi, 2006; Palombo, 2011).

2.2.3 Flavanols

Flavanols exist in both the monomer form (catechins) (Fig. 2.5) and the polymer form (proanthocyanidins). The term *catechins* is also commonly used to refer to the related family of flavonoids and the subgroup flavan-3-ols (or simply flavanols) which are found in a wide variety of vegetables, herbs, wine and especially in teas (Castaignède *et al.*, 2003). The intake of catechins can be expected to be higher in the Asiatic countries and the health effects of green tea may be more apparent when examined in the Asian communities.

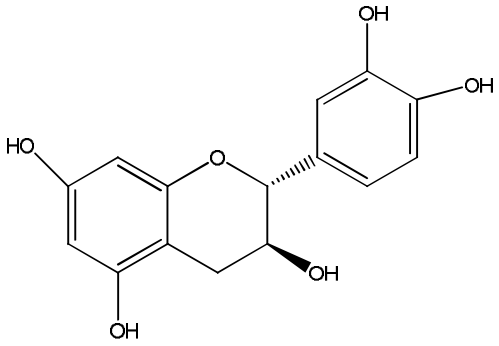

Figure 2.5 Chemical structure of catechin.

Like rutin and naringin, catechin possesses diverse pharmacological properties which include anti-oxidative (Yilmaz & Toledo, 2004), anti-inflammatory (Tipoe *et al.*, 2007; Nichols & Katiyar, 2010), anti-aging (Baxter, 2008) and anti-arteriosclerotic (Horiuchi *et al.*, 2001). It promotes adipocyte differentiation in human bone marrow mesenchymal stem cells (Shin *et al.*, 2009), delaying the degradation of endogenous α-tocopherol and β-carotene and by inhibiting the oxidation of plasma lipids (Lotito & Fraga, 2000; Yilmaz & Toledo, 2004), display a potent antithrombotic activity (Kang *et al.*, 2001) and effective to prevent dental caries and reduce cholesterols and lipids absorption in the gastrointestinal tract (Koo & Cho, 2004).

Due to their antioxidant properties, several studies have been conducted on oxidative coupling for catechin derivatives in order to improve the physiological

properties of the catechins (Uesato *et al.*, 2000; Hosny & Rosazza, 2002; Chung *et al.*, 2003; Jin & Yoshioka, 2005; Velayutham *et al.*, 2008; Spizzirri *et al.*, 2009).

2.3 FATTY ACIDS

A fatty acid is a carboxylic acid with a long aliphatic tail with the general formula of $C_{2n+1}H_{6n+1}COOH$ or $CH_3(CH_2)_{2n}COOH$. Most naturally occurring fatty acids have a chain of an even number of carbon atoms from 4 to 28. Fatty acids can be divided into two groups; saturated and unsaturated. Saturated fatty acids are fatty acids without double bonds while the presence of double bond in the fatty acids made them to be known as unsaturated. Fatty acids also have been classified into short-chain fatty acids, medium-chain fatty acids, long fatty acids and very long fatty acids consisting of 2-5, 6-12, 13-21 and more than 22 carbon atoms, respectively. An example of saturated fatty acid with medium chain length i.e. lauric acid is shown in Fig. 2.6.

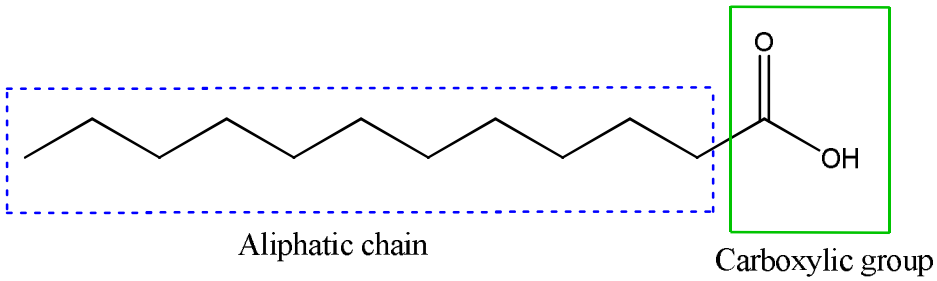

Figure 2.6 Structure of saturated fatty acid with a chain length of 12 carbons i.e. lauric acid (dodecanoic acid).

2.4 LIPASES

Lipases (triacylglycerol acylhydrolases, EC 3.1.1.3) belong to the class of serine hydrolase. Lipases are interfacial enzymes typically meant for the hydrolysis of water insoluble esters like triacylglycerols. Lipases also considered as a versatile enzyme for they can be used in other reactions such as hydrolysis, esterification and

biotransformation. The reactions involved a wide variety of fatty acids, alcohols or esters. Different types of lipases are known as a biocatalyst for non-aqueous synthesis.

Microbial lipases have gained special industrial attention due to their stability, selectivity, and broad substrate specificity (Dutra *et al.*, 2008; Griebeler *et al.*, 2011). Many microorganisms are known as potential producers of extracellular lipases including bacteria, yeast and fungi (Abada, 2008). According to Vakhlu and Kour (2006), the main terrestrial species of yeasts that were found to produce lipases are: *Candida rugosa, Candida tropicalis, Candida antartica, Candida cylindracea, Candida parapsilopsis, Candida deformans, Candida curvata, Candida valida, Yarrowia lipolytica, Rhodotorula glutinis, Rhodotorula pilimornae, Pichia bispora, Pichia Mexicana, Phicia sivicola, Phicia xylose, Phicia burtonii, Saccharomycopsis crataegenesis, Torulaspora globasa,* and *Trichospron asteroids.*

Among the commercially available lipases, *Candida antarctica* lipase B (CAL-B; Novozyme 435) is the most extensively used biocatalyst in both laboratory and industrial scale. Novozym 435 is the commercial preparation of Novozymes for immobilized CAL-B. CAL-B belongs to the hydrolase-fold superfamily with a conserved catalytic triad consisting of Ser105-His224-Asp187 (Uppenberg *et al.*, 1994). It comprises 317 amino acid residues with molecular weight of 33 kDa. The active site of CAL-B consists of a substrate-nonspecific acyl-binding site and a substrate specific alcohol-binding site which is selective for secondary alcohols (Uppenberg *et al.*, 1994). The special characteristic of CAL-B is it has no lid covering the entrance to the active site and shows no interfacial activation (Martinelle *et al.*, 1995). CAL-B is being frequently used in the acylation of various natural compounds such as saccharides, steroids and natural glycosides, including flavonoids (Riva, 2002; Katsoura *et al.*, 2006; Lue *et al.*, 2010; Almeida *et al.*, 2012) due

to its high enantioselectivity and catalytic activity, wide range of substrates, and thermal stability.

2.5 SYNTHESIS OF FLAVONOID ESTERS

Several methods such as Fischer esterification, alcoholysis, transesterfication or biocatalysts methods have been achieved in the synthesis of flavonoid esters. Fischer esterification is the typical route to prepare esters whereby an acid reacts with an alcohol. However, this is straight forward for an aliphatic alcohol. The use of a dehydrating agent is required as water is produce during the reaction.

Alcoholysis or transesterification is a more novel approach to prepare esters which involves the exchange of an alkoxy group of an ester with another alcohol. This reaction produces another ester RCOOR" and liberation of the alcohol R'OH. In chemical synthesis, the reaction is often carried out in the presence of acetyl chloride or acetic anhydride in pyridine (Urano *et al.*, 1991; Mattarei *et al.*, 2010). Perrier *et al.* (2001) patented the preparation of pentaacylated quercetin using lauroyl chloride, palmitoyl chloride, and butyric anhydride. Jin and Yoshioka (2005) reported the synthesis of epigallocatechin with acyl chlorides to produce 3-*O*-acyl epigallocatechin. Moreover, Urano *et al.* (1991) prepared taxifolin pentaacetate with acetic anhydride resulted in good yield. Although the chemical acylation of flavonoids by various fatty acids and ester has been patented, but this process is not regioselective and leads to an unwanted functionalization of phenolic hydroxyl groups.

Biocatalysts are distinguished from common chemical method by their high stereo- and regioselectivity. Recently, enzyme-catalyzed esterification of flavonoids has been reported (Danieli *et al.*, 1997; Gao *et al.*, 2001; Gayot *et al.*, 2003; Chen *et al.*, 2010; Almeida *et al.*, 2012). Selective esterification is often desirable to retain the antioxidant

properties of polyphenol. Therefore, employing lipase enzyme in the acylation of flavonoids with phenolic acids are more preferable in order to introduce non-polar group to the flavonoid molecule.

Results in this research suggest that a high degree of conversion to desired esters can be achieved when optimal reaction conditions are applied. As reviewed by Chebil *et al.* (2006), the factors that influence regioselectivity and the performance of the enzymatic acylation of flavonoids, include type and concentration of enzyme (Danieli *et al.*, 1990), structure (Ardhaoui *et al.*, 2004b) and concentration of the substrates (acyl donor, acyl acceptor and their ratio) (Kontogianni *et al.*, 2001; Kontogianni *et al.*, 2003), nature of the reaction media (Danieli *et al.*, 1997), water content in the media (Gayot *et al.*, 2003), reaction temperature (Katsoura *et al.*, 2006) and nature of the reaction (Nakajima *et al.*, 1999).

To date, lipase-catalyzed reaction using flavonoids such as rutin, naringin, quercetin, and esculin with fatty acids or vinyl esters ranging from C4 to C18 in length had been reported in several literature (Ardhaoui *et al.*, 2004b; Mellou *et al.*, 2006; Viskupicova *et al.*, 2010).

2.6 APPLICATION OF FLAVONOID ESTERS

There is a range of flavonoid-containing preparations that are nowadays available in many forms in some industrial areas. Through the introduction of lipophilic molecules to the basic flavonoid not only physico-chemical properties can be modified but also biological effects of flavonoids are improved.

According to Degenhardt *et al.* (2007), acylation of certain flavonoids may suppress the negative taste properties in food, pharmaceutical preparations and cosmetic products for mouth hygiene. Ghoul *et al.* (2006) reported methods for the preparation of acylated

flavonoid glycosides with improved stability and solubility in various food preparations, while their antioxidant activity retained unmodified or even enhanced.

In order to protect undesirable damage in food caused by free radicals from highly reactive free unsaturated fatty acids, lipophilic antioxidants can be applied (Perrier *et al.*, 2001). Caldwell *et al.* (2009) patented the preparation of alkylated, alkenylated, acetylated and alkoxylated flavonoid derivatives. These modified flavonoids are suitable mainly for stabilisation of food emulsions because their lipophilicity makes them effective for better protection of lipophilic food matrices. Moreover, it was reported that flavonoid esters with unsaturated fatty acids prepared *via* enzymatic synthesis is useful for stabilisation of oxidable compounds (Mellou *et al.*, 2006).

Flavonoid esters acylated with *p*-coumaric acid were found to increase antioxidant (Viskupicova *et al.*, 2010) and anti-inflammatory activities (Harborne & Williams, 2000). According to Katsoura *et al.* (2006), biocatalytic acylation of rutin with various acyl donors affected its antioxidant potential towards both isolated LDL and total serum model *in vitro*. Mellou *et al.* (2006) reported that flavonoids esterified with polyunsaturated fatty acids lowered the formation of vascular endothelial growth factor in human leukemic cells K562. These new, improved compounds are shown to have angiogenic influence to malignant tissues and thereby anticancer effects.

Moussou *et al.* (2007) found that esters of flavonoids with omega-substituted fatty acids (C6 to C22) were able to protect skin cells against damage by UV radiation. These flavonoid esters are more effective than flavonoids themselves. Wirth *et al.* (2008) patented utilization of acylated flavonoid derivatives prepared *via* chemical synthesis into cosmetic preparations. Acylation performed on glycoside moiety of flavonoids with aromatic and aliphatic acylating agents could serve particularly as skin protectors against harmful UV radiation.

2.7 KINETICS OF ENZYME REACTION

Enzymes are the catalysts of biological systems and are extremely efficient and specific. In fact, an enzyme accelerates the rate of a reaction by a factor of at least a million compared to the rate of the same reaction in the absence of the enzyme (Segel, 1975). Enzymes like all positive catalysts dramatically increase the rate of a given reaction.

Enzyme kinetics is the study of rates of chemical reactions that involve enzymes. Principally, enzyme kinetics is concerned with the speed, velocity, or rate which such reaction occur and the factors which influence this rate. The task of enzyme kinetic is the systematic analysis of such processes, involving a study of the dependence of reaction rates on substrate concentration, pH, temperature, ionic strength and other relevant variables (Segel, 1975).

Through kinetic analysis, the kinetic mechanism of a reaction can be determined. The mechanism of enzyme-catalyzed reactions is often studied by making kinetic measurements on enzyme-substrate reaction systems. These studies include measuring rates of the enzyme-catalyzed reactions at different substrate and enzyme concentrations.

2.7.1 Reaction Rates and Rate Constants

When enzyme and substrate are mixed together, reactions begins. As reaction progresses, the concentrations of substrate and product will change as well as the reaction rate (velocity). For example:

$$\mathrm{A} \rightarrow \mathrm{P} \tag{2.1}$$

where A is substrate and P is product. According to law mass of action, the velocity, v is proportional to the concentration of A.

$$v = -\frac{d[\mathrm{A}]}{dt} = \frac{d[\mathrm{P}]}{dt} = k[\mathrm{A}] \tag{2.2}$$

where *k* is the *rate constant* of the reaction.

The velocity or rate of a reaction can be obtained by plotting product formation or substrate reduction curve against the incubation time (Fig. 2.7). The velocity is measured from the slope of the tangent to this curve. Most assays are based on estimation of *initial velocity* which obtained through extrapolation of the progress curve at zero time. Besides, the use of mathematical softwares also provides additional method to examine the variation of initial velocity.

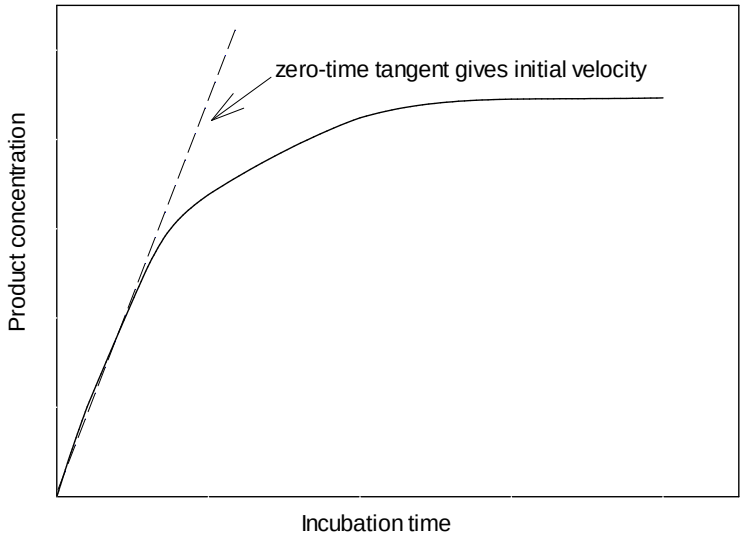

Figure 2.7 Changes in product concentration as a function of time.

After the initial velocity has been estimated for a series of reaction containing different substrate concentrations, a plot of velocity against substrate concentration can be constructed. The general shape of the curve is that of a rectangular hyperbola (Fig. 2.8).

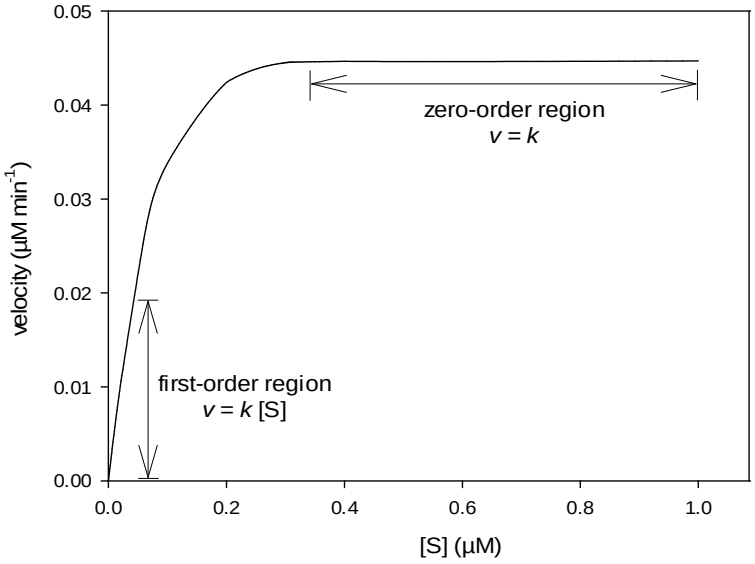

Figure 2.8 Initial velocity versus substrate concentration plot for an enzyme-catalyzed reaction.

If the reaction obeys zero-order reaction, the reaction rate is independent of substrate concentration. By referring to Eq. (2.2), the kinetic expression is:

$$\frac{d[\mathrm{A}]}{dt} = -k_r[\mathrm{A}]^o \tag{2.3}$$

where k_r is the zero rate-order contant. Based on Eq. 2.3, the rate for reaction zero-order action is constant and equal to k_r at all times during reaction.

Integration Eq. (2.3) with initial condition [A] = [A_o] at t = 0 yields:

$$[\mathrm{A}] = \int -k_r dt = [\mathrm{A}_o] - k_r t \tag{2.4}$$

Therefore, when the reaction is zero order, a plot of [A] versus time gives a straight line with slope $-k_r$.

If the reaction obeys first-order kinetics, by referring to Eq. (2.2), the relationship between rate and substrate concentration is as follows:

$$\frac{d[\mathrm{A}]}{dt} = -k_r[\mathrm{A}] \tag{2.5}$$

Separation variables and integration Eq. (2.5) with initial condition [A] = [A_o] at t = 0 gives:

$$\frac{\ln [A]}{\ln [A_o]} = -k_r t \quad \text{or} \quad [A] = [A_o] e^{-k_r t} \tag{2.6}$$

For a first-order reaction, a plot of ln ([A]/[A_o] versus time yield a straight line with slope $-k_r$.

2.7.2 Michaelis- Menten Equation

The kinetics of most enzyme reactions can be represented by Michaelis-menten equation. Michaelis-menten equation was presented by Michaelis and Menten and further developed by Briggs and Heldane. This equation is fundamentally important to study the enzyme kinetics. This model allows enzymologists to predict how fast a reaction will take place based on the concentrations of the chemicals being reacted. Michaelis-Menten scheme defines the relationship between the rate of enzyme-catalyzed reaction and the concentration of the substrate. This equation is characterized by two constants; Michealis-Menten constant (K_m) and the catalytic rate constant, (k_{cat}).

2.7.2.1 Enzymatic reaction involving one substrate

For a single substrate reaction, an enzymatic reaction is usually modeled as a two-step process: substrate (S) binding enzyme (E) and formation of an enzyme-substrate (ES) complex, followed by irreversible breakdown of enzyme-substrate complex to free enzyme and product (P):

$$E + S \underset{k_1}{\overset{k_{-1}}{\rightleftharpoons}} ES \xrightarrow{k_{cat}} E + P \tag{2.7}$$

The velocity of enzyme-catalyzed reaction is limited by the rate of breakdown of the ES complex and therefore the rate of product formation can be expressed as follows:

$$\frac{d[\mathrm{P}]}{dt} = v \quad \text{or} \quad v = k_{cat}[\mathrm{ES}] \tag{2.8}$$

where k_{cat} corresponds to the effective first rate constant for the breakdown of ES complex to free product and free enzyme. At steady state, a balance on the concentration of ES complex can be written as follows:

$$k_1[\mathrm{E}][\mathrm{S}] = k_{cat}[\mathrm{ES}] + k_{-1}[\mathrm{ES}]$$

$$\frac{(k_{cat} + k_{-1})}{k_1} = \frac{[\mathrm{E}][\mathrm{S}]}{[\mathrm{ES}]}$$

$$\frac{k_{cat} + k_{-1}}{k_1} = K_m$$

$$[\mathrm{ES}] = \frac{[\mathrm{E}][\mathrm{S}]}{K_m} \tag{2.9}$$

where K_m is called Michaelis-Menten constant. The total concentration of enzyme is expressed as follow:

$$[\mathrm{E_T}] = [\mathrm{E}] + [\mathrm{ES}]$$

$$[\mathrm{E}] = [\mathrm{E_T}] - [\mathrm{ES}] \tag{2.10}$$

A substitution of Eq. (2.10) in Eq. (2.9) produces the following:

$$[\mathrm{ES}] = \frac{([\mathrm{E_T}] - [\mathrm{ES}])[\mathrm{S}]}{K_m}$$

$$[\mathrm{ES}] = \frac{[\mathrm{E_T}][\mathrm{S}] - [\mathrm{ES}][\mathrm{S}]}{K_m}$$

$$[\mathrm{ES}]\mathrm{K_m} = [\mathrm{E_T}][\mathrm{S}] - [\mathrm{ES}][\mathrm{S}]$$

$$[\mathrm{ES}] = \frac{[\mathrm{E_T}][\mathrm{S}]}{K_m + [\mathrm{S}]} \tag{2.11}$$

As shown in Eq. (2.8), therefore:

$$v = k_{cat}[\mathrm{ES}] \tag{2.8}$$

$$v = k_{cat}\frac{[\mathrm{E_T}][\mathrm{S}]}{K_m + [\mathrm{S}]} \tag{2.12}$$

By defining V_{max} as the maximum reaction velocity:

$$V_{\max} = k_{cat}[\mathrm{ET}] \tag{2.13}$$

Therefore, Eq. (2.12) becomes:

$$v = \frac{V_{\max}[\mathrm{S}]}{K_m + [\mathrm{S}]} \tag{2.14}$$

This equation gives the instantaneous or initial velocity relative to $V_{\max}$ at a given substrate concentration (Fig. 2.9). The rate would probably proportional to [S] for low value of [S], but with the higher value of [S] the rate would asymptotically approach a maximum. The $V_{\max}$ is the maximum velocity that an enzyme could achieve. The measurement is theoretical because at any given time, it would require all enzyme molecules to be tightly bound to their substrates.

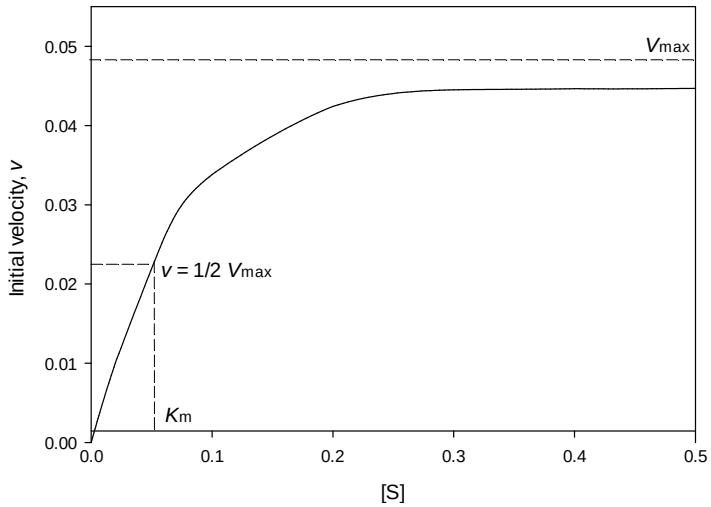

Figure 2.9 Dependence of initial rate on substrate concentration for a typical enzyme-catalyzed reaction.

The definition of K_m is that substrate concentration which gives half the maximum rate. Generally, this Michealis constant, K_m is equal to the reactant concentration at which $v = V_{max}/2$, assuming that the reaction rate is not inhibited by the present of the product (Segel, 1975; Marangoni, 2003). At stable pH, temperature and redox state, K_m for a given enzyme is constant. This parameter provides an indication of the binding strength of that

enzyme to its substrate, where high K_m indicates the enzyme binds the substrate weakly. On the other hand, low K_m indicates higher affinity for the substrate (Segel, 1975). Although derived from a simple, single-substrate, irreversible reaction, the Michaelis–Menten equation also remains valid for more complex reactions.

2.7.2.2 Enzymatic reaction involving two substrates

For a one substrate reaction, there can be no argument about the order of the addition of reactants. However, most enzymes of known function catalyze reactions involving more than one substrate. Two substrates reaction can be classified as *Sequential* or *Ping-Pong* mechanisms (Marangoni, 2003).

In sequential mechanism, the reaction may not occur until both substrates are bound at the active site of the enzyme. Sequential mechanism can be designated *ordered* or *random*, depending on whether the substrates add and the product release in an obligatory sequence or in non-obligatory sequence.

In Ping-Pong mechanism, both substrates are not necessary to be present simultaneously on the enzyme. One of the product must be released between the addition of first and second substrate. This mechanism also can be referred to as double displacement mechanism.

These reactions can be classified even further according to the molecularity of the kinetically important steps in the reaction. These steps can be Uni (unimolecular), Bi (bimolecular), Ter (termolecular), Quad (quadmolecular), Pent (pentmolecular), Hexa (hexamolecular), and so on. Thus a reaction with two substrates and two products is called Bi-Bi as being bireactant in both direction. A Uni-Bi reaction is a unireactant in the forward reaction and bireactant for the reverse reaction. Reactions with three substrates and four products are named as Ter-Quad reactions. Using Cleland's schematics,

examples of Ordered-Sequential Bi-Bi, Random-Sequential Bi-Bi and Ping-Pong Bi-Bi reactions are as follow:

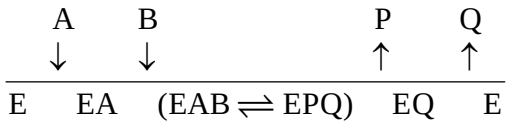

(2.15)

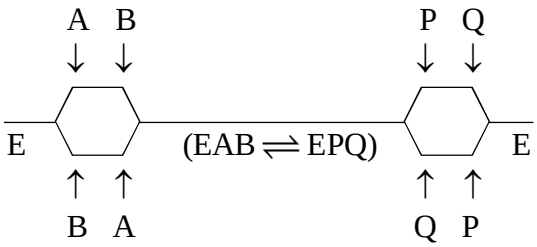

(2.16)

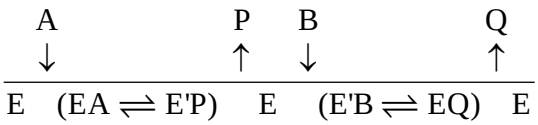

(2.17)

2.7.3 Ordered Sequential Bi-Bi Mechanism

This mechanism describes a sequential addition of A before B to the enzyme in the forward direction, and P before Q in the reverse direction. The attachment of both substrates to the enzyme in ordered sequence yield a ternary complex, EAB. An ordered reaction that is bireactant in both direction is expressed as follow:

$$E + A \underset{}{\overset{K_S^A}{\rightleftharpoons}} EA + B \underset{}{\overset{K^{AB}}{\rightleftharpoons}} EAB \xrightarrow{k_{cat}} E + P + Q \tag{2.18}$$

The rate equation for the formation of product, the equilibrium dissociation constant for the binary enzyme-substrate complex EA (K_s^A), the equilibrium dissociation (K_s), or steady-state Michaelis (K_m) constant for the formation of the ternary enzyme-substrate complex EAB (K^{AB}), and the enzyme mass balance are, respectively:

$$v = k_{cat}[EAB] \tag{2.19}$$

$$K_S^A = \frac{[E][A]}{[EA]} \qquad K^{AB} = \frac{[EA][A]}{[EAB]} \tag{2.20}$$

$$[E_T] = [E] + [EA] + [EAB] \tag{2.21}$$

Normalization of the rate equation by total enzyme concentration ($v/[E_T]$) and rearrangement results in the rate equation for Ordered-Sequential Bi-Bi mechanism produces:

$$\frac{v}{V_{max}} = \frac{[A][B]}{K_S^A K^{AB} + K^{AB}[A] + [A][B]} \tag{2.22}$$

where $V_{max} = k_{cat}[E_T]$.

2.7.4 Random-Sequential Bi-Bi Mechanism

There is no particular order in the sequential binding of substrates A and B to the enzyme to form the ternary complex, EAB for the random-sequential Bi-Bi mechanism. The enzyme may follow either pathway to the central complex, the ratio fluxes through the two path depends on the actual substrate concentrations. A general scheme for Random-Sequential Bi-Bi mechanism is as follow:

$$\begin{array}{ccc} E + A & \overset{K_S^A}{\rightleftharpoons} & EA \\ + & & + \\ B & & B \\ \Big\Updownarrow K_S^B & & \Big\Updownarrow K^{AB} \\ EB + A & \overset{K_S^A}{\rightleftharpoons} & EAB \xrightarrow{k_{cat}} E + P + Q \end{array} \tag{2.23}$$

Rapid equilibrium binding of either substrate A or B to the enzyme takes place in the reaction. For the second stage of the reaction equilibrium binding of A to EB and B to EA, or a steady state in the concentration of the EAB ternary complex.

The rate equation for the formation of product, the equilibrium dissociation constant for the binary enzyme-substrate complex EA and EB (K_s^A and K_s^B), the equilibrium dissociation (K_s), or steady-state Michaelis (K_m) constant for the formation

of the ternary enzyme-substrate complex EAB (K^{AB} and K^{BA}), and the enzyme mass balance are, respectively:

$$v = k_{cat}[\mathrm{EAB}] \tag{2.24}$$

$$\begin{aligned} K_S^{\mathrm{A}} &= \frac{[\mathrm{E}][\mathrm{A}]}{[\mathrm{EA}]} & K_S^{\mathrm{B}} &= \frac{[\mathrm{E}][\mathrm{B}]}{[\mathrm{EB}]} \\ K^{\mathrm{BA}} &= \frac{[\mathrm{EB}][\mathrm{A}]}{[\mathrm{EBA}]} & K^{\mathrm{AB}} &= \frac{[\mathrm{EA}][\mathrm{B}]}{[\mathrm{EAB}]} \end{aligned} \tag{2.25}$$

$$[\mathrm{E}_T] = [\mathrm{E}] + [\mathrm{EA}] + [\mathrm{EB}] + [\mathrm{EAB}] \tag{2.26}$$

A useful relationship exists among these constant:

$$\frac{K_S^{\mathrm{A}}}{K_S^{\mathrm{B}}} = \frac{K^{\mathrm{BA}}}{K^{\mathrm{AB}}} \tag{2.27}$$

Normalization of the rate equation by total enzyme concentration ($v/[\mathrm{E}_T]$) and rearrangement of Eq. (2.27) results in the rate equation for Random-Sequential Bi-Bi mechanism produces:

$$\frac{v}{V_{\max}} = \frac{[\mathrm{A}][\mathrm{B}]}{K_S^{\mathrm{A}} K^{\mathrm{AB}} + K^{\mathrm{AB}}[\mathrm{A}] + K^{\mathrm{BA}}[\mathrm{A}] + [\mathrm{A}][\mathrm{B}]} \tag{2.28}$$

where $V_{\max} = k_{\mathrm{cat}}[\mathrm{E}_T]$.

2.7.5 Ping-Pong Bi-Bi Mechanism

For this mechanism the enzyme must bind substrate A first, following by the release of product P and the formation of the enzyme species E'. This is followed by binding of substrate B to E' and the breakdown of the E'B complex to free enzyme and the second product Q. No ternary is formed for this type of reaction. The scheme for Ping-Pong Bi-Bi mechanism is as follows:

$$\mathrm{E} + \mathrm{A} \underset{k_{-1}}{\overset{k_1}{\rightleftharpoons}} \mathrm{EA} \xrightarrow{k_2} \mathrm{E}' + \mathrm{B} \underset{k_{-3}}{\overset{k_3}{\rightleftharpoons}} \mathrm{E}'\mathrm{B} \xrightarrow{k_4} \mathrm{E} \qquad K_m^{\mathrm{A}} \qquad K_m^{\mathrm{B}} \tag{2.29}$$

The rate equation, steady-state Michaelis constants, and enzyme mass balance for this mechanism are respectively;

$$v = k_4[\mathrm{E'B}] \tag{2.30}$$

$$K_{\mathrm{m}}^{\mathrm{A}} = \frac{k_{-1} + k_{-2}}{k_1} = \frac{[\mathrm{E}][\mathrm{A}]}{[\mathrm{EA}]} \qquad K_{\mathrm{m}}^{\mathrm{B}} = \frac{k_{-3} + k_4}{k_1} = \frac{[\mathrm{E'}][\mathrm{B}]}{[\mathrm{E'B}]} \tag{2.31}$$

$$[\mathrm{E}_T] = [\mathrm{E}] + [\mathrm{EA}] + [\mathrm{E'}] + [\mathrm{E'B}] \tag{2.32}$$

A relationship between E and E' can also be obtained, assuming a steady state in the concentration of E':

$$K_{\mathrm{m}}^{\mathrm{A}} = \frac{k_2}{k_4}\frac{K_m^{\mathrm{A}}}{K_m^{\mathrm{B}}} = \frac{[\mathrm{E'}][\mathrm{B}]}{[\mathrm{A}]} \tag{2.33}$$

Normalization of the rate equation by total enzyme concentration ($v/[\mathrm{E}_T]$) and rearrangement of Eq. (2.33) results in the rate equation for Ping-Pong Bi-Bi mechanism produces:

$$\frac{v}{V_{\max}} = \frac{[\mathrm{A}][\mathrm{B}]}{(k_4/k_2)K_m^{\mathrm{A}}[\mathrm{B}] + K_m^{\mathrm{B}}[\mathrm{A}] + [\mathrm{A}][\mathrm{B}](1 + k_4/k_2)} \tag{2.34}$$

where $V_{\max} = k_{\mathrm{cat}}[\mathrm{E}_T]$ and $k_{\mathrm{cat}} = k_4$. For the case where rate-limiting step of the reaction is the concversion of E'B into EQ (i.e., $k_2 >>> k_4$), Eq. (2.34) reduces to:

$$\frac{v}{V_{\max}} = \frac{[\mathrm{A}][\mathrm{B}]}{\alpha K_m^{\mathrm{A}}[\mathrm{B}] + K_m^{\mathrm{B}}[\mathrm{A}] + [\mathrm{A}][\mathrm{B}]} \tag{2.35}$$

where $\alpha = k_2/k_4$.

Fig. 2.10 shows dependence of the apparent Michaelis constant (*K'*) on the concentration of fixed substrate for Random-Sequential, Ordered-Sequential and Ping-Pong mechanisms.

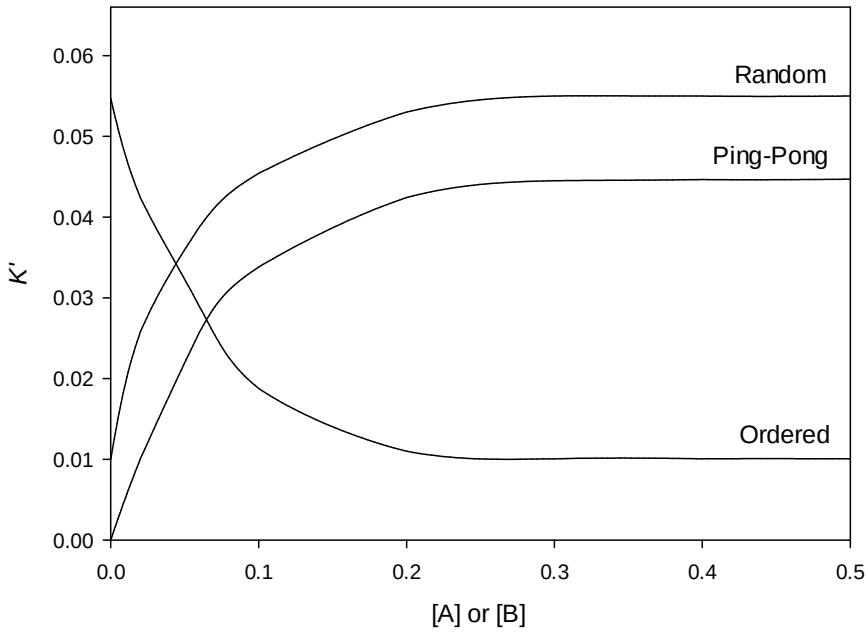

Figure 2.10 Dependence of the apparent Michaelis constant (*K'*) on the concentration of fixed substrate for Random-Sequential, Ordered-Sequential and Ping-Pong mechanisms.

2.7.6 Kinetic Mechanisms on Lipase-catalyzed Esterification Reactions

The kinetics of lipase-catalyzed esterification reactions are useful in not only quantifying a reaction but also in revealing the details of enzyme inhibition and mechanism which have a lot of bearing on its suitability in industrial applications. In lipase-catalyzed esterification, most of the reaction mechanism is reported to follow Michaelis–Menten equation with a Ping–Pong Bi–Bi mechanism. However, in some cases, the reaction obeys the other two mechanisms.

Numerous kinetic studies by lipase have been reported with a variety of homogenous substrates employed in the reaction. The kinetics measurement is practically feasible since there is no solubility limitation by substrates. Zaidi *et al.* (2002) observed kinetic behavior of all the esterification reactions to be following a Ping-Pong Bi-Bi mechanism with competitive inhibition by both substrates used in the reaction. The esterification reactions were carried out using long-chain fatty acids in *n*-hexane

catalyzed by nylon-immobilized lipase from *Candida rugosa*. *Candida rugosa* lipase-catalyzed synthesis of amyl isobutyrate in organic solvent and solvent-free system is showing similar kinetic mechanism (Bezbradica *et al.*, 2006).

Lipase-catalyzed esterification between ethanol and isovaleric acid using immobilized lipase *Rhizomucor michei* in hexane and mixed solvent system were found to follow a Ping-Pong Bi-Bi mechanism where substrates were found to be inhibitory (Chowdary & Prapulla, 2005). They observed the increase in polarity of the media caused an increase in reaction rates and results in lower degree of ethanol inhibition.

In lipase-catalyze esterification using CAL-B, the reaction mechanism is reported to be Ping-Pong Bi-Bi mechanism (Bousquet-Dubouch *et al.*, 2001; Graber *et al.*, 2003; Swarts *et al.*, 2008; Sun *et al.*, 2009). However, Yadav and Trivedi (2003) reported transesterification of *n*-octanol with vinyl acetate at 30ºC showed the reaction obeys the ternary complex (Ordered-Sequential Bi–Bi mechanism) with inhibition by *n*-octanol. The reaction was performed with different lipases (i.e. *Psedomonas, Candida rugosa, Lipozyme* IM 20, CAL-B) amongst which CAL-B was found to be the most active in heptane as a solvent.

Concerning the study of kinetic modeling of lipase-catalyzed esterification in heterogeneous solution most of these studies deal with the esterification of sugar fatty acid esters (Acros *et al.*, 2001; Naoe *et al.*, 2001; Flores & Halling, 2002; Gumel *et al.*, 2011b). Most of the lipase kinetic studies are concerned with miscible substrates reactions, while the kinetic investigation on esterification between immiscible substrates especially on flavonoids has received relatively little attention.

The reaction of glucose esterification catalyzed by immobilized lipase is described by the Ping–Pong kinetic models. The mathematical expressions derived from this model have been tested using several sets of data obtained from reactions carried out under

different reaction conditions. These studies include the kinetics of the lipase-catalyzed synthesis of glucose esters in acetone (Acros *et al.*, 2001) and the esterification of octyl glucoside and octanoic acid by *Candida antarctica* in acetonitrile (Kobayashi *et al.*, 2003).

The similar mechanism also is proposed to described the acylation of glucose by lauric acid in 2-methyl 2-butanol mediated by *Candida antarctica* lipase at 60ºC (Flores & Halling, 2002). To avoid limitations by glucose dissolution rate, a supersaturated glucose solution was used to synthesize lauroyl glucose ester.

Yu *et al.* (2008) reported glucose monoester of stearic acid was obtained by an immobilized lipase from *Candida* sp. They observed the rate constant of monoester reaction increases with the increasing of temperatures from 30 to 40 ºC but decreased at 45ºC due to the low thermostability of the acyl–enzyme complex at higher temperature.

The only data available on flavonoid esterification by lipase was reported by Céliz *et al.* (2012). They studied the kinetic of a new compound, prunin 6"-*O*-laurate which catalyzed by Novozym 435 from vinyl laurate and prunin in acetone. Prunin was obtained through enzymatic hydrolysis of naringin. The kinetic model that best fit the experimental data in these conditions was an Ordered-Sequential Bi-Bi mechanism without inhibition by both substrates.

2.7.7 Activation Energy

The rates of chemicals reactions are greatly dependent on temperature. The rate of the elementary steps in both direction of chemical reaction increases as temperature increases. Arrhenius in 1889 proposed that the effect of temperature on rate constants is adequately describe by a simple equation, now known as *Arrhenius equation,* which can written in several equivalent forms:

Differential form: $$\frac{d \ln k'}{d \mathrm{T}} = \frac{E_a}{RT^2} \quad (2.36)$$

Exponential form: $$k' = Ae^{-E_a/RT} \quad (2.37)$$

Logarithm form $$\ln k' = -\frac{E_a}{RT} + \ln \mathrm{A} \quad (2.38)$$

where E_a is the energy of activation for a chemical reaction, A is the frequency factor, R is the gas constant (8.3145 J mol^{-1} K^{-1}), and T is the absolute temperature (K). Frequency factor is related to the frequency of collisions between reactant molecules. According to the present theories of chemical reactions, a reactant (substrate) must be activated before it can react. The energy must be added to the reactants to allow them to react and form the activated complex (intermediate) before it decomposes into product. This potential energy barrier is therefore called the *energy of activation* of the reaction (Fig. 2.11). For the reaction to take place, this energy of activation is the minimum energy that must be acquired by the system's molecules. Activation energy also can be regarded as an energy

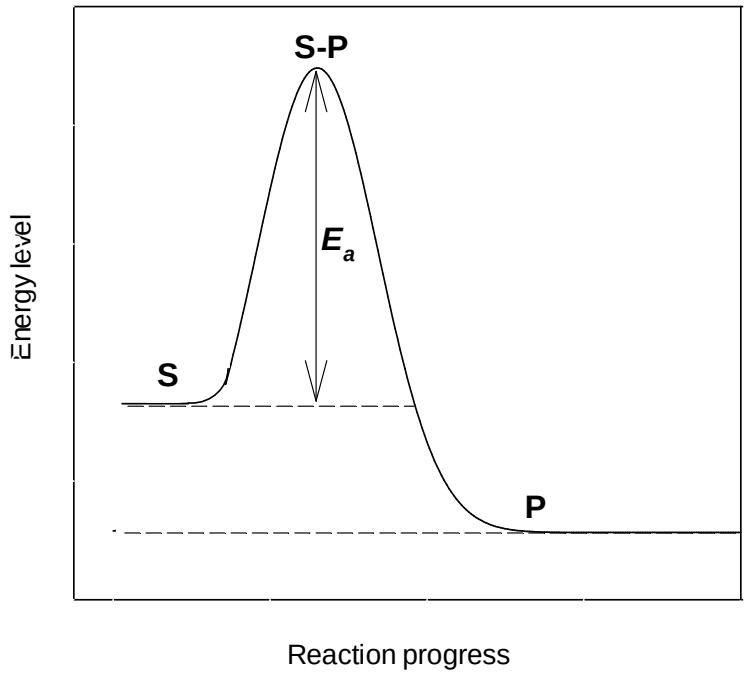

Figure 2.11 Changes in the energy of a chemical reaction from substrate, S to product, P. E_a corresponds to the energy barrier (activation energy) and S-P is corresponds to the activated complex.

difference between the reactants of and activated complex that is an essential intermediate in the reaction step.

In order to determine the energy of activation of a reaction, it is necessary to measure the rate constant (*k'*) of a particular reaction at different temperatures. When *k'* is estimated at a series of different temperature, the activation energy, E_a and frequency factor, *A* can be estimated using Eq. (2.37). By plotting of ln *k'* versus 1/T to yield a straight line with a slope equal to *-E/R* and vertical intercept equal to ln *A* (Fig. 2.12).

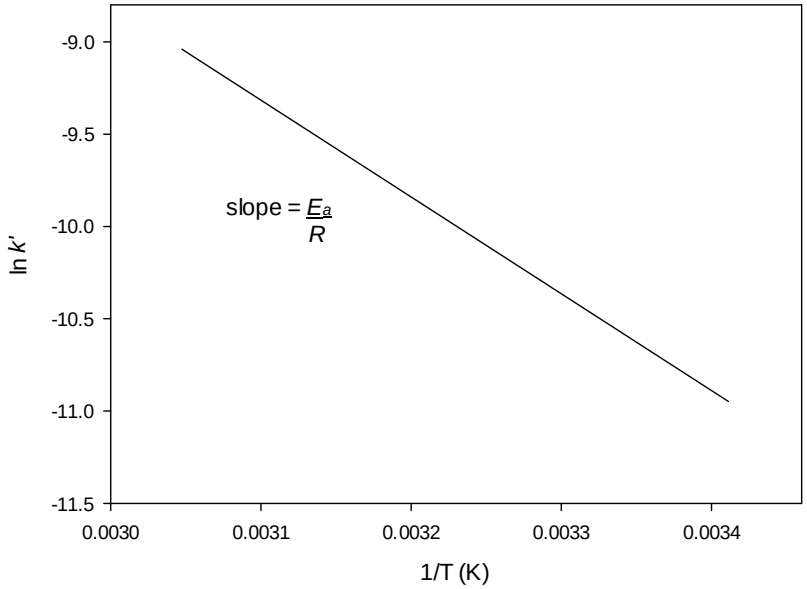

Figure 2.12 Arrhenius plot used in determination of energy of activation, E_a of a reaction.

2.7.8 Activation Energy on Lipase-catalyzed Esterification Reactions

At present, no data is available on the activation energy of lipase-catalyzed synthesis of flavonoid esterification study. However, by taking into consideration of heterogeneous substrates, other comparable activation energy for lipase-catalyzed synthesis of sugar fatty acid esters reported were 19 kJ mol^{-1} (Yu *et al.*, 2008), 50 kJ mol^{-1} i.e. 12 kcal mol^{-1}(Acros *et al.*, 2001), 67.5 × 10^3 kJ mol^{-1} (Šabeder *et al.*, 2006) and 67 kJ mol^{-1} (Gumel *et al.*, 2011b) respectively.

2.8 THERMODYNAMIC OF ENZYME-CATALYZED REACTION

In thermodynamics, a system is defined as that part of the universe which is being studied, such as a bioreactor or a cell, whereas the rest of the universe is referred to as the surroundings. A system is said to be open or closed according to whether it can exchange matter and energy with its surroundings.

The state of a system is defined by a set of state functions which include the free energy ΔG, enthalpy ΔH, and entropy ΔS, as described by the Gibbs-Helmholtz equation at standard state:

$$\Delta G^{\circ} = \Delta H^{\circ} + \Delta S^{\circ} \tag{2.39}$$

Any biochemical reactions must satisfy the laws of thermodynamics. The first law of thermodynamics is simply a conservation of energy statement. The internal energy changes if work and /or heat are exchanged. Enthalpy, ΔH, is used where the heat is exchanged at constant pressure. The second law of thermodynamics introduces the term entropy, ΔS, which is a measure of disorder or randomness in a system.

The thermodynamics of enzyme-catalyzed reactions is based on chemical thermodynamics because it involve substrates, enzymatic sites, and enzyme-substrates complexes. Basically, reactions thermodynamic is concerned with how far a reaction is, and it cannot proceed beyond the point of chemical equilibrium (Doran, 1995).

At equilibrium, there is no net driving force for further change; the reaction has reached the limit of its capacity for chemical transformation in a closed system. Equilibrium concentrations are related by the equilibrium constant, K_{eq} which can be expressed as:

$$K_{eq} = \frac{[\mathrm{P}]_{eq}}{[\mathrm{S}]_{eq}} \tag{2.40}$$

where $[P]_{eq}$ and $[S]_{eq}$ are the concentration of product and substrate at equilibrium respectively.

The equilibrium constant, K_{eq} is also can be determined by the standard free energy change of reaction:

$$\Delta G^{\circ} = -RT \ln K_{eq} \tag{2.41}$$

where ΔG^{o} is the free energy between the product and the substrate in their standard state, R is the gas constant (8.3145 J mol^{-1} K^{-1}), and T is the absolute temperature (K).

Substitution and rearrangement of Eq. (2.40) to Eq. (2.41) yields the van't Hoff equation:

$$\ln K_{eq} = -\frac{\Delta H^{\circ}}{RT} + \frac{\Delta S^{\circ}}{R} \tag{2.42}$$

Thus, for exothermic reactions with negative ΔH^{o}, K_{eq} decreases with increasing temperature. For endothermic reactions with positive ΔH^{o}, K_{eq} increases with increasing temperature.

The van't Hoff equation is used for the determination of the ΔH of a reaction by plotting $\ln K_{eq}$ against 1/T (Fig. 2.13). The slope of the resulting line corresponds to $-\Delta H^{o}/R$. It is also possible to determine the ΔS of the reaction from the *y*-intercept, which corresponds to $\Delta S^{o}/R$.

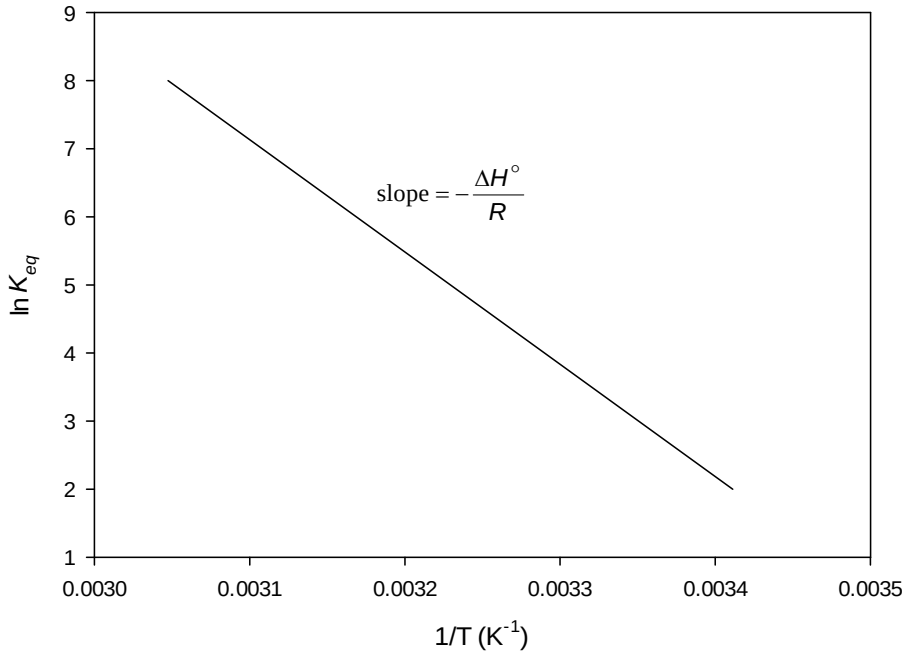

Figure 2.13 van't Hoff plot used in the determination of enthalpy, ΔH and entropy, ΔS.

2.8.1 Thermodynamic on Lipase-catalyzed Esterification Reactions

The values ΔG enthalpy, ΔH and entropy, ΔS an esterification reaction depend on the specific reactants involved. However, to date no information were found in the literature for the specific flavonoid esterification reaction examined in this study. The published data that relevant to this study are reported by Šabeder *et al.* (2006) and Gumel *et al.* (2011b).

Šabeder *et al.* (2006) reported primarily on the enzyme deactivation during the synthesis of fructose palmitate, where a huge decrease in activity was observed with the increase in temperature from 90 to 110 °C. At temperatures above 90 °C, enzymes were deactivated, indicating that free energy during deactivation is negative. Therefore, the Gibb's free energy of deactivation, ΔG_d, enthalpy, ΔH_d and entropy, ΔS_d calculated were at -1.9×10^3 kJ mol^{-1}, 107.8×10^3 kJ mol^{-1} and 302 kJ mol^{-1} K^{-1} respectively.

In addition, Gumel *et al.* (2011b) studied the synthesis of 6-*O*-glucosyldecanoate from *D*-glucose and decanoic acid catalyzed by CAL-B. The researchers found the reaction to be endothermic and become increasingly disordered as the temperature increases. The reaction was performed in dimethyl sulfoxide (DMSO), a mixture of DMSO and *tert*-butanol and *tert*-butanol alone. They found that the values of ΔG, enthalpy, ΔH and entropy, ΔS in the solvent blend were lower compared to the values in the pure solvents.

2.9 CONCLUDING REMARKS

The use of lipase to modify physico-chemical and biological properties of various organic compounds has been of significant scientific and industrial interests. Flavonoids are excellent modification targets due to their potent beneficial biological activities. Although there are a number of studies on lipase-catalyzed modification of flavonoids, the literature on the kinetic model and key parameters affecting the reaction particularly involving immiscible substrates is scarce. Understanding of these fundamental aspects has significant implication in a rational design of the synthesis reaction/reactor for flavonoid esters. Biotransformation represents a useful and ideal tool for the production of valuable commodities in the food processing, pharmaceutical and cosmetic industries.

CHAPTER 3

MATERIALS AND METHODS

3.1 MATERIALS

Lipase from *Candida antarctica* immobilised on acrylic resin (CAL-B), *para*-nitrophenyl palmitate (*p*Npp), sodium hydroxide (NaOH), molecular sieve 4 Å, and the acyl acceptors (rutin, naringin and catechin) were purchased from Sigma–Aldrich Chemical Co. The acyl donors; lauric acid (dodecanoic acid), myristic acid (tetradecanoic acid), palmitic (hexadecanoic acid), deuterated dimethyl sulfoxide (DMSO-d_6), acetic acid, acetone, methanol and *n*-heptane were supplied by Merck. Analytical solvents and reagents were used in this study.

3.2 DETERMINATION OF LIPASE ACTIVITY

Lipase activity was measured by monitoring the rate of hydrolysis of *para*-nitrophenyl palmitate (*p*Npp) (Pencreac'h & Baratti, 1996). Approximately, 20 mM *p*Npp was dissolved in *n*-heptane and used as a substrate for lipase. The hydrolysis reaction was carried out in a two phase solution where immobilized lipase partitioned between heptane and 0.1 M NaOH solution interphase. The assay was done by adding 2.5 mL of 0.1 M NaOH into a cuvette and 0.5 mL of 20 mM *p*Npp in *n*-heptane was added into the solution. Two immiscible solution formed where *p*Npp in *n*-heptane was in the upper part and 0.1 M NaOH was in the bottom part. Then, 10 mg of immobilized lipase was added and the spectrophotometic absorbance was measured immediately at 410 nm for 20 minutes using UV/VIS Spectrophotometer Jasco V-630 (Japan). To ensure proper mixing of the solutions, a tiny magnetic stirrer bar was located at the bottom of the cuvette. Hydrolysis of *p*Npp releases *p*-nitrophenol resulting in yellow coloration in the 0.1 M NaOH solution.

Reaction within the temperature range of 20 to 80 °C were performed in order to investigate the effect of temperature on lipase activities. By employing Beer-Lambert relationship, lipase activity was calculated using Eq. (3.1),

$$\text{U/ ml} = \frac{\Delta Abs_{410\text{nm}} \text{ x } V_s}{V_{ls} \text{ x } l \text{ x } \xi_{410}} \tag{3.1}$$

where

$\Delta Abs_{410\text{nm}}$ = Absorbance difference at 410 nm at for a specific interval (min^{-1})

ξ_{410} = Extinction coefficient of *p*-nitrophenol i.e. 1070.43 L mol^{-1} min^{-1}

V_s = Volume of substrate (mL)

V_{ls} = Total assay volume (mL)

l = path length of cuvette (1 cm)

One unit activity is defined as the amount of lipase that hydrolyzed 1 μmol of *p*Npp per minute.

3.3 PRELIMINARY TEST OF FLAVONOID ESTERS SYNTHESIS

Prior to the determination of the efficiency of lipase-catalyzed acylation of flavonoids, preliminary tests were conducted. Three different classes of flavonoids with different representative structures were selected; rutin (flavonols), naringin (flavanones) and catechin (flavanols) and the acylation of these flavonoids with lauric acid were carried out. Filtered rutin (5 x 10^{-3} M) and lauric acid (0.25 M) were solubilized in 5 mL acetone that was previously dried with 4 Å molecular sieves. Direct esterification was started by the addition of 50 mg of immobilized lipase. The reaction was carried out in screw-capped glass tubes shaken horizontally at 200 rpm, 55 ºC. Similar experiments were conducted for naringin and catechin. The identity and molecular weight calculation of flavonoid

esters were obtained from Liquid Chromatography/Mass Spectrometry/Mass Spectrometry (LC/MS/MS) analysis.

3.4 FULL FACTORIAL EXPERIMENTAL DESIGN

Based on the LC/MS/MS results and preliminary investigation of reaction conditions, only rutin flavonoid was selected for further investigation. Due to the low solubility, rutin stock was dissolved in dried acetone and the filtered using Buchner funnel. The rutin filtrate was collected and the actual concentration of rutin was assayed using High Performance Liquid Chromatography (HPLC). The solubility of rutin stock solution in acetone was determined at 1.48×10^{-2} g g^{-1} solvent (molality = 2.42×10^{-2} mol kg^{-1}) at 25 ± 1 ºC and 1 atm. The rutin residue was dried at 55 ºC, kept at -4 ºC and reused for other esterification process.

For experimental design experiment, the rutin concentration was held constant at 5 x 10^{-3} M in 5 mL of acetone. Reaction was carried out in a screw-capped glass tube agitated horizontally at 200 rpm and 55 ºC. After 4 days, 0.2 mL of sample was taken from the reaction. Each sample was dried at 70 ºC and re-suspended in 1 mL of methanol and filtered through a 0.22 μm PTFE filter for subsequent analysis by HPLC.

In order to study the effects of selected process parameter, experimental design was performed using full factorial design (FFD) in MINITAB® 15 software. The effects of three selected operating variables *viz.* lauric acid concentration (M), temperature (ºC) and enzyme loading (g) were screened using full factorial design (FFD). Synthesis of rutin ester was performed in random triplicates with lowest, middle and highest factor levels (Table 3.1). These effects were evaluated in terms of rutin ester yield as the response variable.

Table 3.1 Factor and level set up for FFD screening experiment

Factor	Level		
	Lowest	**Middle**	**Highest**
Lauric acid (M)	0.05	0.15	0.25
Temperature (ºC)	35	45	55
Enzyme loading (g)	0.03	0.04	0.05

Since there are three factors, each with three levels (minimum, middle and maximum point values), there were 27 experimental runs including triplicates generated from MINITAB®15. The design was completely randomized along with the sampling.

3.5 ENZYMATIC SYNTHESIS OF RUTIN ESTERS: KINETIC AND THERMODYNAMIC EXPERIMENT

In order to investigate the kinetic and thermodynamic of lipase-catalyzed synthesis of rutin laurate, the range of variables studied were selected based on screening results. The enzymatic synthesis of rutin esters were carried out at fixed amount of filtered rutin (5×10^{-3} M) at different concentration of lauric acid (0.05 to 0.55 M) in acetone. Batch esterification process were performed in screw-capped glass tubes shaken horizontally at 200 rpm. The reaction was initiated by adding 0.15 g (10 gL^{-1}) of lipase into 15 mL of reaction media. A fixed reaction temperature (20-55 ºC) was maintained at the specific set of experimental combination. In order to determine the progress of the reaction, 0.2 mL aliquot of the reaction medium was withdrawn at predetermined time intervals. Each sample was dried at 70 ºC and re-suspended in 1 mL of methanol and filtered through a 0.22 μm PTFE filter for subsequent analysis by HPLC. Three

independent replicates were made for every experiments conducted. Control experiments (without catalyst) were also conducted in parallel.

3.6 ANALYTICAL METHODS

3.6.1 High Performance Liquid Chromatography (HPLC)

Quantitative analysis of rutin and their esters was performed by HPLC (Jasco, Japan) system equipped with degasser (DG 980 50), binary pump (PU 980), auto sampler (AS 950), column oven (CO 965), and ultraviolet (UV) detector (UV 975). The detector was operated at ultraviolet wavelength detection at 280 nm. A Chromolith® HR RP-18^{e} column (4.6 x 10 mm, 2 μm, Merck) fitted with analytical guard column (4.6 x 10 mm x 2μm) was used for the chromatographic separation. The temperature of the column was maintained at 35 °C with flow-rate of 1 ml min^{-1}. The injection volume of 20 μL was used. The separation of the different components of the reaction medium was performed using a gradient of methanol (A) and water with 0.1% acetic acid (B): 0.1 min (30/70), 5 min (100/0), 10 min (100/0), 11 min (30/70), 15 min (30/70). Data acquisition was performed using ChromNav software (Jasco, Japan). The conversion yield was calculated between the molar concentration of acylated flavonoid (rutin) and its initial molar concentration,

$$Conversion\ yield = \frac{[F]_{initial} - [F]_{residual}}{[F]_{initial}} x100 \qquad (3.2)$$

where $[F]_{initial}$ is the initial rutin concentration and $[F]_{residual}$ is the remaining rutin concentration in the reaction. Calibration curve for rutin was obtained using standards dissolved in methanol. Rutin ester was collected from the elution of HPLC and the external calibration curve was plotted using purified samples.

3.6.2 Liquid chromatography/mass spectrometry/mass spectrometry (LC/MS/MS)

The molecular weight analysis for the flavonoids and their esters were performed using a liquid chromatograph (LC, Shimadzu, LC 20 AD, binary pump) interfaced to AB Sciex 3200QTrap LC/MS/MS with Perkin Elmer FX 15 uHPLC system was used for the integration, calibration, collection of LC/MS spectra and data processing for qualitative and quantitative analysis. Separation was achieved on a Phenomenex Aqua C18 reversed phase column with an ID of 5 µm and dimensions of 50 mm × 20 mm × 5 µm. Reaction components separation was achieved using different gradients of 0.1% formic acid and 5 mM ammonium formate in water (A) and acetonitrile with 0.1% formic acid and 5mM ammonium formate (B) as follows: 0.01 min (90/10), 8 min (10/90), 11 min (10/90), 11.10 min (90/10), 15 min (90/10) at constant flow rate of 0.25 mL min^{-1}. The column oven temperature was operated at 40 ºC and the injection volume was 20 µL with the total running time of 15 min. The mass spectra was operated in the negative turbo ion spray (ESI) mode and the electrospray source parameters were fixed as follows: electrospray capillary voltage 3.5 kV, source temperature 500 ºC. Nitrogen was used in the electrospray ionization source. The de-solvation gas and source gas flows were at 40 psi. The de-clustering potential and entrance potential were at 40 V and 10 V respectively.

3.6.3 Nuclear Magnetic Resonance (NMR) spectroscopy

Authentication of the chemical structure of the purified product was done *via* NMR analysis using Brucker AC 600 MHz spectrometer. Prior to analysis, the purified product was dried in a oven at 60 ºC to get rid of solvent and water. 5 to 20 mg of product was weighed for ^{1}H-NMR and ^{13}C-NMR analysis. Deuterated DMSO-d_6 was used as solvent

and internal standard reference. A total of 1 mL filtered sample solution was pipetted into the 300 MHz NMR tubes.

3.7 KINETICS PARAMETERS

3.7.1 Initial Rate of Rutin Ester Synthesis

Esterification rate was determined from the polynomial regression plot of apparent product concentration as a function of time. A tangent was drawn from the origin on the polynomial regression. In the case of rutin ester, initial volumetric rate (r_{vol}, $M^{-1}\,h^{-1}$) was calculated using Eq. (3.3):

$$r_{vol} = \frac{\Delta C}{\Delta t} \tag{3.3}$$

where ΔC (M) is the change in the rutin ester concentration over the time interval Δt (h).

The rate equation for this reaction described by a Ping-Pong Bi-Bi kinetic model, assuming there is no inhibition of both substrates and products. The expression for the reaction rate is given by Segel (1975) as:

$$v = \frac{V_{\max}[\mathrm{LA}][\mathrm{F}]}{K_m^{[\mathrm{F}]} + K_m^{[\mathrm{LA}]} + [\mathrm{LA}][\mathrm{F}]} \tag{3.4}$$

where v is the initial reaction rate, V_{max} is the maximum reaction rate ($M\,h^{-1}$) and K_m^{LA} and K_m^{F} are the binding constants (Michaelis constants) for both substrates lauric acid (LA) and the flavonoid, rutin (F) The reaction rates obtained at various lauric acid and rutin concentrations were fitted to this model using non-linear regression (Polymath® software).

3.7.2 Activation Energy of Rutin Ester Synthesis

Activation energy (E_a) is defined as minimum energy required by reactant molecules to overcome energy barrier and pass through a transition state before

proceeding on to the product of the reaction (Segel, 1975). The activation energy (E_a, J mol^{-1}) of esterification process was calculated using the linearized Arrhenius equation as shown in Eq. (3.5):

$$\ln k_1^{'} = -\frac{E}{RT} + \ln \mathrm{A} \tag{3.5}$$

where A is the frequency factor, R is the gas constant (8.3145 J mol^{-1} K^{-1}), and T is the absolute temperature (K). To calculate k_1', the volumetric rate of rutin esterification was plotted against different initial fatty acid concentration for each temperature tested (20 to 55 °C). The rate constant k_1' was obtained from the slope of the resulting linear plot.

3.8 THERMODYNAMIC PARAMETERS OF RUTIN ESTER SYNTHESIS

The esterification reaction is assumed to be at equilibrium state when the formation of rutin ester in acetone showed no further changes in concentration over time at a particular temperature. The transition of the rutin to rutin ester was also considered a one-step process, thus employing Eq. (2.39) the apparent equilibrium constant K_{eq} was calculated as follows:

$$K_{eq} = \frac{[\mathrm{P}]_{eq}}{[\mathrm{S}]_{eq}} \tag{2.40}$$

$$K_{eq} = \frac{[\mathrm{FE}]_{eq}[\mathrm{W}]_{eq}}{[\mathrm{F}]_{eq}[\mathrm{LA}]_{eq}} \tag{3.6}$$

where K_{eq} is the apparent equilibrium constant, $[\mathrm{FE}]_{eq}$ and $[\mathrm{W}]_{eq}$ are the flavonoid ester (rutin ester) and water concentration (in mole) at equilibrium respectively. $[\mathrm{F}]_{eq}$ and $[\mathrm{LA}]_{eq}$ are the respective concentration of residual rutin and lauric acid (in mole) at equilibrium. $[\mathrm{FE}]_{eq}$ and $[\mathrm{F}]_{eq}$ were determined from the plotted external calibration curve. Meanwhile $[\mathrm{W}]_{eq}$ was calculated from the ester synthesis stoichiometry where 1 mole of water is produced per mole of ester synthesized. Based on the same stoichiometry, 1 mole

of lauric acid is used per mole of ester synthesized, therefore $[LA]_{eq}$ was calculated from the initial lauric acid concentration and minus the $[FE]_{eq}$ concentration.

K_{eq} was measured at various temperatures. The temperature dependence of K_{eq} is expressed according to van't Hoff equation as follows:

$$\ln K_{eq} = -\frac{\Delta H}{RT} + \frac{\Delta S}{R} \tag{3.7}$$

where ΔH is van't Hoff enthalpy (J mol^{-1}) and ΔS is entropy (J mol^{-1} K^{-1}).

At constant pressure and temperature, Gibbs free energy change (ΔG, J mol^{-1}) for the reaction at non-standard conditions was calculated using the following equation:

$$\Delta G = \Delta H + \Delta S \tag{3.8}$$

Gibbs free energy at standard condition (ΔG^{o}, J mol^{-1}) was calculated as follows:

$$\Delta G = \Delta G + RT \ln K_{eq} \tag{3.9}$$

where K_{eq} is the apparent equilibrium constant at standard condition (1 atm).

3.9 WORKFLOW OF THE STUDY

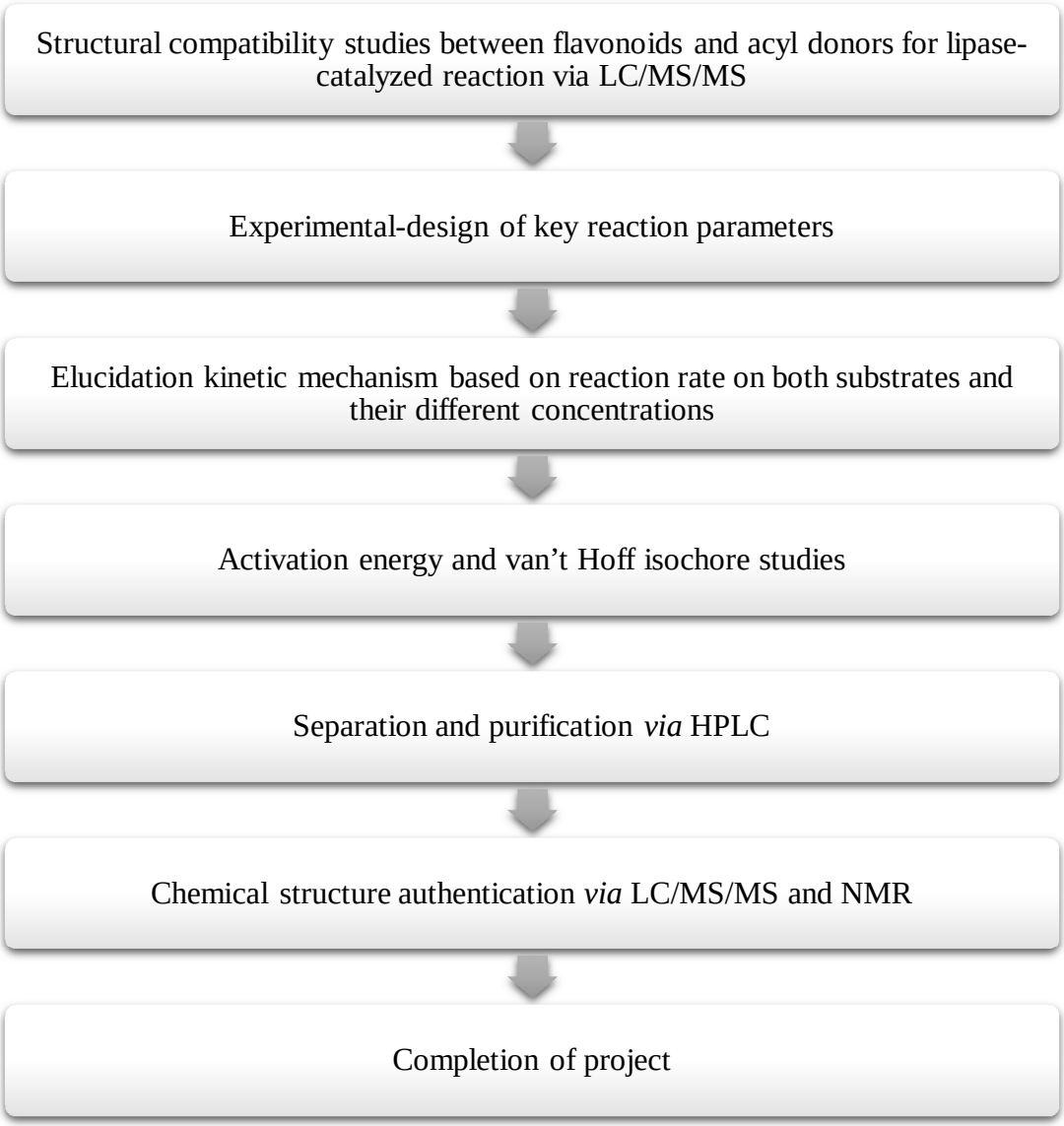

Figure 3.1 Work flow of flavonoid esterification study.

Fig. 3.1 showed the workflow of flavonoid esterification study. Initially, three different flavonoid structures *viz.* rutin, naringin and catechin (flavanols) were reacted with lauric acid as an acyl donor catalyzed by lipase (CAL-B). By using full factorial design (FFD), the effects of three selected operating variables *viz.* lauric acid concentration (M), temperature (ºC) and enzyme loading (g) were investigated for the synthesis of rutin ester. Next, to elucidate the reaction mechanism, various fixed initial quantities of rutin were reacted with different initial concentrations of lauric acid. The

reaction was also carried out at various temperatures for van't Hoff isochore studies and also to determine the activation energy. The separation and purification of the flavonoid ester i.e. rutin laurate was done using HPLC. Finally, the authentication of the chemical structure of the purified product was performed *via* LC/MS/MS and NMR.

CHAPTER 4

RESULTS AND DISCUSSION

4.1 DETERMINATION OF LIPASE ACTIVITY

Prior to the determination of the thermal stability of lipase enzyme in organic solvent, lipase activity was measured by monitoring the rate of hydrolysis of *para*-nitrophenyl palmitate (*p*Npp) (Pencreac'h & Baratti, 1996). Reactions were carried out within the temperature range of 20 to 80 °C.

Table 4.1 Lipase activities assayed at different temperatures

Temperature (°C)	**Lipase activity (U L^{-1})**	**Fold of increase in activity**
30	2.06	1.0
40	3.13	1.5
50	6.34	3.0
60	8.57	4.1
70	11.97	5.7
80	14.98	7.1

Standard deviation of the triplicate measurements was <5 %

As shown in Table 4.1, lipase activity increased with the increase in reaction temperature. It was found that the enzyme remained active within the temperature range tested. CAL-B is known as a thermostable enzyme and able to retain its catalytic activities during the reaction even up to 90 °C (Yoshida *et al.*, 2006). Thus, the suitable temperature range for the esterification reaction investigated in this study was deemed to be in which the enzyme was thermally stable without a significant loss of catalytic activity. Using 30

^{o}C as a references temperature, an increase in enzyme activity up to seven times was observed within the reaction temperature range studied.

4.2 PRELIMINARY TEST OF FLAVONOID ESTERS SYNTHESIS

4.2.1 Effects of the flavonoid structure on its acylation

Three different classes of flavonoids (5 x 10^{-3} M) with different representative structures were selected; rutin (flavonols), naringin (flavanones) and catechin (flavanols). The acylation of these flavonoids with lauric acid (0.25 M) was carried out.

Initial investigation using LC/MS/MS in negative mode showed flavonoids acylation with lauric acid was successful for the flavonoid glucosides; rutin (Fig. 4.1 and 4.2) and naringin (Fig. 4.3 and 4.4). For an aglycone flavonoid, such as catechin, no desired product was observed (Fig. 4.5)

From the LC/MS/MS spectra of rutin (Fig. 4.1 b) and naringin (Fig. 4.3 b), only one product was identified after the reaction. Based on *m/z* values and MS/MS fragmentation pattern, rutin exhibited principal fragments at *m/z* 300 and *m/z* 609 (Fig. 4.2 a). In the case of acylated rutin, dominant signal was present at *m/z* 792 (Fig. 4.2 b). In the mass spectrogram of naringin (Fig. 4.4 a), principal fragments were observed at *m/z* 151, *m/z* 271, *m/z* 459 and *m/z* 579. An additional dominant signal at *m/z* 762 was found for the acylated naringin (Fig. 4.4 b). Since only monoester was produced, these results showed that enzymatic acylation of rutin and naringin was regioselective, which were in agreement with other reported literature (Danieli *et al.*, 1997; Ishihara *et al.*, 2002; Gayot *et al.*, 2003; Mellou *et al.*, 2005; Lue *et al.*, 2010; Almeida *et al.*, 2012).

Precursor scanning of LC/MS/MS for catechin showed two major peaks appeared at t_R = 0.40 min and t_R = 1.05 min (Fig. 4.5 a). The first peak was detected as catechin meanwhile the second peak was identified catechin isomer, epicatechin. The major ion

peaks for catechin was found at *m/z* 289, *m/z* 109 and *m/z* 245 (Figure 4.3 c) but no prominent signal was observed after acylation (Figure 4.5 b). The non-reactivity with catechin seemed to be due to the lack of glycoside moiety in the acyl acceptor molecule. Gao *et al.* (2001) reported that synthesis of catechin glycoside esters were achieved by the sequential use of two enzymes; glycosidase and lipase. Initially the synthesis of catechin glycosides was carried out using glycosidase and the resulting flavonoid glycosides were further modified by acylation with vinyl esters using *C. antarctica* lipase *B (*CAL-B). Thus, it was hypothesized that the acylation of catechin with lauric acid using CAL-B lipase as biocatalyst will occur when the catechin molecule in the glycosylated form. Moreover, the absence of reactivity with catechin might be due to the incompatibility of the active site of CAL-B to the aglycone form of flavonoids.

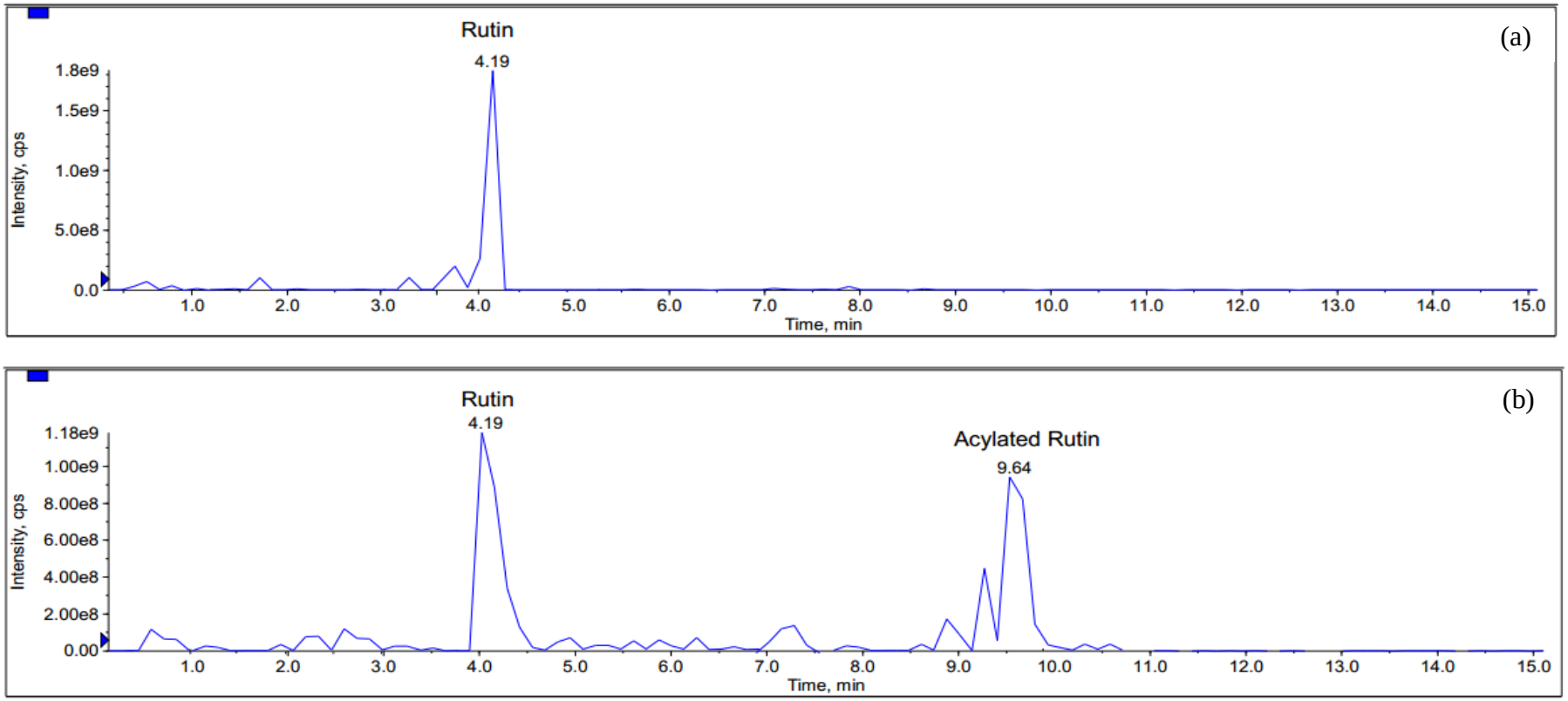

Figure 4.1 LC/MS/MS chromatogram for rutin flavonoid and its ester (a) rutin peak (b) acylated rutin with lauric acid.

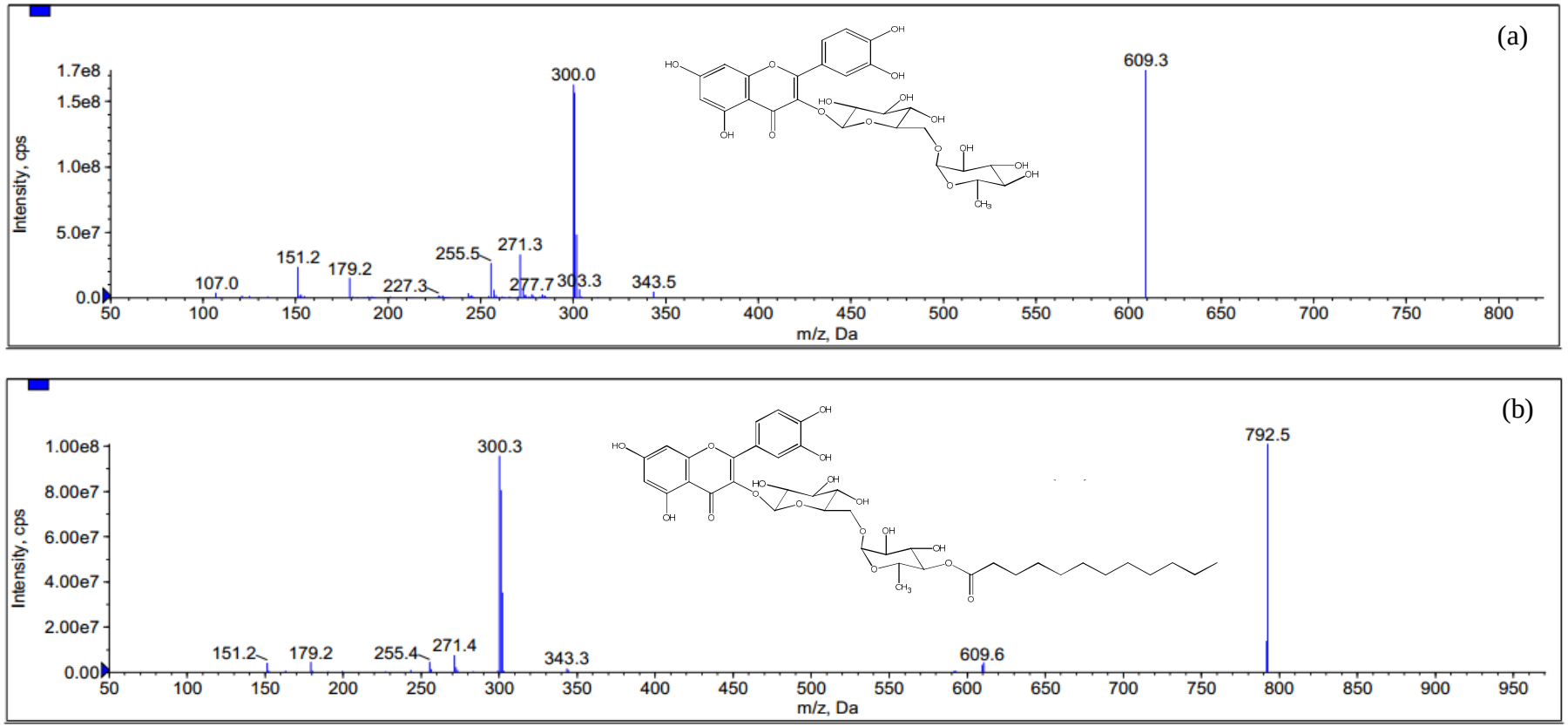

Figure 4.2 LC/MS/MS chromatogram for rutin flavonoid and its ester (a) fragmentation pattern of rutin (b) fragmentation pattern of acylated rutin.

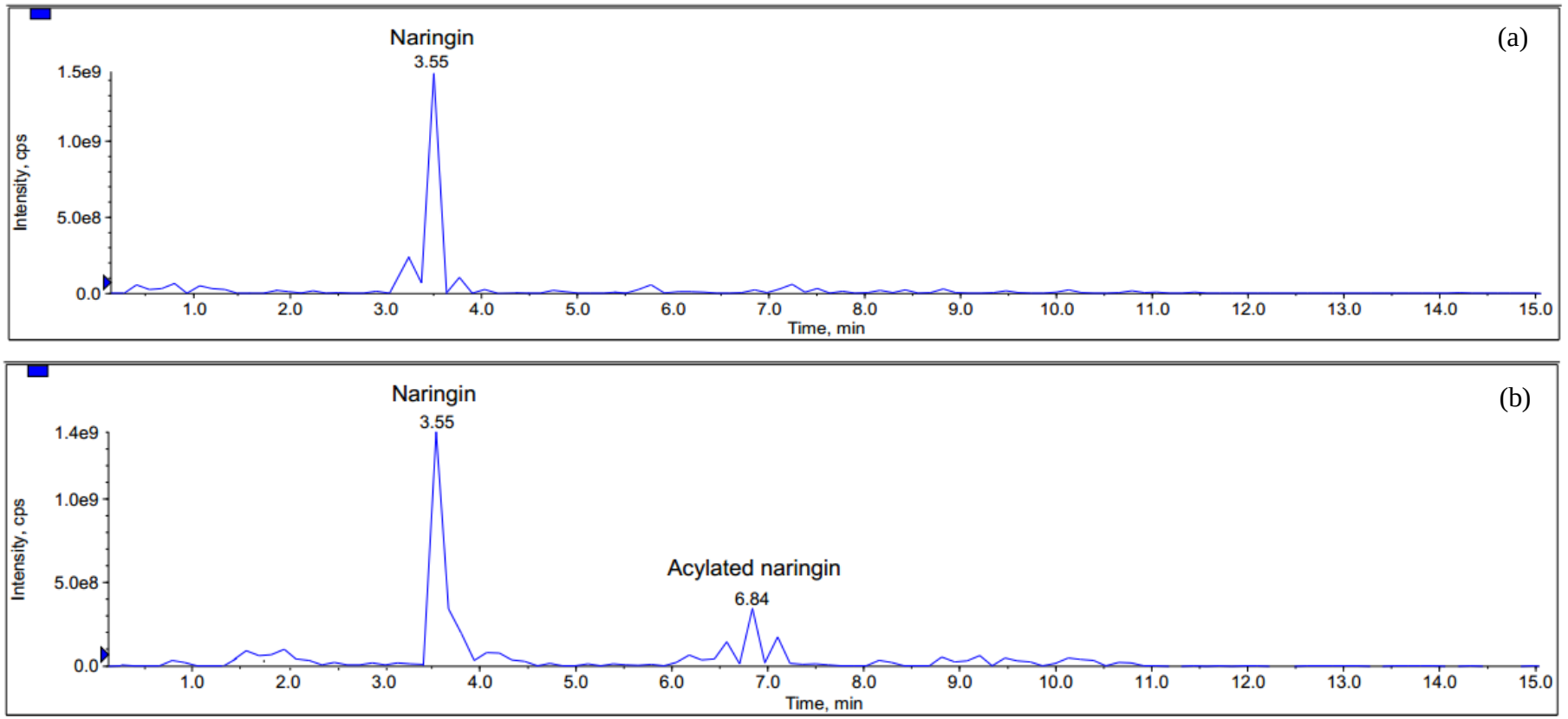

Figure 4.3 LC/MS/MS chromatogram for naringin flavonoid and its ester (a) naringin peak (b) acylated naringin with lauric acid.

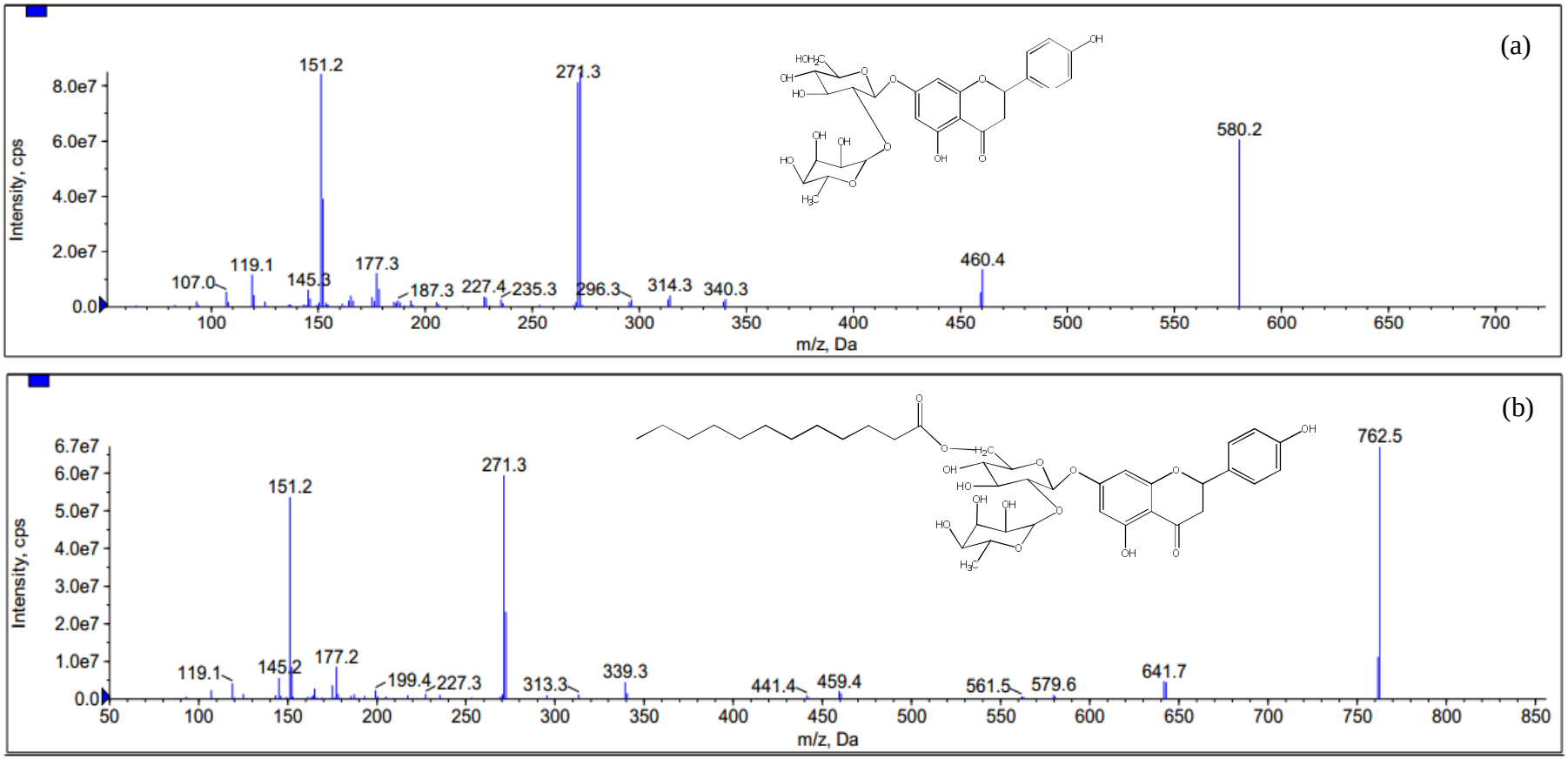

Figure 4.4 LC/MS/MS chromatogram for naringin flavonoid and its ester (a) fragmentation pattern of naringin (b) fragmentation pattern of acylated naringin.

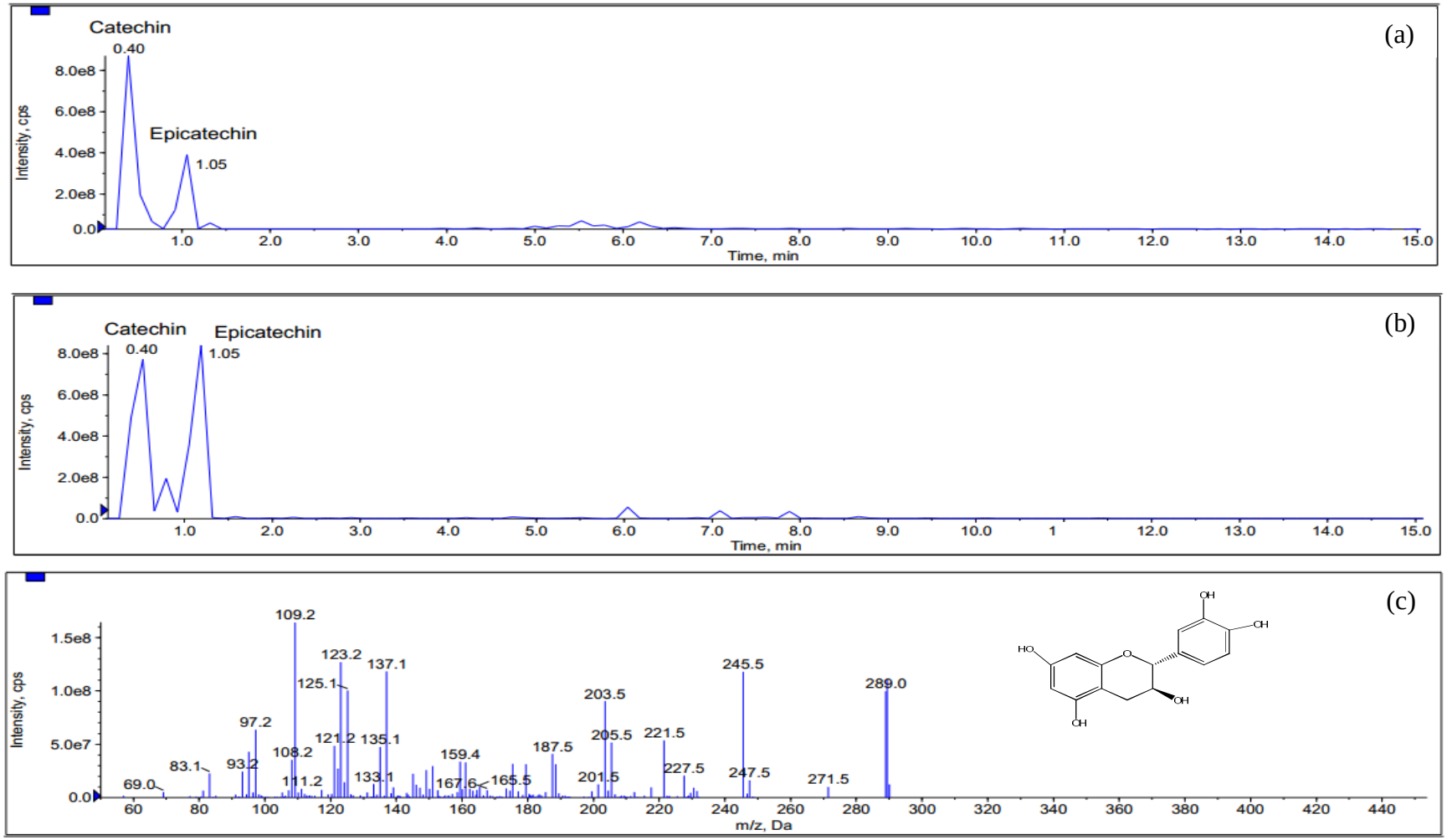

Figure 4.5 LC/MS/MS chromatogram for catechin flavonoid (a) catechin peak (b) acylated catechin with lauric acid (c) fragmentation pattern of catechin.

4.2.2 Effects of the flavonoid structure and carbon-chain length of the acyl donors on reaction conversion yield

Based on the preliminary results, rutin and naringin were selected for further studies. The effects of the carbon-chain length and the substitution pattern of the acyl donors were investigated for the most reactive substrate.

As shown in Fig. 4.6, the conversion yield obtained was higher in the case of rutin (55 %) than that of naringin (47 %). These observations were in accordance with other investigations (Danieli. *et al.*, 1990; Nakajima *et al.*, 1999; Kontogianni *et al.*, 2001; Kontogianni *et al.*, 2003). They observed that the acylation of naringin with fatty acid or vinyl esters takes place at the primary hydroxyl group of the glucose meanwhile acylation of rutin takes place at the secondary hydroxyl group of the glucose. By considering the differences in structure of these two flavonoids, it was suggested that the efficiency of the conversion catalyzed by *C. antarctica* lipase was relatively by the unaffected structure of the aglycone moiety of the two of the flavonoids.

Since acylation of rutin exhibited better conversion yield as compared to naringin, the effect of the carbon-chain length of the acyl donors on the acylation of the flavonoids was investigated using aliphatic fatty acids with carbon number ranging from 12 to 16 with rutin as acyl acceptor. The comparable conversion (> 50 %) was obtained when long chain fatty acids (C12–C16) were reacted with rutin (Fig. 4.6). Similar findings were reported in literature (Kontogianni *et al.*, 2001; Kontogianni *et al.*, 2003; Ardhaoui *et al.*, 2004a; Mellou *et al.*, 2005; Lue *et al.*, 2010) that showed the fatty acid chain length had no significant effect on conversion yield when fatty acids of medium and high chain length were used.

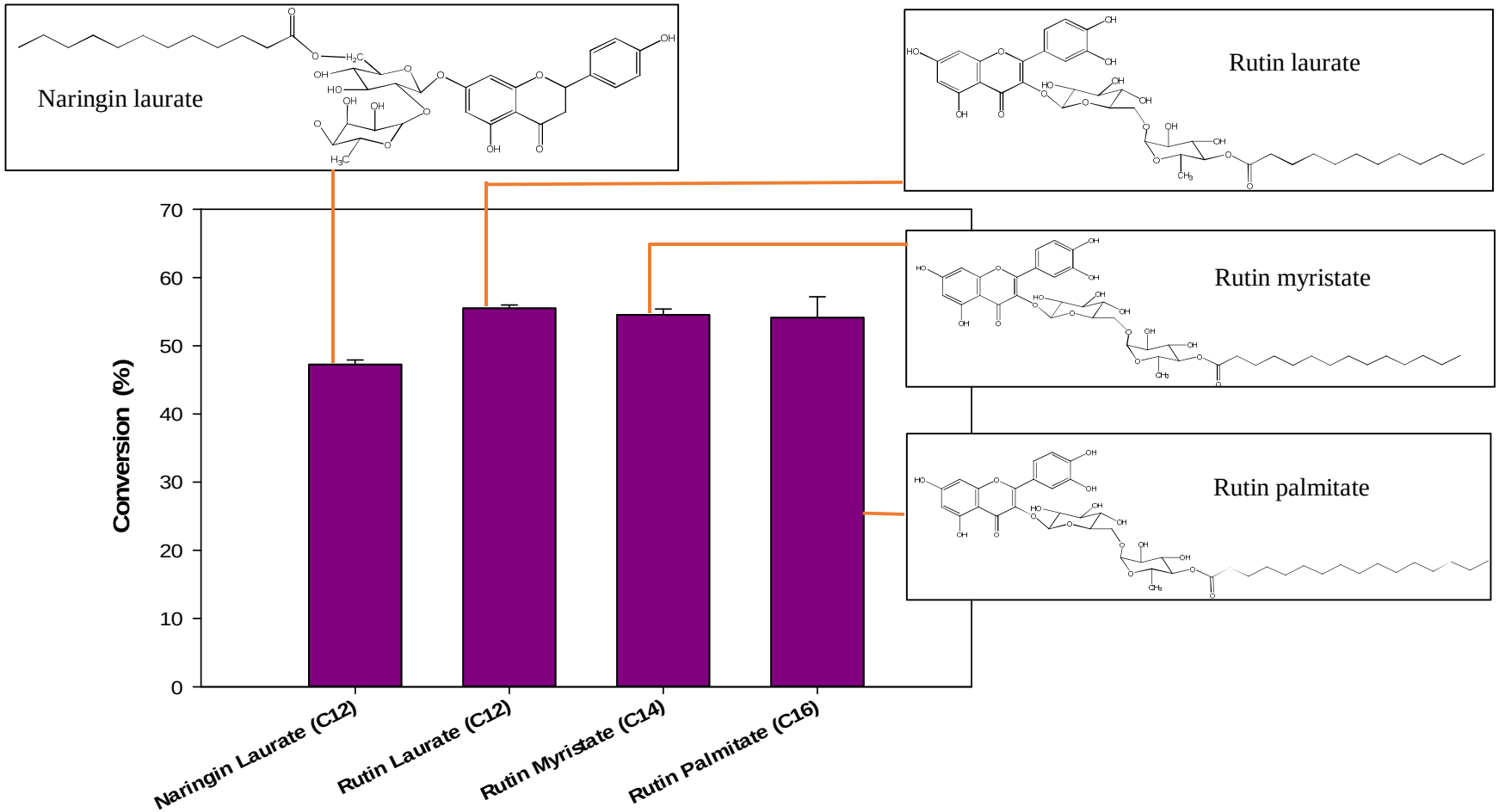

Figure 4.6 Conversion yield (%) for naringin ester and rutin esters.

However, Viskupicova *et al.* (2010) and Katsoura *et al.* (2006) reported that increasing the carbon number of the aliphatic fatty acids (from C12 up to C18) resulted in gradual decrease in conversion yield of esters with steric hindrance is suggested as the primary reason. Therefore, the effect of the chain length of the fatty acid (the acyl donor) on esterification yield is difficult to generalize and remains a matter of discussion (Gumel *et al.*, 2011a; Viskupicova *et al.*, 2012).

LC/MS/MS spectra revealed that only one product was formed (Fig. 4.7 a) for each of the aliphatic fatty acid used. As mentioned earlier, LC/MS/MS analysis showed a dominant signal at *m/z* 791.4 (t_R = 9.54 min), which confirmed that only a single lauric acid was acylated to each molecule of rutin (rutin laurate). The longer the carbon chain of fatty acid used in the reaction, the longer was the retention time for the acylated flavonoid and the larger its *m/z* value. Major peak for myristic acid rutin ester (rutin myristate) appeared at *m/z* of 819.5 (t_R = 10.85 min) (Fig. 4.7 c) while palmitic acid rutin ester (rutin palmitate) showed its major ion peak at *m/z* 848.8 (t_R = 12.27 min) (Fig. 4.7 d). For every rutin esters, consistent fragmentation pattern was observed at *m/z* 463.2 and *m/z* 591.4 indicating an additional attachment of aliphatic fatty acid molecule to the rutin molecule.

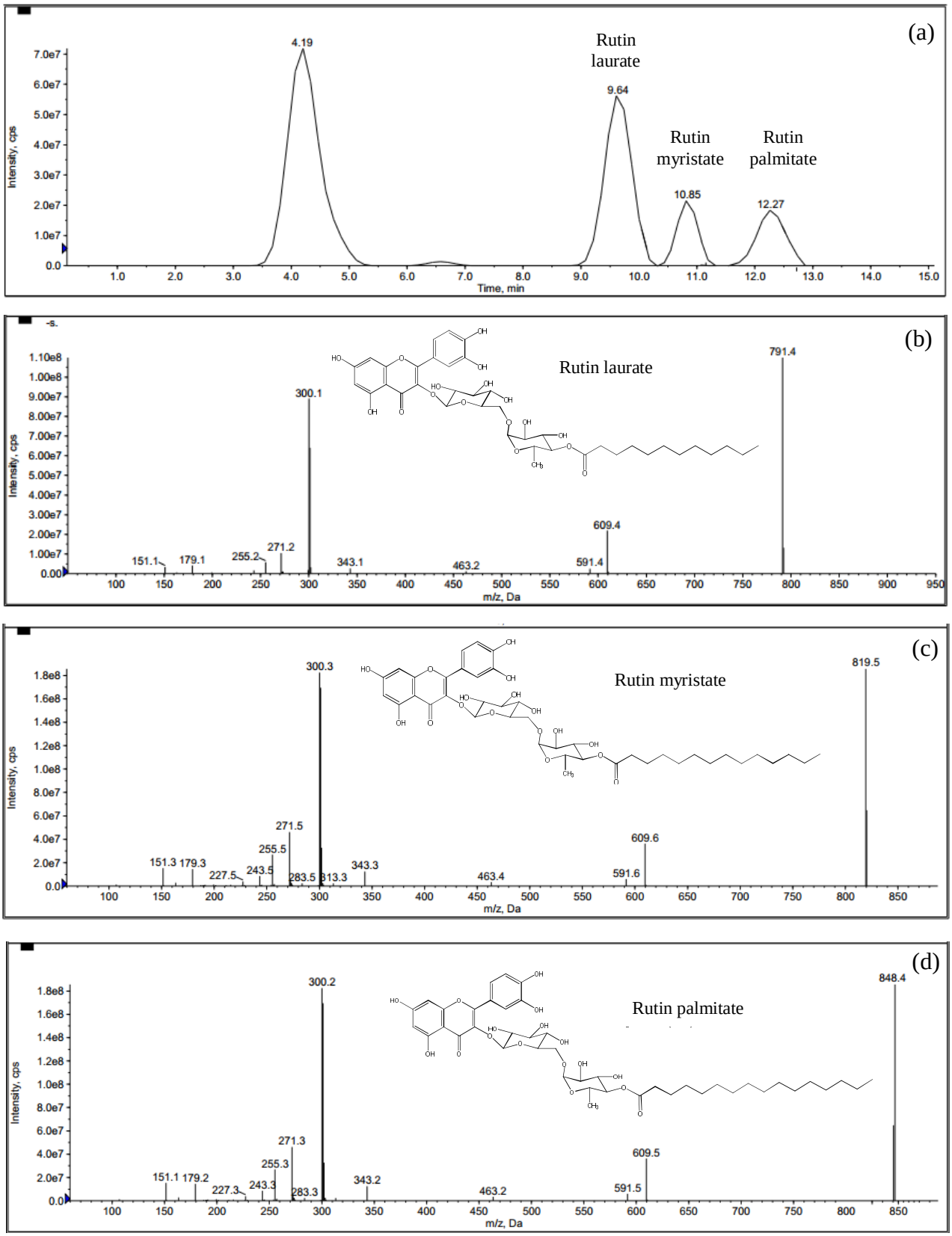

Figure 4.7 LC/MS/MS chromatogram for rutin esters (a) rutin and their ester peaks (b) fragmentation pattern of acylated rutin with lauric acid (c) fragmentation pattern of acylated rutin with myristic acid (d) fragmentation pattern of acylated rutin with palmitic acid.

4.3 QUANTIFICATION OF RUTIN AND RUTIN ESTER (RUTIN LAURATE)

Calibration of rutin standard was prepared in order to quantify the residual rutin concentration following the esterification reaction (Fig. 4.8). For rutin laurate, standard calibration was prepared using the purified sample (Fig. 4.9).

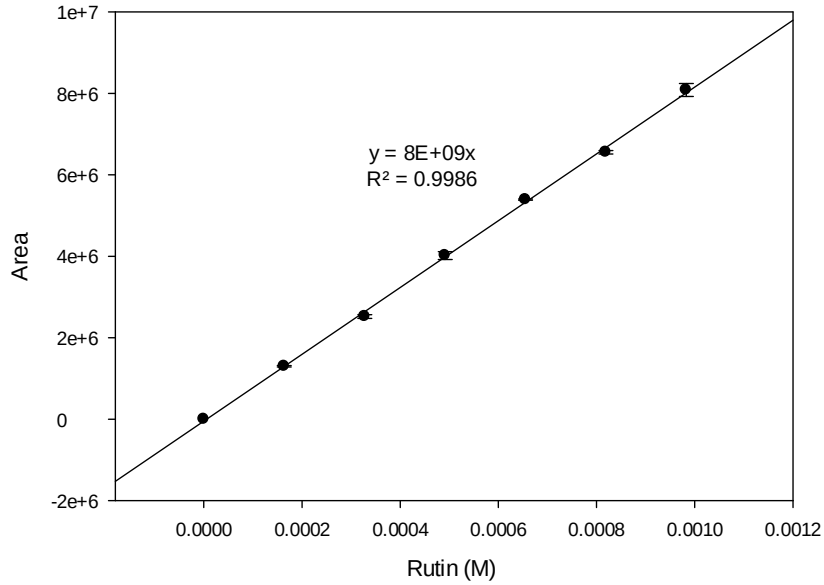

Figure 4.8 Standard calibration of rutin.

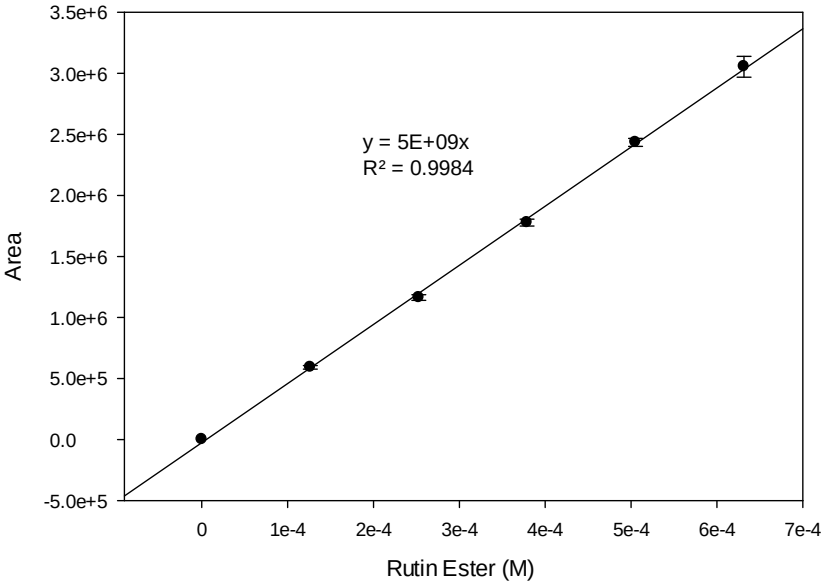

Figure 4.9 Standard calibration of rutin laurate.

4.4 RUTIN LAURATE PROFILE

Among the three aliphatic fatty acid tested (C12–C16), the acylation of rutin with lauric acid was selected as a model reaction. The progress of esterification reaction was followed as it is of particular interest to determine equilibrium time of the reaction. Filtered rutin at 5 x 10^{-3} M and lauric acid at 0.25 M lauric acid were used as reactants. Reaction was carried out in 15 mL dried acetone at 55 ºC, 200 rpm and was started by the addition of 0.15 g lipase. Samples were taken regularly for 168 h.

Acetone was chosen as a reaction medium due to its low toxicity (Kontogianni *et al.*, 2003). However, the solubility of rutin in this solvent proved to be rather low. In this study, insoluble rutin was filtered after its dissolution in acetone and its actual concentration in acetone was measured using HPLC prior to use in esterification reaction. Acetone was also dried with molecular sieves 4 Å in order to lower the presence of water molecules in the solvent prior to dissolution of rutin.

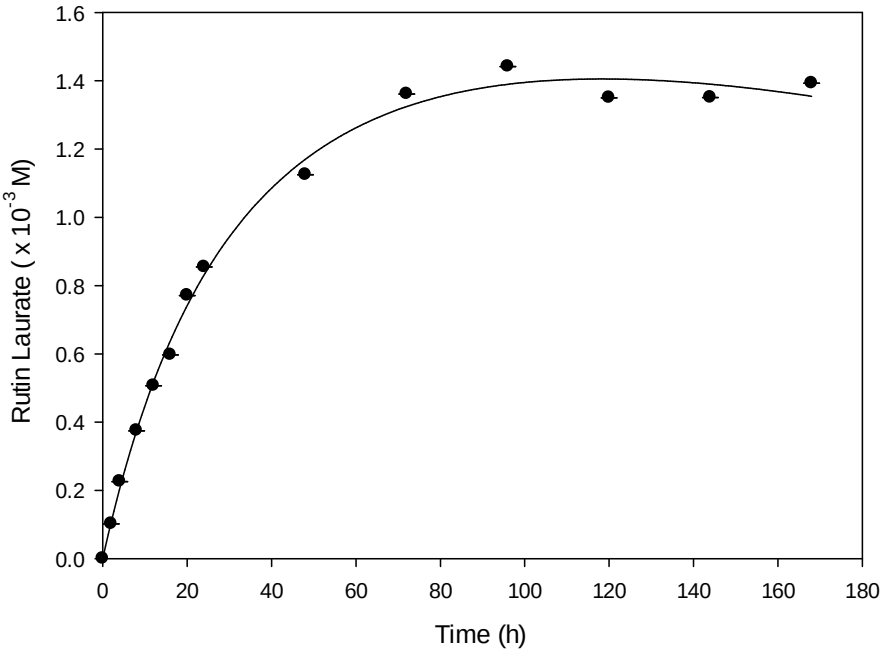

Figure 4.10 Rutin laurate formation (M) as a function of time (h).

A hyperbolic curve was obtained when synthesized rutin laurate concentration was plotted against incubation time (Fig. 4.10). It can be observed that formation of rutin laurate increased with time. However, above 96 h of reaction no change in rutin laurate concentration was observed which could probably due to water accumulation in the reaction. Lipase-catalyzed esterification of flavonoid esters generally take few days to reach equilibrium (Riva *et al.*, 1996; Kontogianni *et al.*, 2001; Ishihara *et al.*, 2002; Kontogianni *et al.*, 2003; Ardhaoui *et al.*, 2004b; Mellou *et al.*, 2005; Katsoura *et al.*, 2006; Mellou *et al.*, 2006). The water molecules present in the medium originates either from the different components of the reaction medium or from the ester synthesis itself where 1 mol of water is produced per mol of ester synthesized.

4.5 SCREENING OF SELECTED OPERATING VARIABLES USING FULL FACTORIAL DESIGN (FFD)

The effects of selected operating variables namely lauric acid concentration (M), temperature (ºC) and enzyme loading (g) were screened using full factorial design (FFD). A total 27 number of runs were generated and the concentration of rutin laurate was taken at 96 h of reaction. Responses for operating variables screening experiments were shown in Table 4.2.

Table 4.2 Responses of FFD experiment on the screening of selected esterification operating variables.

Runs	Lauric acid (M)	Enzyme loading (g)	Temperature (ºC)	Rutin laurate (µM)
1	0.05	0.03	55	4.97
2	0.05	0.05	55	7.02
3	0.15	0.04	45	11.62
4	0.25	0.03	35	3.16
5	0.25	0.05	55	12.06
6	0.15	0.04	45	11.35
7	0.05	0.03	35	2.11
8	0.05	0.03	35	2.08
9	0.25	0.03	55	10.12
10	0.25	0.03	55	9.61
11	0.05	0.05	55	7.11
12	0.25	0.05	35	7.56
13	0.25	0.03	35	3.01
14	0.25	0.03	35	3.13
15	0.25	0.05	35	7.80
16	0.05	0.05	35	5.61
17	0.05	0.05	35	5.41
18	0.25	0.03	55	9.89
19	0.05	0.03	55	4.83
20	0.25	0.05	35	7.61
21	0.15	0.04	45	11.30
22	0.05	0.05	35	5.63
23	0.05	0.03	55	4.66
24	0.25	0.05	55	12.16
25	0.05	0.03	35	2.19
26	0.05	0.05	55	6.73
27	0.25	0.05	55	12.12

The highest rutin laurate formation was observed when the concentration of lauric acid, enzyme loading and temperature were set at 0.25 M, 0.05 g and 55 ºC respectively. Conversely, lowest rutin laurate concentration were obtained at the lowest level of each variable combination.

4.5.1 Analysis of FFD Experiments on Screening of Selected Operating Variables

Factorial analysis using analysis of variance (ANOVA) using full order model terms (main-, 2-way and 3-way effects) was performed. The ANOVA analysis was carried out using Minitab® 15 software (Table 4.3).

Table 4.3 ANOVA analysis for the effects of lauric acid concentration, temperature and enzyme on rutin laurate formation

Factor	***DoF***	***Adj SS*** **(x 10^{-7})**	***Adj MS*** **(x 10^{-7})**	***F***	***P***
Main factor	3	21.2	7.1	3112.43	0.000
Lauric acid		6.6	6.6	2929.40	0.000
Enzyme		5.7	5.7	2523.37	0.000
Temperature		8.8	8.8	3884.53	0.000
2-way interactions	3	2.5	0.8	360.75	0.000
Lauric acid*Enzyme		0.1	0.1	25.56	0.000
Lauric acid*Temperature		1.9	1.9	841.36	0.000
Enzyme*Temperature		0.5	0.5	215.33	0.000
3-way interactions	1	0.000	0.000	17.41	0.001
Lauric acid*Enzyme*Temperature		0.000	0.000	17.41	0.001
Residual Error	18	0.000	0.000		
Total	26	6.6	6.6		

DoF: Degrees of freedom; *Adj SS*: Adjusted sum of squares; *Adj MS*: Adjusted mean of squares; *F*: F-statistic; *P*: P-statistic.

The full order term model showed good correlation with R^2- and R^2- *adjusted* value of 0.9986 and 0.9980 respectively. The effect of lauric acid concentration, enzyme and temperature and their interaction effect (Lauric acid*Enzyme, Lauric acid*Temperature, Enzyme*Temperature) were significant in all cases ($P < 0.05$). The single effect of full interaction (Lauric acid*Enzyme*Temperature) was also significant as the main effects were significant. The *F*-value for the factors studied showed temperature ($F = 3884.52$) has the strongest influence on the response followed by lauric acid concentration ($F = 2929.40$) and enzyme loading ($F = 2523.37$). Furthermore, based on the normal plot of standardized effect graph (Fig. 4.11), all selected variables were found to be significant towards the reaction.

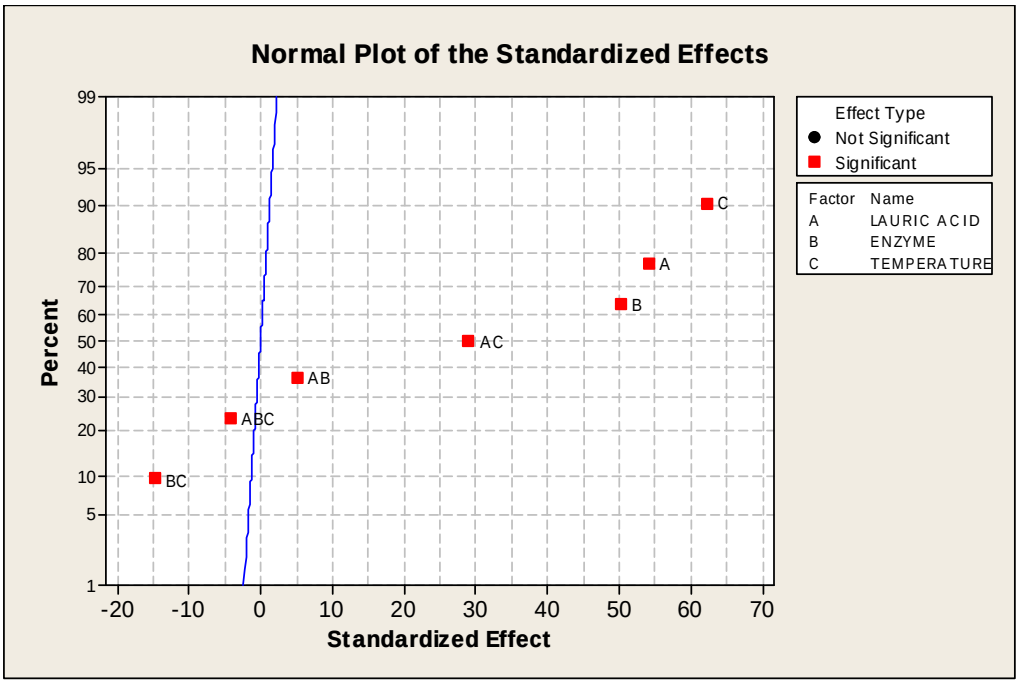

Figure 4.11 Normal plot of the standardized effects of lauric acid concentration, temperature and enzyme loading on rutin laurate yield.

4.5.2 Residual Analysis of FFD Experiments on Screening of Selected Operating Variables

In order to evaluate the fitted model, the residual analysis was performed with standardized residual (Fig. 4.12). Residual values are derived from experimental values deducted by the model fitted values (Residuals = Experimental values – Model fitted values).

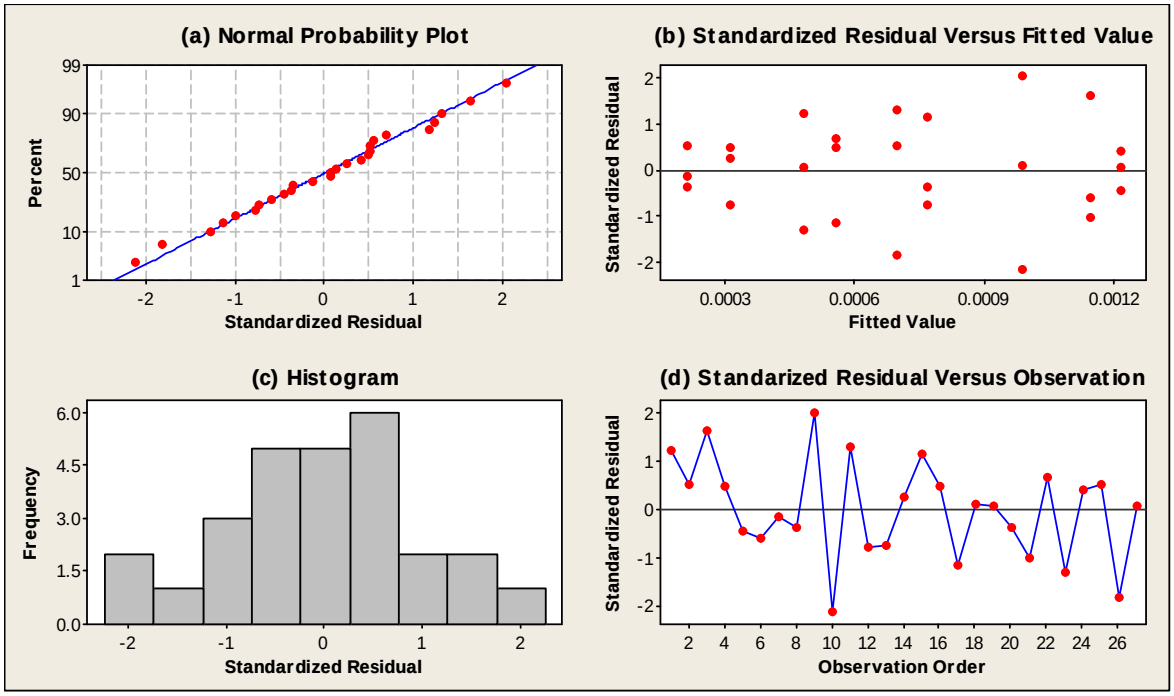

Figure 4.12 Residual plots of FFD model for the effect of lauric acid concentration, temperature and enzyme loading on rutin laurate yield.

The normal probability plot of residuals (Fig. 4.12 a) showed that the residuals were normally distributed as all standardized residuals fell on the straight line. By observing the residuals against fitted (predicted) value graph (Fig. 4.12 b), a random pattern of residuals on both sides of standardized zero line indicated the absence of systematic errors in the experiment (± 2). This normal probability assumption was supported by the approximate bell-shape curve of the histogram (Fig. 4.12 c). This indicates that the error generated from the experimental data collected were largely due to random error. The order of collecting data has no influence on the data collected as

shown by the lack of strong pattern in standardized residuals versus the observation order graph (Fig. 4.12 d). Moreover, based on Anderson-Darling (*AD*) analysis for violation of normality assumption, the *AD* value was insignificant 0.552 (P = 0.141). Overall, it can be concluded that the pattern of residual data were approximately normally distributed and thus the data obtained were less likely influenced by non-random and systematic errors.

4.5.3 Main Effect Plot of FFD Experiments on Screening of Selected Operating Variables

The response for main effect plots was based on mean of observed rutin laurate formation for each factor level. The slope in main effect plot can be used to determine the magnitude of response change with respect to variable change (Fig. 4.13). The steeper the line indicates the stronger effect of the variable on the experiment. However, the differences in the relative steepness of the slope for lauric acid concentration, temperature and enzyme were not pronounced and mean response showed comparable rate of change

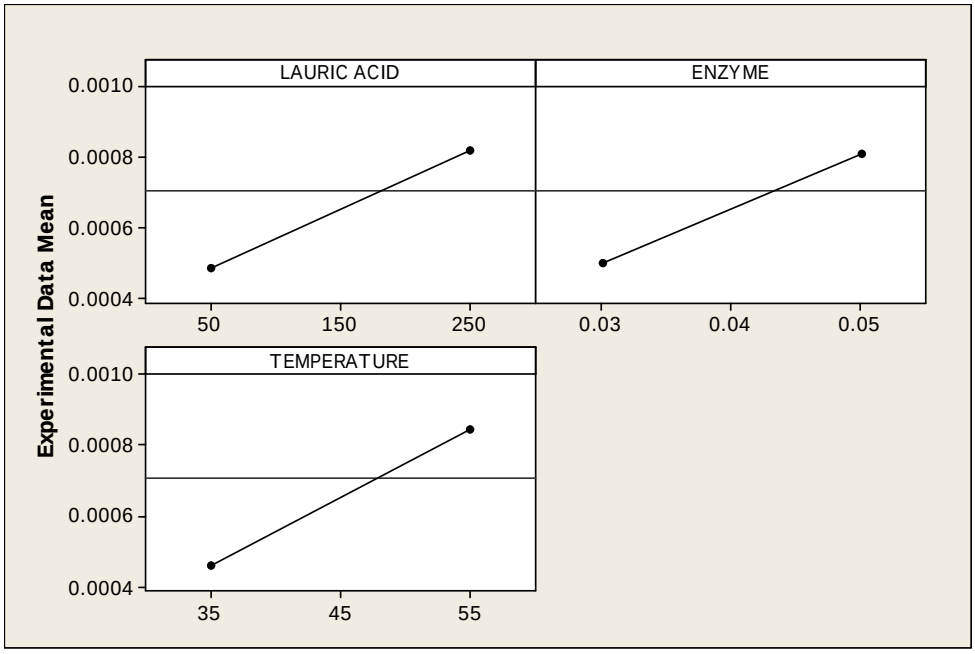

Figure 4.13 Main effect plot of FFD experiments on the effects of lauric acid concentration, temperature and enzyme towards rutin laurate yield.

(slope) with respect to variable change. Thus, it was suggested that all variables *viz.* lauric acid concentration, temperature and enzyme exerted almost similar influence on the esterification process.

4.6 EFFECTS OF SELECTED PARAMETERS ON RUTIN LAURATE SYNTHESIS

4.6.1 Effects of temperature on esterification of rutin

Temperature is an important factor in enzymatic synthesis. Temperature affects the viscosity of the medium, the activation energy and the thermal denaturation of the enzyme and the solubility of substrates and products (Chebil *et al.,* 2006; Stergiou *et al.*, 2013). Based on the FFD experiment, temperature had the strongest effect on the reaction (Section 4.5.1). With increasing temperature, the solubility of the flavonoid and flavonoid ester increased and therefore significant increase of rutin laurate was observed at the elevated temperatures. The temperature effect on the conversion yield has been reported for the enzymatic acylation of sugars and glycosides in conventional organic media (Enaud *et al.,* 2004; Šabeder *et al.,* 2006; Yu *et al.,* 2008; Viskupicova *et al.,* 2010). To date, flavonoid transformation has been carried out in the temperature range of 30 to 100°C (Nakajima *et al.*, 1999; Ishihara *et al.*, 2002; Gayot *et al.*, 2003; Kontogianni *et al.*, 2003; Passicos *et al.*, 2004; Katsoura *et al.*, 2006; Lue *et al.*, 2010)

Moreover, the choice of temperature depends on the enzyme and solvent used. In this study, the maximum reaction temperature limit is dictated by the boiling point of the acetone i.e. 56 ºC. Acetone was selected as a medium for the acylation of rutin and fatty acid due to its relatively low cost, low toxicity and inert towards the biocatalyst. Besides, its polarity facilitates the solubilization of flavonoid glycoside (acyl acceptor) thus allowing for high conversion yield. Kontogianni *et al.* (2001) and Mellou *et al.* (2005)

compared different solvents and reported that the highest conversion of rutin and naringin was observed in the presence of acetone at 45 ºC and 50 ºC respectively.

Temperature also affects the stability of the biocatalyst. However, CAL-B demonstrated a high thermostability which could be attributed to its immobilization on resin. Lower temperatures resulted in poor conversion levels because of the low enzyme activities (Table 4.1).

4.6.2 Effects of lauric acid (acyl donor) concentration on rutin laurate synthesis.

The ideal acyl donor should be inexpensive, fast acylating, and completely non-reactive in the absence of the enzyme. One way to move esterification equilibrium towards synthesis is to work with a large excess of one substrate which could also function as a solvent for the second substrate (melting media). It was observed that rutin laurate formation increased with increasing lauric acid from 0.05 to 0.25 M. The excess of the fatty acid in the medium increases rutin conversion and thus, the final rutin laurate concentration. This observation could be explained by the fact that an excess of substrate shifts the equilibrium in favor of flavonoid esters synthesis rather than their hydrolysis. Similar observations were also reported in the literature. Kontogianni *et al.* (2001) and Mellou *et al.* (2005) tested the effects of the fatty acid and the vinyl ester concentrations respectively in the presence of CAL-B. They observed that concentration of the acyl donor affected both the initial rate and the conversion yield of flavonoids to their esters.

In the case of solvent-free system where the reaction mixture composed solely of the substrates (Hari Krishna & Karanth, 2002), Kontogianni *et al.* (2001) reported that the conversion yields of naringin and rutin decreased when fatty acids were used both as an acyl donor and a solvent. In spite of its attractiveness, the use of melting media is

characterized by a serious drawback due to the necessity of the elimination of the excess of the acyl donor for the recovery of the synthesized products.

4.6.3 Effects of amount of enzyme on synthesis of rutin laurate

Because of the high cost of lipase, experiment was conducted to determine the minimum amount of lipase that maximizes the amount of rutin laurate synthesized during the reaction. In this case, 10 g L^{-1} (0.05 g in 5 mL) was chosen for the highest lipase concentration. Kontogianni *et al.* (2003) observed that the variation of lipase CAL-B concentration during the acylation of naringin flavonoid in the presence of decanoic acid as an acyl donor and *tert*-butanol as a solvent, led to an increase of the conversion yield. However, a plateau was reached when lipase concentrations were higher than 15 g L^{-1} which may be due to the increase in the water byproduct. Its excessive production results in a reversible reaction. Furthermore, high loading of biocatalyst decreased the conversion yield due to the mass transfer limitation in the media following altered reaction mixture viscosity. They reported the highest value of the conversion yield was about 40 % after 240 h of incubation at maximum lipase loading (15 g L^{-1}).

In this study, the highest conversion (55 %) was obtained when the enzyme concentration was 10 g L^{-1} at 55ºC. Comparable conversion has been reported by Nakajima *et al.* (1999) and Viskupicova *et al.* (2010) for the synthesis of rutin esters using 10 g L^{-1} of CAL-B in acetone and 2-methylbutan-2-ol respectively. High loading of biocatalyst also increase the possibilities for both agglomeration of solids and precipitation of the intermediate monoesters in locations that may render the immobilized enzyme less accessible (Acros *et al.*, 2001; Šabeder *et al.*, 2006). Therefore all further investigation in this study were done at this biocatalyst concentration (10 g L^{-1}).

4.7 KINETICS PARAMETERS OF RUTIN ESTERIFICATION

In order to investigate the kinetic and thermodynamic of lipase-catalyzed synthesis of rutin laurate, the range of operating variables used were selected based on the previous screening results. Based on the ANOVA (Section 4.5.1), the effects of lauric acid, temperature and enzyme were significant. Since temperature has the strongest influence on the response, the temperature range was expanded from 20 to 55 ºC (293 to 328 K). Rutin and lauric acid concentrations ranges were expanded from 0.003 to 0.012 M and 0.5 to 0.55 M respectively in order to better understand the esterification kinetic and to obtain higher product yield and concentration. The enzyme loading fixed at the maximum amount used in the screening experiment i.e. 10 g L^{-1}.

4.7.1 Initial Rate of Rutin Esterification

In order to determine the initial rate of esterification, the amounts of organic solvent (acetone), and enzyme were held constant whereas various fixed initial quantities of rutin were reacted with different initial concentrations of lauric acid. To counterbalance low probability of successful reaction due to low solubility of rutin, lauric acid was provided in the excess of 10-110 to rutin (mole:mole) so that high initial rate of esterification and yield of rutin laurate could be achieved. Fig. 4.14 showed the regression plot of apparent rutin laurate formation (M) as a function of time (h) performed at various lauric acid and rutin concentration (M).

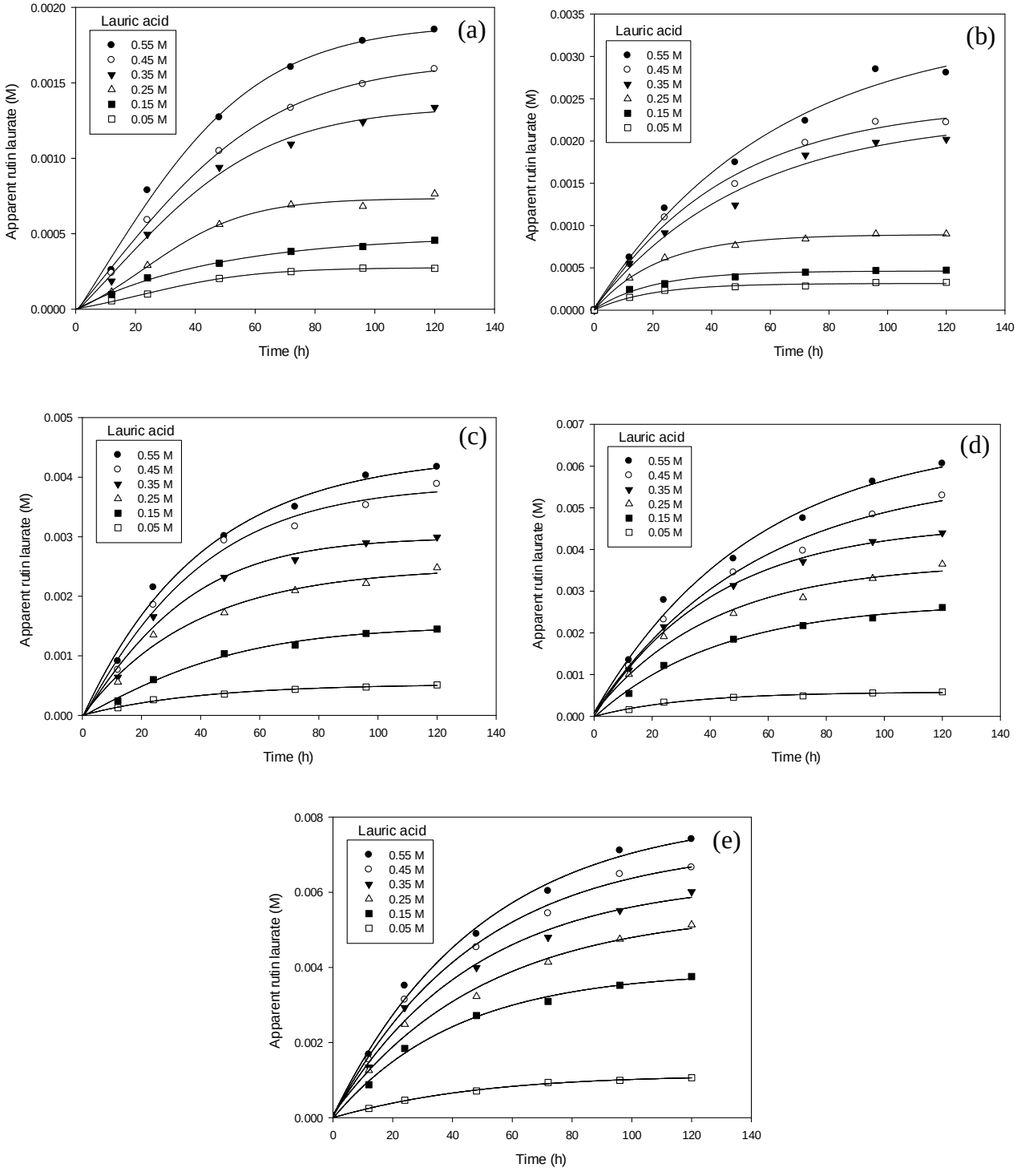

Figure 4.14 Regression plot of apparent rutin laurate formation (M) as a function of time (h) performed at various rutin concentration (M) (a) 0.003 M (b) 0.005 M (c) 0.007 M (d) 0.010 M (e) 0.012 M Reaction conditions: enzyme 0.15 g; 55 °C (328 K) and 200 rpm *(Standard deviation of the triplicate measurements was <5 %).*

From the initial slope of each graph, initial of esterification was calculated using Eq. (3.3). Based on Fig. 4.15, increasing the substrates concentration (i.e rutin and lauric acid) lead to a rapid increase in the initial rates of the reaction and the esterification product (rutin laurate). Assuming the mass transfer limitations of immobilized catalyst (CAL-B) was negligible based on reported studies (Hari Krishna & Karanth, 2001; Romero *et al.*, 2007; Mahmud *et al.*, 2009), the effect of these substrates and enzyme were in accordance to Michaelis-Menten kinetics in a homogenous, single-phase solution (Doran, 1995).

The higher the concentration of both substrates present in the reaction medium, the higher concentration of rutin laurate obtained. This is simply explained by the high availability of substrate to be transformed. Moreover, these results were in agreement with other studies concerning the optimal molar ratio of flavonoid/acyl donor in order to achieve the highest possible yield (Ishihara *et al.*, 2002; Gayot *et al.*, 2003; Kontogianni *et al.*, 2003; Mellou *et al.*, 2006). The maximum initial rate of 1.52×10^{-4} M h^{-1} was achieved at 0.55 M of lauric acid and 0.012 M of rutin (Fig. 4.15).

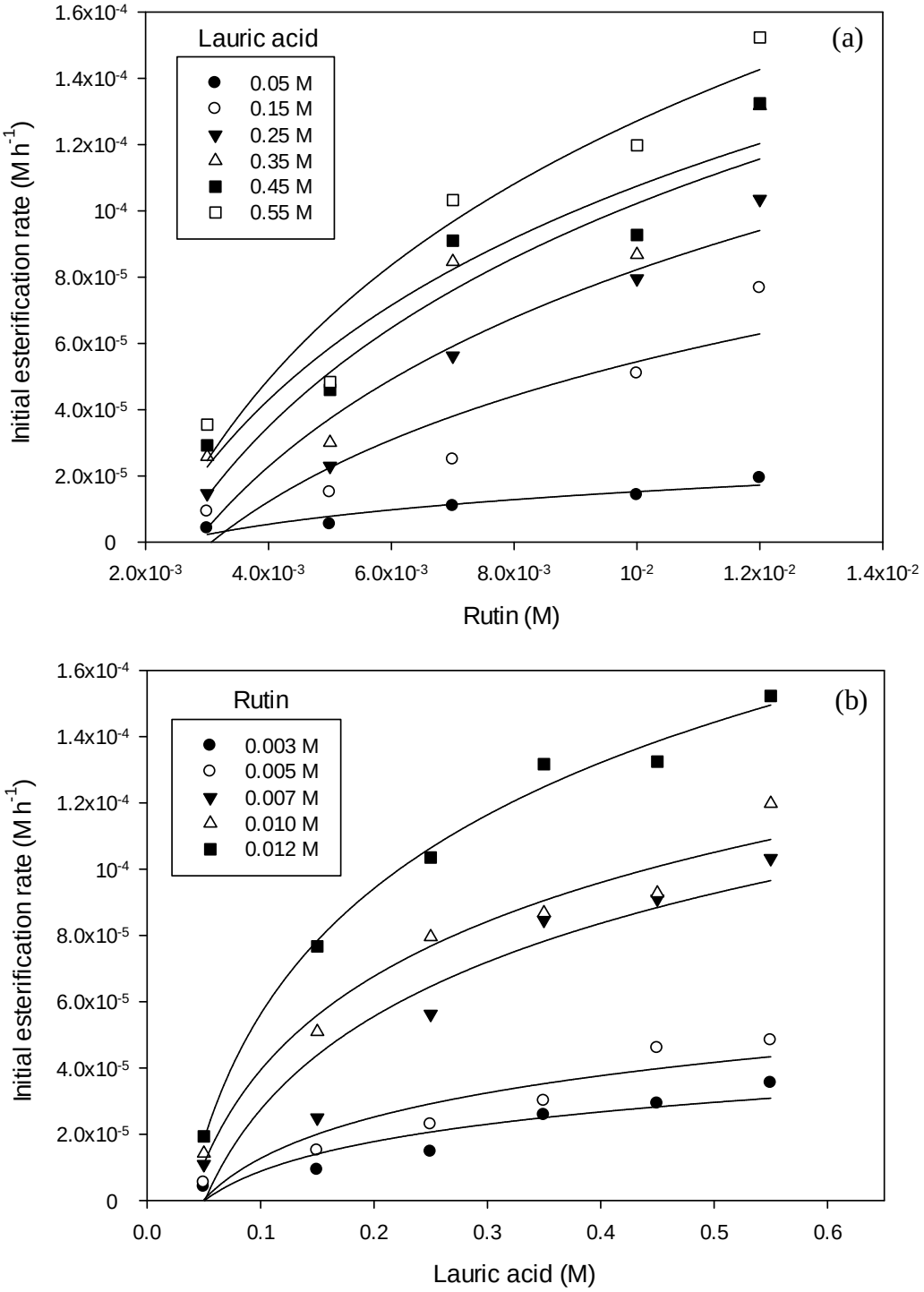

Figure 4.15 (a) Initial esterification rate as a function of rutin concentrations at varying concentrations of lauric acid performed at 55 ºC (328 K), 0.15 g enzyme and 200 ppm. (b) Initial esterification rate as a function of lauric acid concentrations at varying concentrations of rutin performed at 55 ºC (328 K), 0.15 g enzyme and 200 ppm. *(Standard deviation of the triplicate measurements was <5 %).*

4.7.2 Kinetic Model

In order to verify the mechanism of the present reaction, double-reciprocal plot was applied in this work. Reciprocal initial reaction rates (v^{-1}) were plotted versus the inverse lauric acid (s^{-1}) for several initial rutin concentrations and *vice versa*. As shown in Fig. 4.16, the lines in the double-reciprocal plot verify that the reaction followed a Ping-Pong Bi–Bi mechanism. A similar mechanism has been also proposed for lipase-catalyzed esterification in other reactions as reported elsewhere in the literature (Stamatis *et al.*, 1993; Zaidi *et al.*, 2002; Chowdary & Prapulla, 2005; Prlainović *et al.*, 2010).

In addition, there was no inhibition exerted by both substrates as no upward curvature found in both plots (Fig. 4.16). The present study appears to be different from the other reported esterification kinetics by lipase, which indicate inhibition at high concentration of substrate (Hari Krishna & Karanth, 2001; Chowdary & Prapulla, 2005; Romero *et al.*, 2007). These reports, however, have considered alcohols and medium- or long chain carboxylic acids. To date, the only kinetics data available on flavonoid ester is in esterification of prunin 6”-*O*-laurate (Céliz *et al.*, 2012). Similar to this finding, the authors indicated there were no inhibition patterns found for both substrates (i.e prunin and vinyl laurate) even at high concentration of vinyl laurate (4000 mM) used in the reaction.

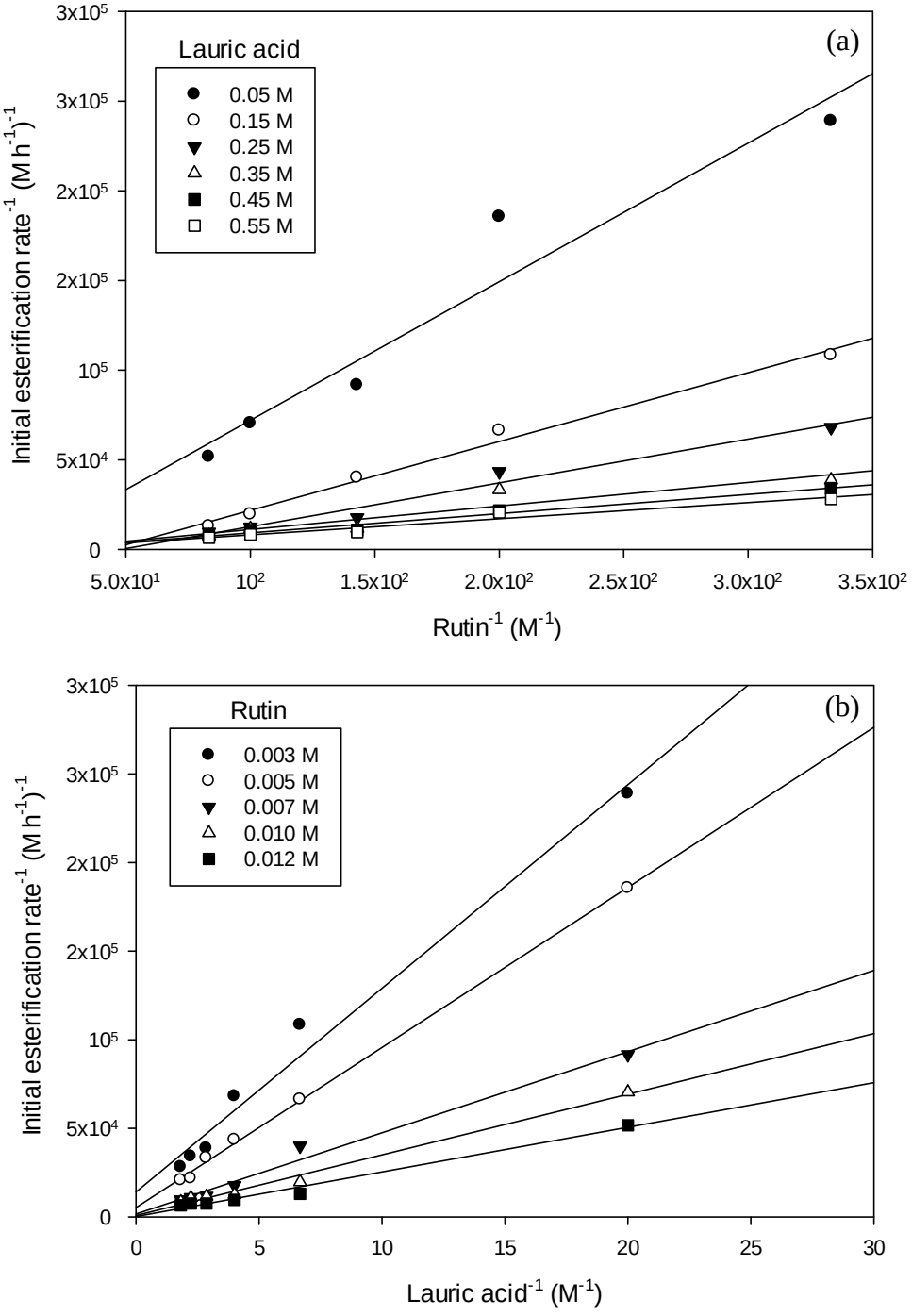

Figure 4.16 (a) Double-reciprocal plot of rutin concentrations against initial reaction rates at fixed lauric acid concentrations. Reaction conditions: enzyme 0.15 g; 55 °C (328 K) and 200 rpm. (b) Double-reciprocal plot of lauric acid concentrations against initial reaction rates at fixed rutin concentrations. Reaction conditions: enzyme, 0.15 g; 55 °C (328 K) and 200 rpm.

In this reaction mechanism (Fig. 4.18), lauric acid (acyl donor) first binds to the hydroxyl group of serine in active site of lipase by a nucleophilic attack forming an enzyme–lauric acid complex. The enzyme–lauric acid complex is then transformed to enzyme–acyl intermediate with the concomitant release of the first product, water. This is followed by an attack of the second substrate, rutin on this intermediate to form enzyme–acyl-rutin complex. Later this complex dissociated into rutin laurate, while the enzyme returns to its initial catalytic state ready for the next cycle of catalysis.

The reaction also can be presented using Cleland's schematics;

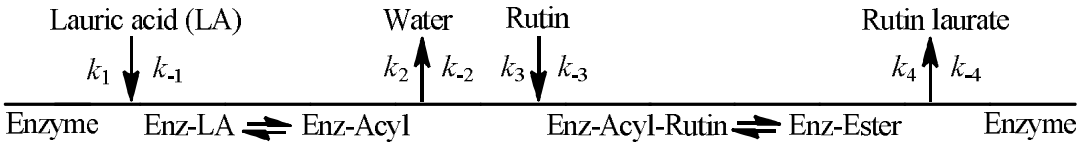

Figure 4.17 Cleland's schematic on rutin laurate synthesis

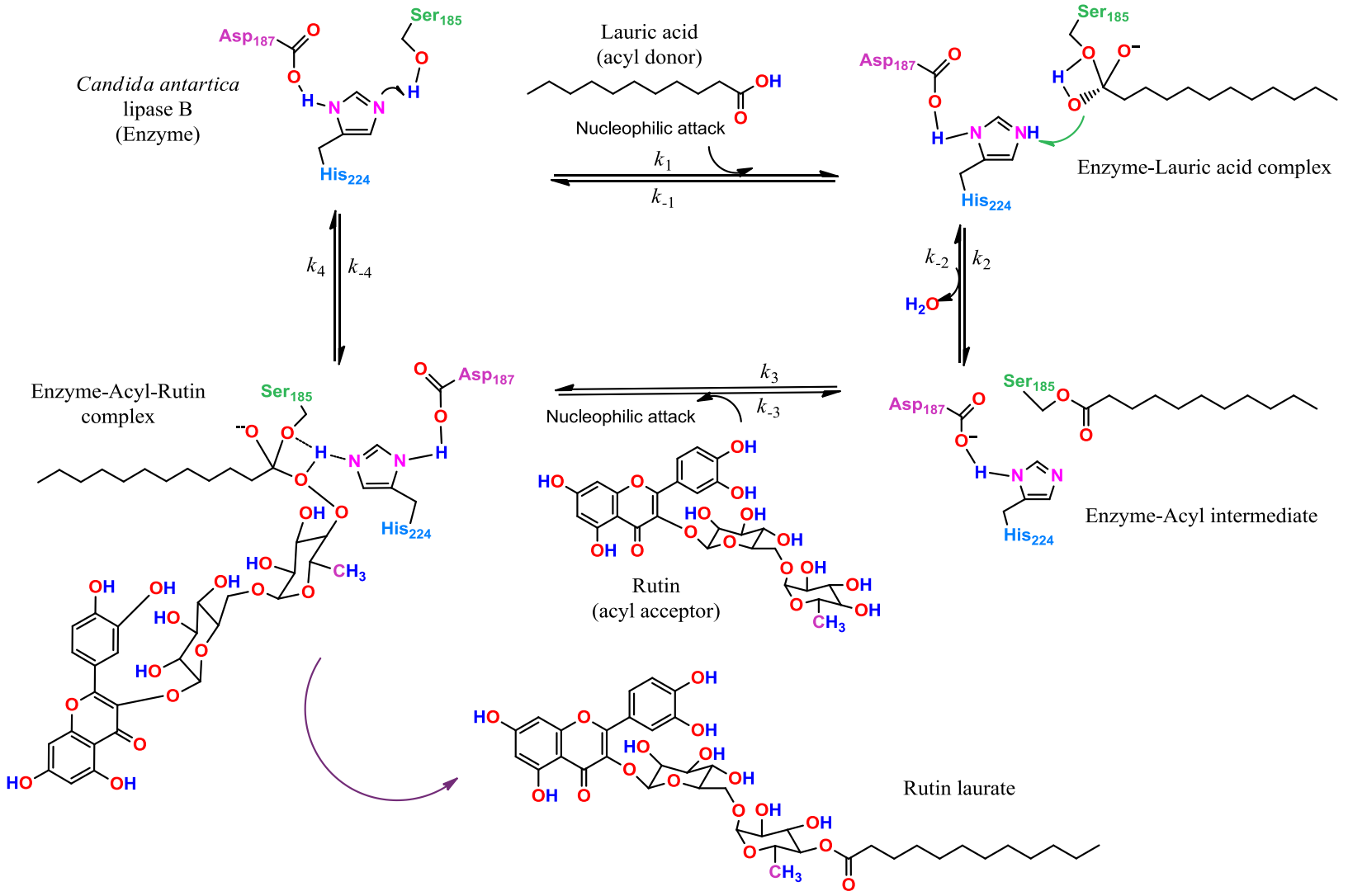

Figure 4.18 Schematic representation of lipase-catalyzed esterification of rutin and lauric acid by Ping-Pong Bi-Bi mechanism.

Since the reaction agreed with a Ping-Pong Bi–Bi mechanism with no substrate inhibition, the kinetic parameters of Eq. (3.4) were calculated using multiple regressions fitting of the experimental values. The final kinetic equation that best fitted the enzymatic synthesis of rutin laurate using rutin and lauric acid is as follows:

$$v = \frac{7.49 \times 10^{-4}[\mathrm{LA}][\mathrm{F}]}{0.044\,[\mathrm{LA}] + 0.99[\mathrm{F}] + [\mathrm{LA}][\mathrm{F}]} \qquad (4.1)$$

where V_{max} = 7.45 x 10^{-4} (M h^{-1}),, K_m^R = 0.044 M and K_m^{LA} = 0.99 M. The verification experimental data fitted with Eq. (4.1) is shown in Fig. 4.19. It was found that the experimental initial rates agreed very well with the calculated value, obtaining the R^2 value of 0.99, which showed that the kinetic model fitted well the experimental data. Based on the kinetic parameters determined, it is clearly shown that the affinity of the enzyme towards rutin flavonoid was higher than lauric acid, since K_m^R was lower than K_m^{LA}.

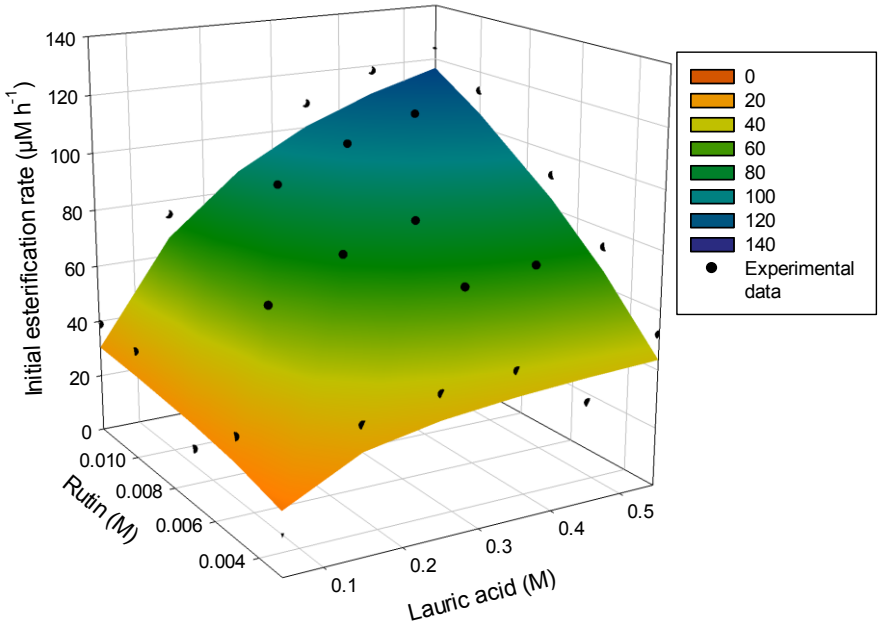

Figure 4.19 Illustration of the proposed Ping-Pong Bi-Bi model.

Moreover, the reaction also was carried out at various temperature ranging from 293 to 328 K at fixed rutin concentration *viz.* 5 x 10^{-3} M (Fig. 4.20). Initial rate of was determined from the polynomial regression plot of apparent product concentration as a function of time for each temperature tested. A tangent was drawn from the origin on the polynomial regression.

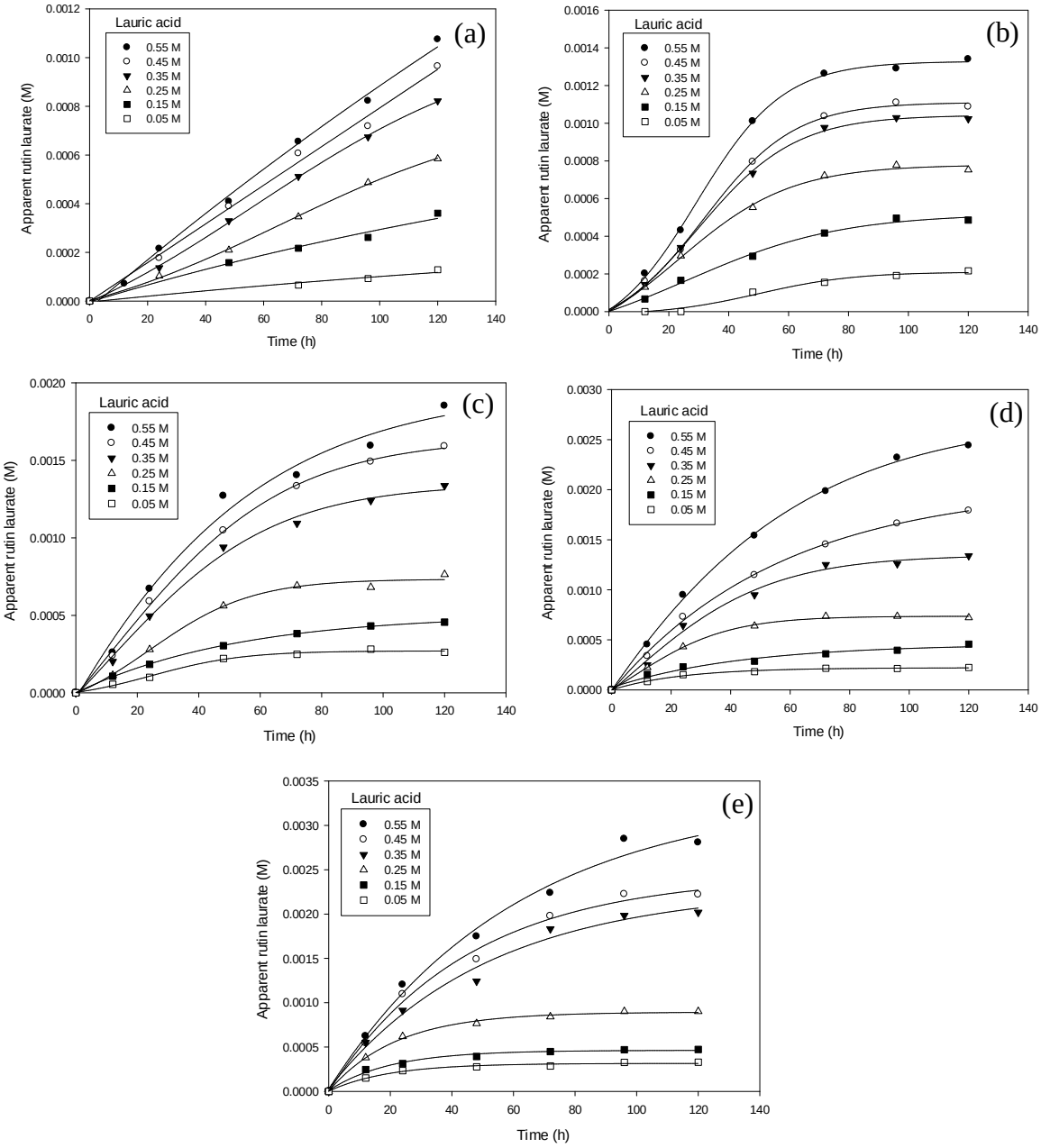

Figure 4.20 Regression plot of apparent rutin laurate formation (M) as a function of time performed at various temperature (h) (a) 293 K (b) 303 K (c) 313 K (d) 318 K (e) 328 K. Reaction conditions: rutin, 0.005 M; enzyme, 0.15 g; and 200 rpm *(Standard deviation of the triplicate measurements was <5 %).*

As can be seen in Fig. 4.20, the highest rutin laurate concentration (3 x 10^{-3} M) was achieved at the highest concentration at lauric acid (55 x 10^{-2} M) and temperature (323 K). No formation of product was observed at any temperature in control experiments (data not shown). In addition, initial rate of esterification is directly proportional to the lauric acid concentration (0.05 to 0.55 M) at any given temperature (293 to 328 K) (Fig. 4.21).The magnitude of product formation also increased with the increasing of temperature. This could be explained by the fact that, besides improving the wriggling motions of enzyme molecules at higher temperature, substrates diffuse faster and increase the chances of their successful binding to the active site of the enzyme.

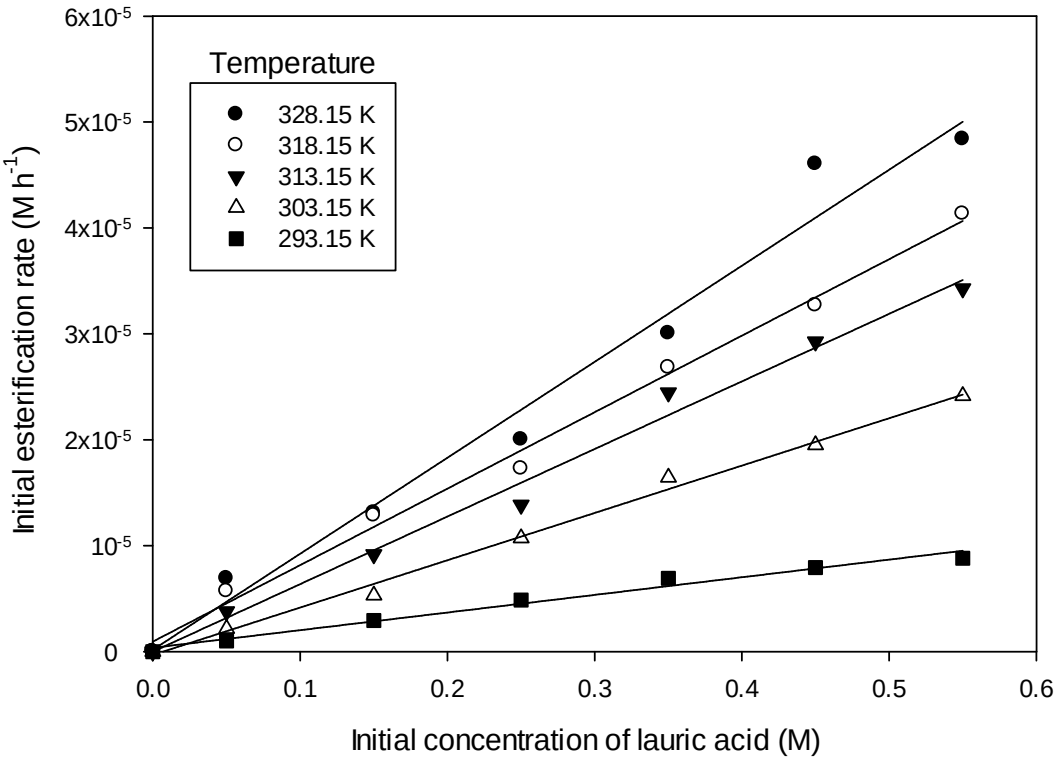

Figure 4.21 Volumetric rate of esterification (M h^{-1}) as a function of initial concentration of lauric acid (M) performed at various temperatures. Reaction conditions: rutin, 0.005 M; enzyme, 0.15 g; and 200 rpm *(Standard deviation of the triplicate measurements was <5 %).*

The evolution with time of substrates and rutin laurate concentrations at 5 x 10^{-3} M rutin, 55 x 10^{-2} M lauric acid and at a fixed temperature of 55ºC (328 K) is shown in Fig. 4.22. Reduction in rutin concentration was high during the first 12 h and gradually decreased until negligible change in its concentration was observed. Similarly, after the rapid increase of conversion during the first 24 h of the reaction (44 %), a nominal increase in the rate of conversion could be observed between 48 and 120 h of reaction. Rutin laurate concentration continued to increase up to 96 h, which then remained unchanged as the reaction reached its equilibrium state. It has been observed that at higher lauric acid concentrations there was a progressive decrease in rutin concentration, which gradually approached plateau with increasing reaction time (Fig. 4.23). This pattern representative for all reaction temperatures tested.

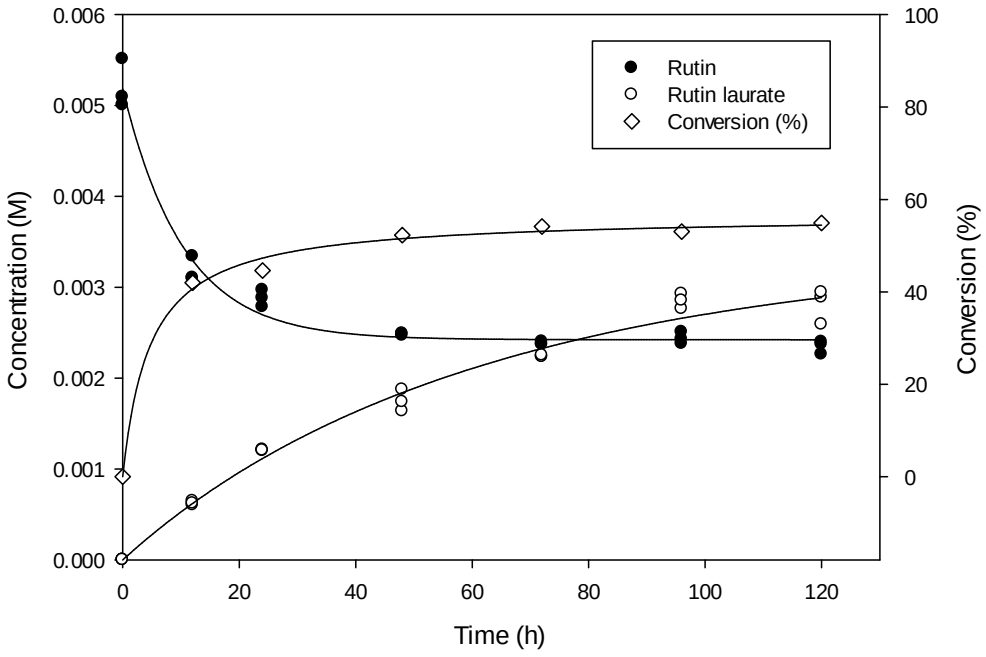

Figure 4.22 Evolution of substrate, rutin and product, rutin laurate and conversion yield (%). Reaction conditions: rutin, 0.005 M; enzyme, 0.15 g; 55 °C (328 K) and 200 rpm *(Standard deviation of the triplicate measurements was <5 %).*

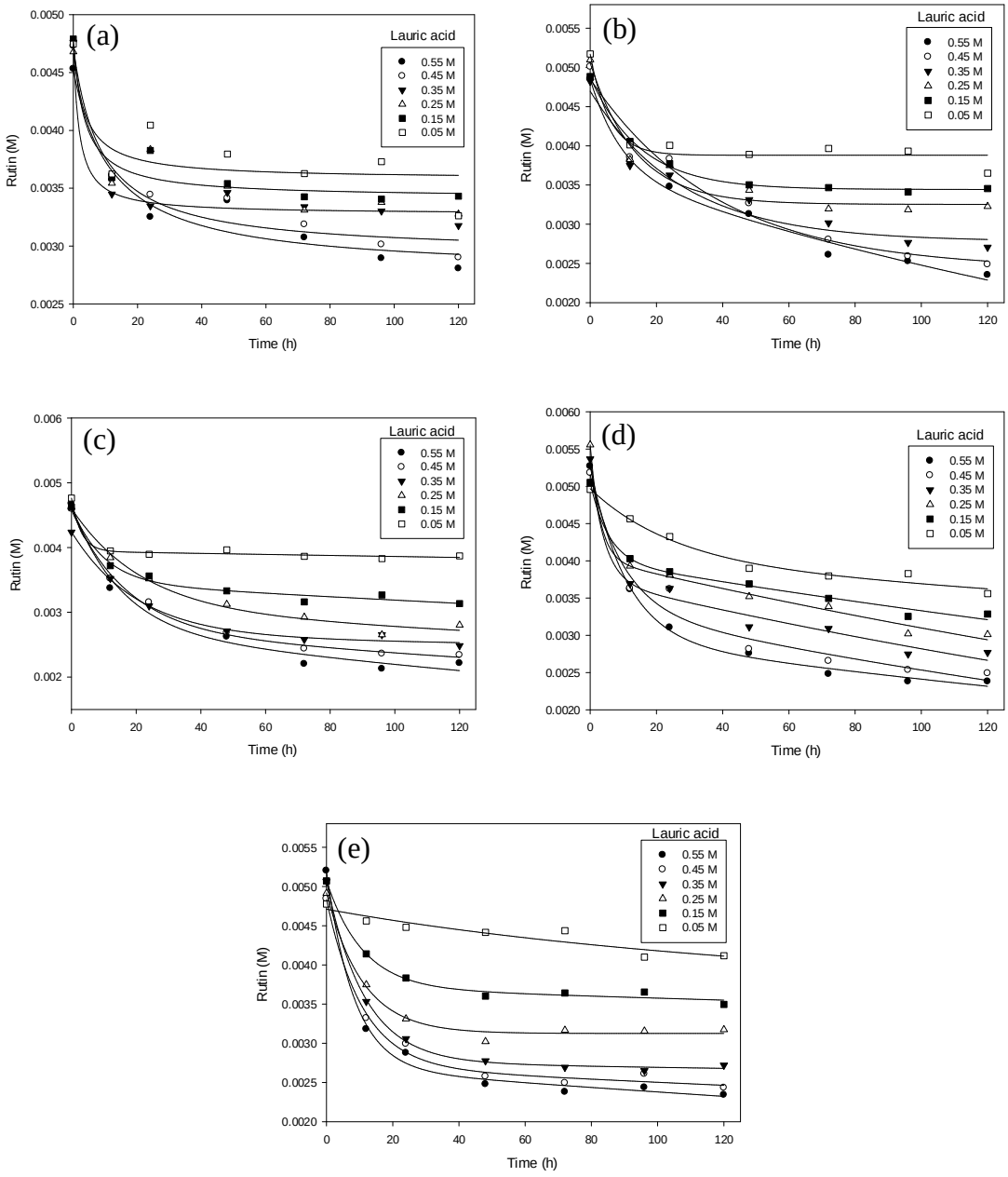

Figure 4.23 Regression plot of rutin concentration reduction (M) as a function of time (h) and lauric acid concentrations (M) performed at various temperatures (a) 293 K (b) 303 K (c) 313 K (d) 318 K (e) 328 K. Reaction conditions: rutin, 0.005 M; enzyme, 0.15 g; and 200 rpm *(Standard deviation of the triplicate measurements was <5 %).*

The maximum conversion of the rutin was about 56 % at the highest temperature tested (Table 4.4). At 328 K, further increase in rutin concentration (0.007 to 0.012 M) did not change the conversion yield. This could be due to the accumulation of water byproduct within the milieu as the reaction progresses thus unfavorable for a high yield conversion. An excess amount of water present in the solvent will drive the reaction backwards where the rutin laurate will be hydrolyzed back into its components.

Table 4.4 Percentage of conversion yield at various temperatures.

Concentration of lauric acid ($\times 10^{-2}$ M)	**Percentage of conversion yield (%) at equilibrium at different temperatures (K)**				
	293	**303**	**313**	**318**	**328**
5	21	24	20	23	20
15	28	30	30	37	27
25	28	37	43	46	47
35	30	43	47	48	49
45	36	48	49	51	52
55	36	49	55	54	56

Standard deviation of the triplicate measurements was <5 %

The maximum conversion yield was lower from the other reported rutin esterification. Other reported conversion were 20 to 30 % for acylated rutin with aliphatic fatty acid (Kontogianni *et al.*, 2001; Kontogianni *et al.*, 2003), 68 to 80 % for acylated rutin with unsaturated fatty acid (Mellou *et al.*, 2006), 70 to 77 % for acylated rutin with lauric acid and palmitic acid (Lue *et al.*, 2010) and more than 50 % reached when short and medium chain fatty acids (C4–C12) were reacted with rutin (Viskupicova *et al.*, 2010). The difference in conversion yields could be attributed to the presence of molecular sieve in the current reaction.

Molecular sieves 4 Å is the most commonly desiccant used in the esterification reaction. However, it was not included in this reaction mixture as it has strong affinity to adsorb rutin molecules resulting in less rutin available for esterification. From Table 4.5, the molecular sieves 4 Å absorption of rutin increased with an increase in rutin concentration. After the addition of molecular sieves, a two-fold reduction of the rutin concentrations was observed. Application of molecular sieves to remove water byproduct in esterification reaction should be reconsidered due to this reason. In addition, it is also impractical since the regeneration of the desiccant is an energy-intensive process.

Table 4.5 The effect of molecular sieve 4 Å addition on rutin concentration dissolved in acetone

Rutin concentration (M)	**Concentration of filtered rutin ($\times 10^{-3}$ M)**	**Concentration of filtered rutin after the addition of 0.05 g g^{-1} molecular sieve 4 Å ($\times 10^{-3}$ M)**
0.01	3.46 ± 1.34	1.33 ± 0.97
0.02	6.31 ± 1.03	3.46 ± 1.40
0.03	7.68 ± 1.21	3.58 ± 0.79
0.04	8.08 ± 1.45	3.77 ± 1.17
0.05	9.16 ± 0.66	3.88 ± 1.32

Standard deviation of the duplicate measurements was <5 %

4.7.3 Apparent First-Order Rate Constant, k_1'

Based on the initial volumetric rates of esterification as a function of initial concentration of lauric acid, k_1' were calculated from the slope for each graph (Fig. 4.15).

Table 4.6 Apparent first-order rate constant, k_1' at various temperatures

Tempe-rature (K)	**Volumetric rate of rutin laurate ($\times 10^{-6}$ M^{-1} h^{-1}) at different concentration of lauric acid (x 10^{-2} M)**						**Apparent first-order rate constant, k_1' (x 10^{-6} h^{-1})**
	5	**15**	**25**	**35**	**45**	**55**	
293	1.01	2.94	4.87	6.92	7.93	8.82	17.6
303	2.15	5.32	10.7	16.4	19.5	24.1	43.9
313	3.78	9.18	13.8	24.4	29.3	34.3	63.8
318	5.7	12.8	17.3	26.8	32.7	41.3	74.6
328	6.89	13.1	20	30	46	48.4	91.1

Standard deviation of the triplicate measurements was < 5%

As shown in Table 4.6, the apparent kinetics of the esterification were found to follow a first-order behaviour. As the temperature increases, the slope of the line became steeper, which reflected the linear increase in k_1' values (Table 4.6). A higher k_1' values implies faster esterification reaction. First-order esterification kinetics are also observed during the esterification of fatty acid lauric alcohol by *Lipolase* lipase (Shintre *et al.*, 2002), and interesterification of triolein and caprylic acid by *Rhizomucor miehei* lipase (Camacho Paez *et al.*, 2003).

4.7.4 Apparent Activation Energy of Esterification (E_a)

Based on k_1' values obtained at different temperatures (Table 4.6), the apparent activation energy (E_a) for the esterification was estimated using Arrhenius plot. A plot of the ln k_1' vs. reciprocal temperature was obtained with a regression coefficient of 0.9211 (Fig. 4.24).

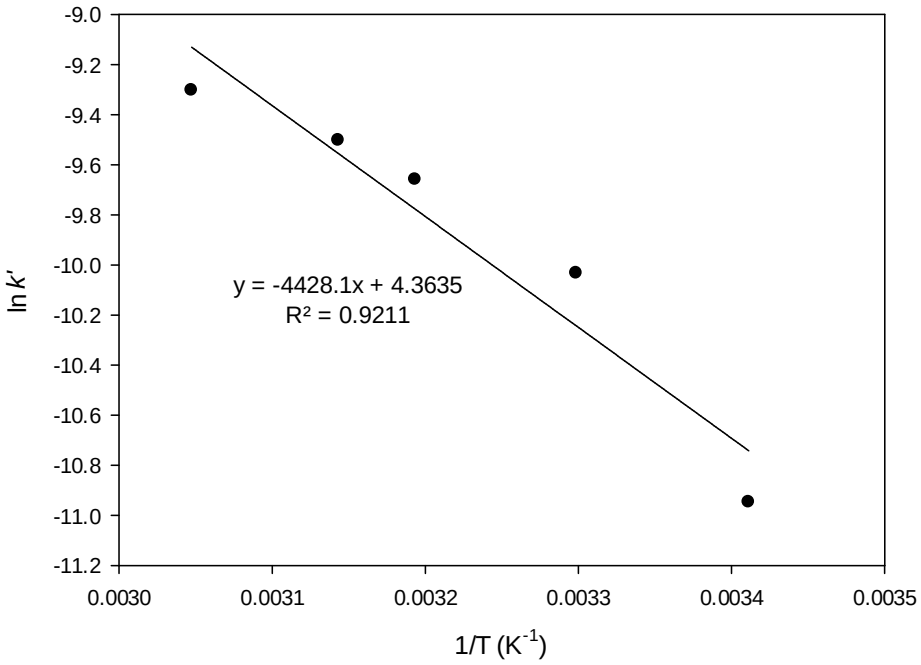

Figure 4.24 Arrhenius plot for esterification of rutin with lauric acid by lipase enzyme.

From the slope of the line, the E_a value was calculated at 37 kJ mol^{-1}, which is consistent with activation energy of enzyme-catalyzed reactions i.e. 25 to 83 kJ mol^{-1} (Dixon & Webb, 1986). At present, no data available on the activation energy of lipase-catalyzed synthesis of flavonoid ester. Since the acylation of rutin takes place at the hydroxyl group of its sugar moiety, (Ishihara *et al.*, 2002; Mellou *et al.*, 2006; Lue *et al.*, 2010; Viskupicova *et al.*, 2010) other comparable activation energy for lipase-catalyzed synthesis of sugar fatty acid esters were 50 kJ mol^{-1} (12 kcal mol^{-1}) for glucose ester synthesized in acetone (Arcos *et al.*, 2001), 67.5×10^3 kJ mol^{-1} for the synthesis of

fructose palmitate (Šabeder *et al.*, 2006), 19 kJ mol^{-1} for esterification of glucose with stearic acid (Yu *et al.*, 2008) and 67 kJ mol^{-1} for the synthesis of 6-*O*-glucosyldecanoate (Gumel *et al.*, 2011b) respectively.

4.8 THERMODYNAMICS PARAMETER OF RUTIN ESTER SYNTHESIS

Employing van't Hoff equation, apparent enthalpy (ΔH) and entropy (ΔS) were determined from the slope and the *y* intercept of the straight line (Fig. 4.25). A plot of ln K_{app} against reciprocal temperature fitted a straight line with a regression coefficient of 0.983.

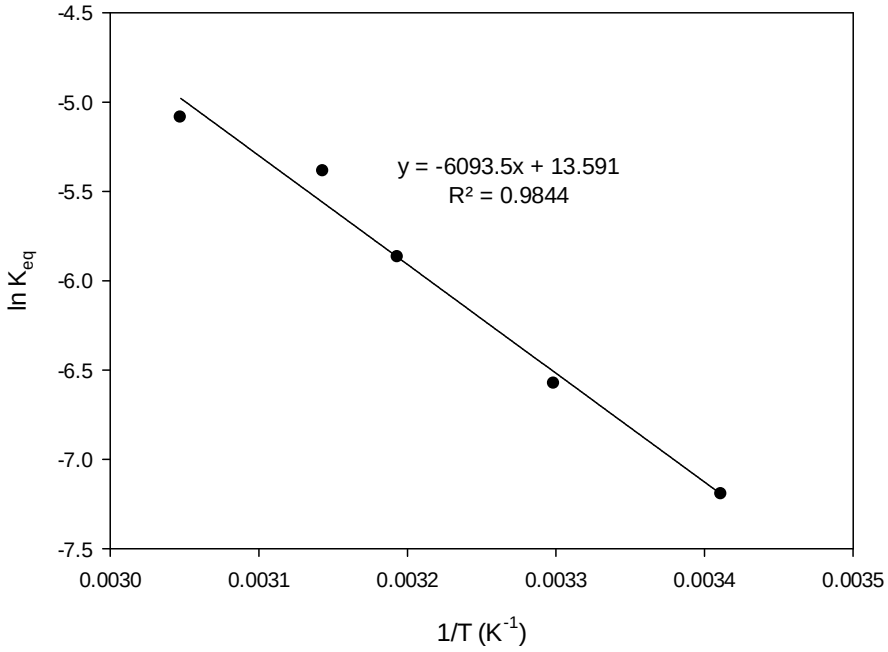

Figure 4.25 van't Hoff plot for esterification of rutin with lauric acid.

K_{eq} refers to the apparent equilibrium constant for esterification process, which was calculated for the highest lauric acid concentration i.e. 0.55 M at each temperature tested (Table 4.7). The K_{eq} value increased with the increase in temperature.

From this work, enthalpy (ΔH) and entropy (ΔS) were calculated at +51 kJ mol^{-1} and +113 J $mol^{-1}K^{-1}$, respectively. The positive value of enthalpy change (ΔH) for the

processes implies the endothermic nature of the esterification system, whereas the positive value of entropy change (ΔS) reflects an esterification system that is becoming increasingly disordered as the temperature increases. The disorder in the system was attributed primarily to the dispersal of water molecules byproduct. Since the reaction is endothermic, as shown by the positive value of ΔH, the increase in temperature is expected to favor the direction of product formation (Segel, 1975).

The values of enthalpy and entropy changes obtained subsequently were used in the calculation of Gibbs free energy change, ΔG using Eq. (3.8). The ΔG value indicates the degree of spontaneity of the esterification process. A strong positive value reflects a more energetically non-favorable process. As shown in Table 4.7, esterification reaction occurs non-spontaneously for temperatures studied ranging of 293 to 318 K and became spontaneous at 328 K. At the temperature below 318 K, esterification reaction occurs non-spontaneously for temperatures studied ranging of 293 to 328 K. Therefore, the esterification of rutin to rutin laurate is an energetically non-favorable process hence non-spontaneous in nature. However, as more energy in the form of heat is supplied to the system the greater is the tendency of the system to move towards spontaneous reaction as shown by the decrease in positive value of ΔG. This could be explained as follow; as temperature increases, more heat is absorbed (ΔH) during the process resulting in the increase of thermal energy of the system. This resulted in energetically favorable path to overcome the activation energy barrier for rutin laurate formation. In addition, thermal effects also help to increase the probability of successful collision between both substrates (rutin and lauric acid) and the catalyst (lipase) to form rutin laurate as a final product. This eventually resulted in high probability of successful esterification.

Table 4.7 Gibbs free energy (ΔG) of esterification at 0.55 M lauric acid

Absolute temperature, *T* (K)	***T*$^{-1}$ (x 10^{-3} K^{-1})**	**Apparent K_{eq}**	**ln K_{eq}**	**Δ*G* (kJ mol^{-1})**	**Δ*G*° (kJ mol^{-1})**	**Δ*G*-Δ*G*° (kJ mol^{-1})**
293	3.41	0.8	-7.2	+18	+35	-18
303	3.30	1.4	-6.6	+16	+33	-17
313	3.19	2.8	-5.9	+15	+31	-15
318	3.14	4.6	-5.4	+14	+29	-14
328	3.05	6.2	-5.1	+13	+28	-13

From Table 4.7, the differences between the energy change for the reaction under the conditions applied in the study and the energy change for the reaction under certain defined standard conditions (ΔG - ΔG^o) exhibited a significant deficit of energy for the temperature range studied. This further supported the endothermic nature of the esterification and the energy investment required to push the reaction forward in the absence of biocatalyst such as CAL-B.

A plot of the Gibbs free energy (ΔG) for the esterification reaction at various temperatures is shown in Fig. 4.26. The ΔG values were calculated with the assumption that the ΔH and ΔS calculated earlier are constant within the temperature range examined. This assumption is not unreasonable as the temperature range studied is relatively narrow due to limited thermal stability of the enzyme catalyst and the boiling point of the solvent used in the system. It showed $\Delta G = 0$ at approximately 448 K (or 175.1 ºC), which means that at this temperature, the energy of the products and reactants are at the equilibrium.

As described before, values of ΔG were positive at 293 to 318 K showing that esterification process is favored when temperature is greater than 175.1 ºC. Extrapolated graph showed that the reaction is spontaneous (i.e., ΔG is negative) above 175.1 ºC (448

K). The increase in temperature amplifies the influence of positive value of ΔS so that the entropic effect could overcome an endothermic process i.e. $T\Delta S > \Delta H$.

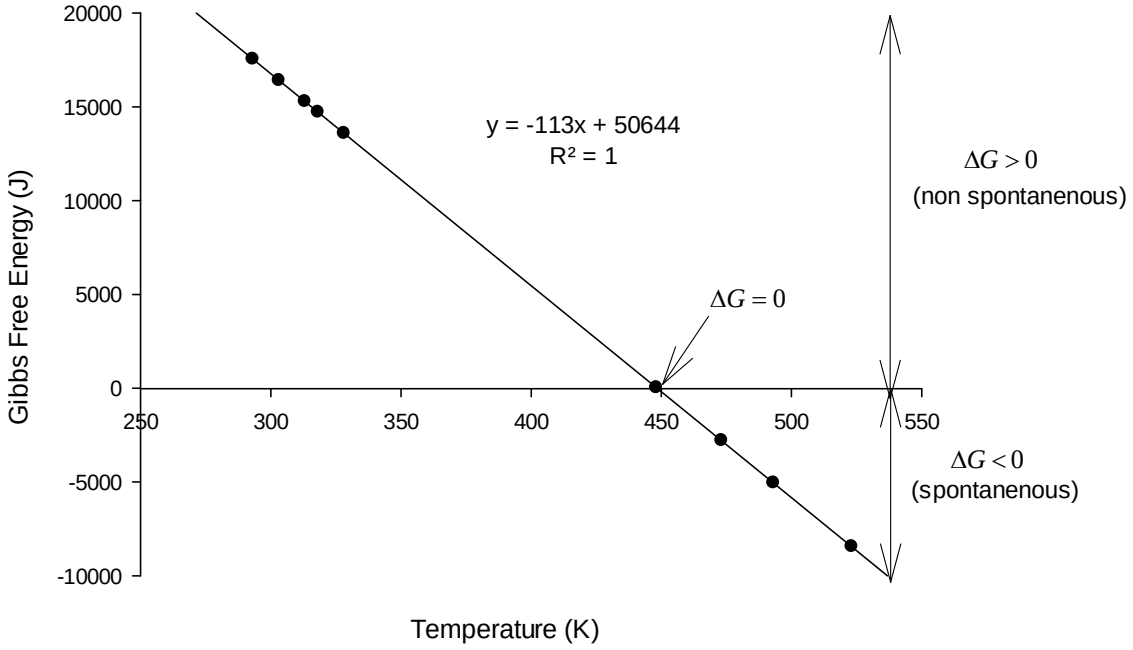

Figure 4.26 Gibbs free energy change for esterification reaction as a function of temperature.

4.9 PRODUCT AUTHENTICATION

NMR spectroscopy allowed the products to be identified and authenticated thus giving an insight as to the site(s) of substitution. The authentication of the chemical structure of the purified rutin laurate was performed using ^{1}H-NMR. Thereafter, the exact position of esterification was deduced from ^{13}C-NMR analysis. The NMR analysis was carried out in DMSO-d_6 using Brucker AC 600 MHz spectrometer.

The ^{1}H-NMR spectrum of rutin exhibited a characteristic proton signal at δH 12.56 corresponding to a chelated hydroxyl group at C-5 (Fig. 4.27). The presence of five aromatic protons were seen in the ^{1}H-NMR spectrum; two orthocoupling protons assignable to H-6' (δ7.55, 1H, d, J = 8.5 Hz) and H-5' (δ6.84, 1H, d, J = 8.5 Hz); two-meta coupling protons at H-6 (δ6.20, 1H, d, J =1.2 Hz) and H-8 (δ6.39, 1H, d, J

= 1.2 Hz); a singlet aromatic proton at H-2' (δ7.53, 1H, s). The ^{1}H-NMR spectrum also supported the presence of rhamnose and glucose moieties with the rhamnose anomeric proton signal at δH 4.39 and glucose H-1 signal at δH 5.35. A doublet of methyl group of rhamnose was observed at δH 1.00. The rest of the protons in the sugar moiety resonated between 3.06 to 3.72 ppm.

For rutin laurate ^{1}H-NMR, a downfield at 4.65 ppm was observed in the spectrum of the glycoside moiety (Fig. 4.28). For the flavone protons, no significant change in chemical shift was observed. The terminal methyl (-CH_3) protons of the ester occurred at 0.75 ppm and the chemical shift due to methylene (-CH_2) protons in the fatty acid moiety of the rutin ester occurred at 1.85 ppm to 1.23 ppm.

^{1}H-NMR chemical shifts for rutin (DMSO-d_6): δ (ppm) 12.59 (1H, s, C5-OH), 7.55 (1H, dd, J = 2.5, 8.5 Hz, C6'-H), 7.53 (1H, d, J = 2.5 Hz, C2'-H), 6.84 (1H, d, J = 8.5 Hz, C5'-H), 6.39 (1H, d, J = 1.2 Hz, C8-H), 6.20 (1H, d, J = 1.2 Hz, C6-H), 5.35 (1H, d, J = 7.5 Hz, C1"-H), 4.65 (1H, t, J = 9.8 Hz, C4"'-$H_{acylated}$), 4.39 (1H, s, C1"'-H), 3.06-3.72 (12H, m, sugar H), 1.85 (2H, m, CH_2 fatty chain), 1.45 (2H, m CH2 fatty chain), 1.23 (24H, m, CH_2 fatty chain), 0.85 (3H, d, J = 6.0 Hz, C6"'-H), 0.75 (3H, t, CH_3 fatty chain).

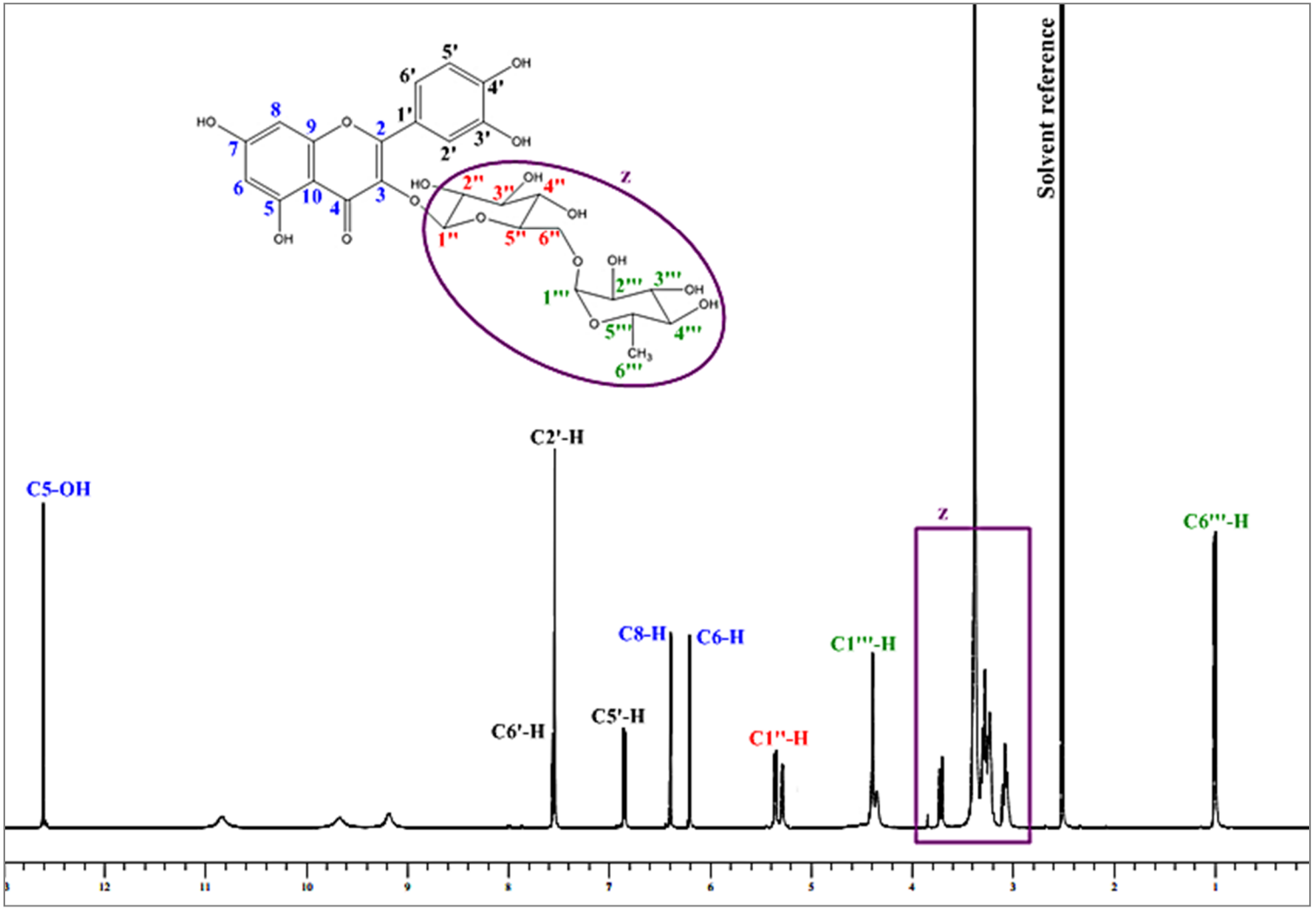

Figure 4.27 ^{1}H-NMR spectrum of rutin.

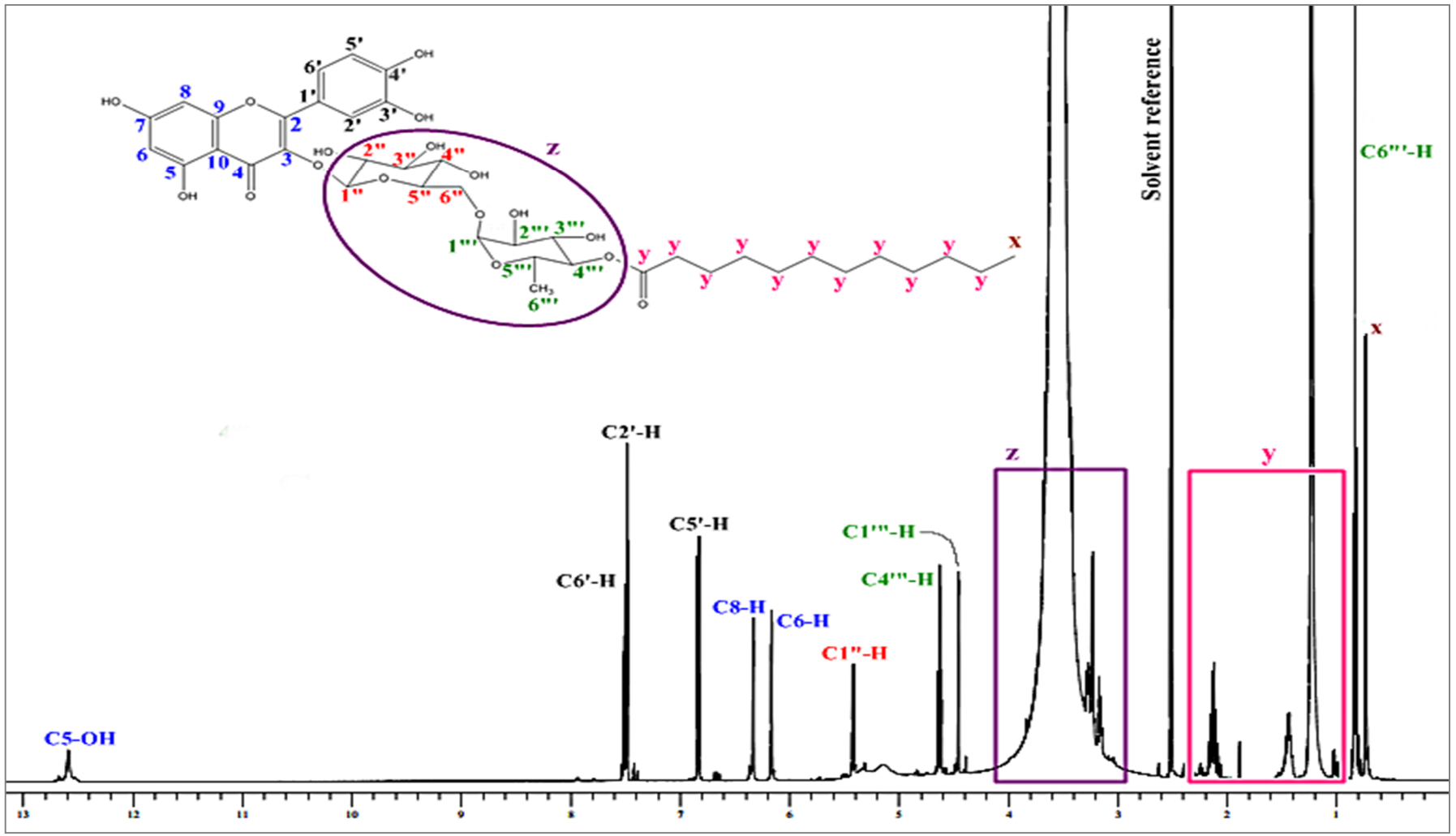

Figure 4.28 ^{1}H-NMR spectrum of rutin laurate.

The ^{13}C-NMR spectrum of rutin molecules showed 27 carbon signals which indicated the presence of one methyl carbon (δC = 17.5 ppm) of rhamnose, one methylene carbon (δC = 67.3 ppm), 15 methine carbons (flavonol skeleton) and 10 quaternary carbons (rutinoside moiety). The signals for two anomeric carbons C1”’ and C1” of rhamnose and glucose were observed at 100.9 and 101.4 ppm respectively (Fig. 4.29).

Meanwhile ^{13}C-NMR spectrum for rutin laurate (Fig. 4.30), occurrence of peaks from 33.9 ppm to 22.5 ppm suggested the formation of an ester with aliphatic chain, which the terminal methyl protons (-CH_3) appeared at 14.4 ppm. The peak at 173.2 ppm was associated with the methylene protons linked directly to the carbonyl (C=O) group of the ester. It was found that the signal of the C4”’ position (Rha, C4”’) for the rhamnose moiety shifted by 1.5 ppm (from 72.3 ppm to 73.7 ppm). Hence, based on this observation, the acylation took place specifically on the secondary 4’”-OH of the rhamnose moiety. This finding provided an important experimental confirmation to the exact location of rutin esterification as speculated by earlier reports (Ardhaoui *et al.*, 2004b; Mellou *et al.*, 2006; Viskupicova *et al.*, 2010).

^{13}C-NMR chemical shifts for rutin laurate (DMSO-d_6): δ (ppm) 177.7 (C4), 173.2 (C=O), 164.3 (C7), 161.7 (C9), 156.9 (C2), 156.8 (C5), 148.9 (C3’), 145.3 (C4’), 133.5 (C3), 121.9 (C1’), 121.5 (C6’), 116.6 (C5’), 115.6 (C2’), 104.1 (C10), 101.4 (C1”), 100.9 (C1’”), 99.3 (C6), 94.1 (C8), 76.9 (C3”), 75.9 (C5”), 74.5 (C2”), 73.7 (C4’”), 70.8 (C2’”), 70.0 (C4”), 68.6 (C3’”), 67.3 (C6”), 66.2 (C5”’), 33.9 (aliphatic chain), 31.7 (aliphatic chain), 29.4 (aliphatic chain), 29.3 (aliphatic chain), 29.2 (aliphatic chain), 29.1 (aliphatic chain), 28.8 (aliphatic chain), 24.9 (aliphatic chain), 22.5 (aliphatic chain), 17.5 (C6”’), 14.4 (CH_3 aliphatic chain).

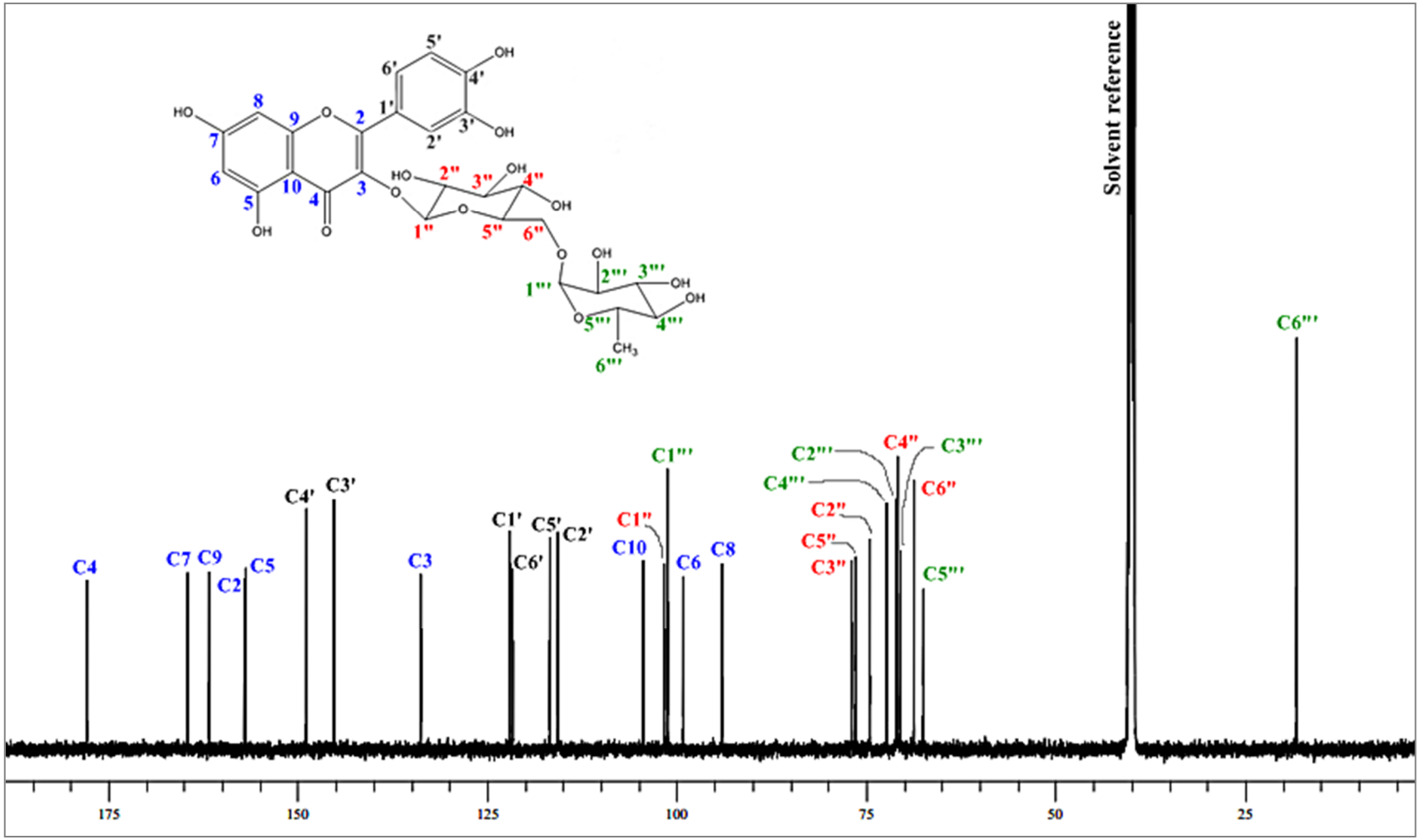

Figure 4.29 ^{13}C-NMR spectrum of rutin.

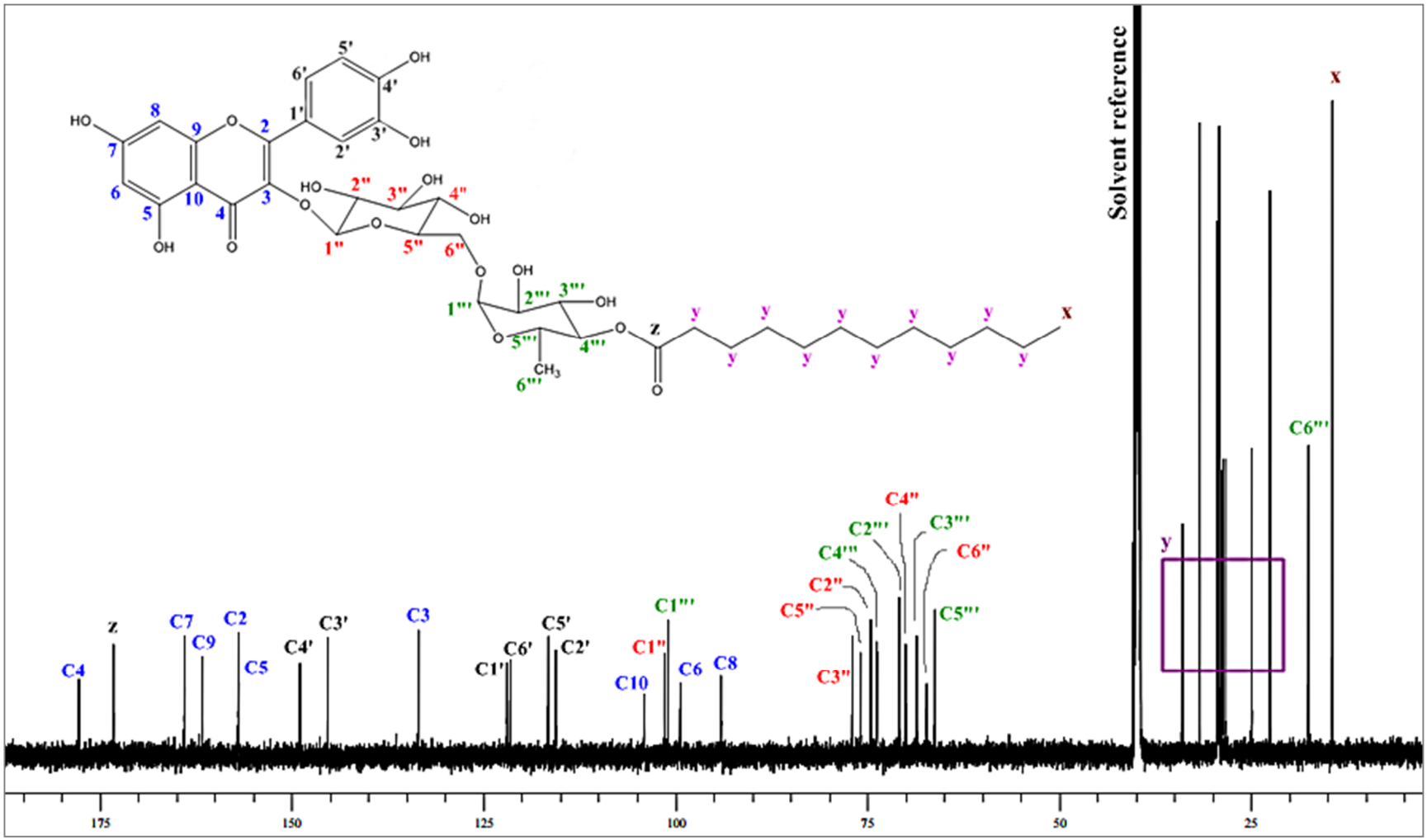

Figure 4.30 ^{13}C-NMR spectrum of rutin laurate.

CHAPTER 5

CONCLUSION

5.1 CONCLUSION

The findings presented in this research showed the general applicability of enzyme-mediated process for the biosynthesis of flavonoid esters. It demonstrated an important investigation of key strictures that could affect the synthesis of flavonoid ester with pharmaceutical, food, cosmetic and health importance. Acylation yield and efficiency in the enzyme process could be manipulated *via* simple parameters such acyl donor concentration, reaction temperature and biocatalyst loading. The process itself is specific and uncomplicated by other competing, unwanted side-reaction(s) as shown in this study where the enzymatic acylation of rutin with lauric acid took place specifically on the secondary 4’”-OH of the rhamnose moiety. Thermal energy investment is minimal, limited by the enzyme stability and solvent boiling point, alongside the advantages previously outlined. Energetic input is primarily to push the endothermic reaction forward, improvement of solubility and mass transfer for immiscible substrates, concomitantly increase the rate of product formation. It is expected that other related and/or similar enzyme-mediated flavonoid esterification may also follow a Ping-Pong Bi–Bi mechanism as shown in this study. The analytical route outlined in this study provides crucial, fundamental information for the development of the said process.

5.2 FUTURE RECOMMENDATIONS

Kinetic models are among the tools that can be used for optimization of bio-catalytic reactions, as well as for facilitating process design and up scaling to improve productivity and reduce the cost of bioprocesses. Although the thermo-kinetic of lipase-catalyzed synthesis of flavonoid ester has been established in the present study, it was found that the number of organic solvents capable of solubilizing adequate amounts of both polar flavonoids and non-polar fatty acid substrates are limited. Furthermore, the reaction itself requires a relatively extended reaction time to reach equilibrium. The yield of flavonoid ester also was not exceptionally high.

The low solubility of flavonoid in the reaction media was the major challenge in the non-aqueous biosynthesis of flavonoid ester. In this study, acetone was employed as a medium during enzymatic esterification of flavonoid. Rutin was apparently most soluble in DMSO whereas lauric was observed to be more soluble in acetone. Therefore, the mixed solvent system might be an excellent choice in order to dissolve both the reactants reasonably well. The polarity and ionization capacity of a non-aqueous reaction medium could be improved by blending of two or more solvents.

The performance of the current system could be enhanced through ultrasonication and microwave irradiation. These methods were thought to be beneficial to accelerate chemical transformation, improve yield and reduce reaction time.

A better understanding and knowledge in some of the aspects mentioned above will help to pave a way for an economically viable commercial scale application of the process.

BIBLIOGRAPHY

Abada, E. A. E. (2008). Production and characterization of a mesophilic lipase isolated from *Bacillus stearothermophilus* AB-1. *Pakistan Journal of Biological Sciences, 11*, 1100-1106.

Acros, J. A., Hill, C. G., & Otero, C. (2001). Kinetics of the lipase-catalyzed synthesis of glucose esters in acetone. *Biotechnology and Bioengineering, 73*(2), 104-110.

Aherne, S. A., & O'Brien, N. M. (2002). Dietary flavonols: chemistry, food content, and metabolism. *Nutrition, 18*(1), 75-81.

Ahmed, O. M., Moneim, A. A., Yazid, I. A., & Mahmoud, A. M. (2010). Antihyperglycemic, antihyperlipidemic and antioxidant effects and the probable mechanisms of action of *Ruta graveolens* infusion and rutin in nicotinamide-streptozotocin-induced diabetic rats. *Diabetologia Croatica, 39*(1), 15-35.

Almeida, V., Branco, C., Assis, S., Vieira, I., Braz-Filho, R., & Branco, A. (2012). Synthesis of naringin 6"-ricinoleate using immobilized lipase. *Chemistry Central Journal, 6*(1), 41.

Amaro, M. I., Rocha, J., Vila-Real, H., Eduardo-Figueira, M., Mota-Filipe, H., Sepodes, B., & Ribeiro, M. H. (2009). Anti-inflammatory activity of naringin and the biosynthesised naringenin by naringinase immobilized in microstructured materials in a model of DSS-induced colitis in mice. *Food Research International, 42*(8), 1010-1017.

Arcos, J. A., Hill, C. G., & Otero, C. (2001). Kinetics of the lipase-catalyzed synthesis of glucose esters in acetone. *Biotechnology and Bioengineering, 73*(2), 104-110.

Arct, J., & Pytkowska, K. (2008). Flavonoids as components of biologically active cosmeceuticals. *Clinics in Dermatology, 26*(4), 347-357.

Ardhaoui, M., Falcimaigne, A., Engasser, J., Moussou, P., Pauly, G., & Ghoul, M. (2004a). Acylation of natural flavonoids using lipase of *Candida antarctica* as biocatalyst. *Journal of Molecular Catalysis B: Enzymatic, 29*(1-16), 63 - 67.

Ardhaoui, M., Falcimaigne, A., Ognier, S., Engasser, J. M., Moussou, P., Pauly, G., & Ghoul, M. (2004b). Effect of acyl donor chain length and substitutions pattern on the enzymatic acylation of flavonoids. *Journal of Biotechnology, 110*(3), 265-272.

Ashok, P. K., & Saini, B. (2013). HPLC analysis and isolation of rutin from stem bark of *Ginkgo biloba. Journal of Pharmacognosy and Phytochemistry, 2*(4), 68-71.

Baxter, R. A. (2008). Anti-aging properties of resveratrol: review and report of a potent new antioxidant skin care formulation. *Journal of Cosmetic Dermatology, 7*(1), 2-7.

Bezbradica, D., Mijin, D., Siler-Marinkovic, S., & Knezevic, Z. (2006). The *Candida rugosa* lipase-catalyzed synthesis of amyl isobutyrate in organic solvent and solvent-free system: A kinetic study. *Journal of Molecular Catalysis B: Enzymatic, 38*(1), 11-16.

Bharti, S., Rani, N., Krishnamurthy, B., & Arya, D. S. (2014). Preclinical evidence for the pharmacological actions of naringin: A review. *Planta Medica, 80*(6), 437-451.

Boligon, A. A., Pimentel, V. C., Piana, M., Zanini, D., Schmatz, R., Bagatini, M. D., Athayde, M. L., Morsch, V. M., & Schetingera, M. R. C. (2014). *Scutia buxifolia Reiss* inhibit platelet aggregation and alters the activities of enzymes that hydrolyze adenine nucleotides in lymphocytes and platelets. *Journal of Applied Biomedicine, 12*(4), 219-227.

Bourogaa, E., Bertrand, J., Despeaux, M., Jarraya, R., Fabre, N., Payrastre, L., Demur, C., Fournié, J.-J., Damak, M., & El Feki, A. (2011). *Hammada scoparia*

flavonoids and rutin kill adherent and chemoresistant leukemic cells. *Leukemia Research, 35*(8), 1093-1101.

Bousquet-Dubouch, M.-P., Graber, M., Sousa, N., Lamare, S., & Legoy, M.-D. (2001). Alcoholysis catalyzed by *Candida antarctica* lipase B in a gas/solid system obeys a Ping-Pong Bi-Bi mechanism with competitive inhibition by the alcohol substrate and water. *Biochimica et Biophysica Acta (BBA) - Protein Structure and Molecular Enzymology, 1550*(1), 90-99.

Bridson, J. H., Grigsby, W. J., & Main, L. (2013). Synthesis and characterization of flavonoid laurate esters by transesterification. *Journal of Applied Polymer Science, 129*(1), 181-186.

Caldwell, S. T., Bennett, C. J., Hartley, R. C., McPhail, D. B., & Duthie, G. G. (2009). Flavonoid compounds as therapeutic antioxidants. Patent US 7601754.

Camacho Paez, B., Robles Medina, A., Camacho Rubio, F., Esteban Cerdán, L., & Molina Grima, E. (2003). Kinetics of lipase-catalysed interesterification of triolein and caprylic acid to produce structured lipids. *Journal of Chemical Technology and Biotechnology, 78*(4), 461-470.

Camargo, C. A., Gomes-Marcondes, M. C. C., Wutzki, N. C., & Aoyama, H. (2012). Naringin inhibits tumor growth and reduces interleukin-6 and tumor necrosis factor α-levels in rats with walker 256 carcinosarcoma. *Anticancer Research, 32*(1), 129-133.

Castaignède, V., Durliat, H., & Comtat, M. (2003). Amperometric and potentiometric determination of catechin as model of polyphenols in wines. *Analytical Letters, 36*(9), 1707-1720.

Céliz, G., Martearena, M. R., Scaroni, E., & Daz, M. (2012). Kinetic study of the alkyl flavonoid ester prunin 6″-*O*-laurate synthesis in acetone catalysed by immobilised *Candida antarctica* lipase B. *Biochemical Engineering Journal, 69*, 69-74.

Chebil, L., Humeau, C., Falcimaigne, A., Engasser, J., & Ghoul, M. (2006). Enzymatic acylation of flavonoids. *Process Biochemistry, 41*, 2237 - 2251.

Chen, Z. G., Tan, R. X., & Huang, M. (2010). Efficient regioselective acylation of andrographolide catalyzed by immobilized *Burkholderia cepacia* lipase. *Process Biochemistry, 45*(3), 415-418.

Chiva-Blanch, G., & Visioli, F. (2012). Polyphenols and health: moving beyond antioxidants. *Journal of Berry Research, 2*(2), 63-71.

Chowdary, G., & Prapulla, S. (2005). Kinetic study on lipase-catalyzed esterification in organic solvents. *Indian Journal Of Chemistry, 44*(11), 2322-2327.

Chung, J., Kurisawa, M., Uyama, H., & Kobayashi, S. (2003). Enzymatic synthesis and antioxidant property of gelatin-catechin conjugates. *Biotechnology Letters, 25*(23), 1993-1997.

Cui, X.-d., & Wang, Z.-h. (2012). Preparation and properties of rutin-hydrolyzing enzyme from tartary buckwheat seeds. *Food Chemistry, 132*(1), 60-66.

Danieli, B., De Bellis, P., Carrea, G., & Riva, S. (1990). Enzyme-mediated regioselective acylations of flavonoid disaccharide monoglycosides. *Helvetica Chimica Acta, 73*(7), 1837-1844.

Danieli, B., Luisetti, M., Sampognaro, G., Carrea, G., & Riva, S. (1997). Regioselective acylation of polyhydroxylated natural compounds catalyzed by *Candida antarctic*a lipase B (Novozym 435) in organic solvents. *Journal of Molecular Catalysis B: Enzymatic, 3*(1), 193-201.

Degenhardt, A., Ullrich, F., Hofmann, T., & Stark, T. (2007). Flavonoid sugar addition products, method for manufacture and use thereof. Patent US 20070269570.

Dixon, M., & Webb, E. C. (1979). *Enzymes,* 3rd Edition. London: Longman Group Ltd.

Doran, P. M. (1995). *Bioprocess Engineering Principles*. London: Academic Press Limited.

Dubey, S., Ganeshpurkar, A., Shrivastava, A., Bansal, D., & Dubey, N. (2013). Rutin exerts antiulcer effect by inhibiting the gastric proton pump. *Indian Journal of Pharmacology, 45*(4), 415.

Dutra, J. V., C. Terzi, S., Bevilaqua, J., Damaso, M. T., Couri, S., Langone, M. P., & Senna, L. (2008). Lipase production in solid-state fermentation monitoring biomass growth of *Aspergillus niger* using digital image processing. *Applied Biochemistry and Biotechnology, 147*(1-3), 63-75.

Enaud, E., Humeau, C., Piffaut, B., & Girardin, M. (2004). Enzymatic synthesis of new aromatic esters of phloridzin. *Journal of Molecular Catalysis B: Enzymatic, 27*(1), 1-6.

Ferrazzano, G. F., Amato, I., Ingenito, A., Zarrelli, A., Pinto, G., & Pollio, A. (2011). Plant polyphenols and their anti-cariogenic properties: A review. *Molecules, 16*(2), 1486-1507.

Flores, M. V., & Halling, P. J. (2002). Full model for reversible kinetics of lipase-catalyzed sugar–ester synthesis in 2-methyl 2-butanol. *Biotechnology and Bioengineering, 78*(7), 795-801.

Gao, C., Mayon, P., MacManus, D., & Vulfson, E. (2001). Novel enzymatic approach to the synthesis of flavonoid glycosides and their esters. *Biotechnology and Bioengineering, 71*(Suppl 3), 235 - 243.

Gayot, S., Santarelli, D., & Coulon, D. (2003). Modification of flavonoid using lipase in non-conventional media: effect of the water content. *Journal of Biotechnology, 101*, 29 - 36.

Ghoul, M., Engasser, J.-M., Moussou, P., Pauly, G., Ardhaoui, M., & Falcimaigne, A. (2006). Enzymatic production of acyl flavonoid derivatives. Patent US 20060115880.

Gonçalves, A. F. K., Friedrich, R. B., Boligon, A. A., Piana, M., Beck, R. C. R., & Athayde, M. L. (2012). Anti-oxidant capacity, total phenolic contents and HPLC determination of rutin in *Viola tricolor* (L) flowers. *Free Radicals and Antioxidants, 2*(4), 32-37.

Graber, M., Bousquet-Dubouch, M.-P., Lamare, S., & Legoy, M.-D. (2003). Alcoholysis catalyzed by *Candida antarctica* lipase B in a gas/solid system: effects of water on kinetic parameters. *Biochimica et Biophysica Acta (BBA) - Proteins and Proteomics, 1648*(1–2), 24-32.

Griebeler, N., Polloni, A., Remonatto, D., Arbter, F., Vardanega, R., Cechet, J., Luccio, M., Oliveira, D., Treichel, H., Cansian, R., Rigo, E., & Ninow, J. (2011). Isolation and screening of lipase-producing fungi with hydrolytic activity. *Food and Bioprocess Technology, 4*(4), 578-586.

Guardia, T., Rotelli, A. E., Juarez, A. O., & Pelzer, L. E. (2001). Anti-inflammatory properties of plant flavonoids. Effects of rutin, quercetin and hesperidin on adjuvant arthritis in rat. *Il Farmaco, 56*(9), 683-687.

Gumel, A. M., Annuar, M. S. M., Heidelberg, T., & Chisti, Y. (2011a). Lipase mediated synthesis of sugar fatty acid esters. *Process Biochemistry, 46*(11), 2079-2090.

Gumel, A. M., Annuar, M. S. M., Heidelberg, T., & Chisti, Y. (2011b). Thermo-kinetics of lipase-catalyzed synthesis of 6-*O*-glucosyldecanoate. *Bioresource Technology, 102*(19), 8727-8732.

Gupta, N., Naik, P., & Chauhan, R. (2012). Differential transcript profiling through cDNA-AFLP showed complexity of rutin biosynthesis and accumulation in seeds of a nutraceutical food crop (*Fagopyrum* spp.). *BMC Genomics, 13*(1), 231.

Hamad, M. N. (2012). Isolation of rutin from *Ruta graveolens (Rutaceae)* cultivated in Iraq by precipitation and fractional solubilization. *Pharmacie Globale (IJCP), 4*, 1-3.

Harborne, J. B., & Williams, C. A. (2000). Advances in flavonoid research since 1992. *Phytochemistry, 55*, 481-504.

Hari Krishna, S., & Karanth, N. G. (2001). Lipase-catalyzed synthesis of isoamyl butyrate: A kinetic study. *Biochimica et Biophysica Acta (BBA)-Protein Structure and Molecular Enzymology, 1547*(2), 262-267.

Hari Krishna, S., & Karanth, N. G. (2002). Lipases and lipase-catalyzed esterification reactions in nonaqueous media. *Catalysis Reviews, 44*(4), 499-591.

Hassan, Z., Yam, M. F., Ahmad, M., & Yusof, A. P. M. (2010). Antidiabetic properties and mechanism of action of *Gynura procumbens* water extract in streptozotocin-induced diabetic rats. *Molecules, 15*(12), 9008-9023.

Havsteen, B. H. (2002). The biochemistry and medical significance of the flavonoids. *Pharmacology & Therapeutics, 96*(2), 67-202.

Hollman, P. C., Cassidy, A., Comte, B., Heinonen, M., Richelle, M., Richling, E., Serafini, M., Scalbert, A., Sies, H., & Vidry, S. (2011). The biological relevance of direct antioxidant effects of polyphenols for cardiovascular health in humans is not established. *The Journal of Nutrition, 141*(5), 989-1009.

Hollman, P. C., & Katan, M. B. (1999). Health effects and bioavailability of dietary flavonols. *Free Radical Research, 31 Suppl*, 75-80.

Horiuchi, M., Osakabe, N., Takizawa, T., & Seyama, Y. (2001). The inhibitory effect of cacao liquor crude polyphenols (CLP) on experimental arteriosclerosis with calcification in rat soft tissue. *Journal of Health Science, 47*(2), 208-212.

Hosny, M., & Rosazza, J. P. N. (2002). Novel oxidations of (+)-catechin by horseradish peroxidase and laccase. *Journal of Agricultural and Food Chemistry, 50*(20), 5539-5545.

Ishihara, K., Nishimura, Y., Kubo, T., Okada, C., Hamada, H., & Nakajima, N. (2002). Enzyme-catalyzed acylation of plant polyphenols for interpretation of their functions. *Plant Biotechnology, 19*(3), 211-214.

Jadhav, R., & Puchchakayala, G. (2012). Hypoglycemic and antidiabetic activity of flavonoids: boswellic acid, ellagic acid, quercetin, rutin on streptozotocin-nicotinamide induced type 2 diabetic rats. *Group, 1*, 100g.

Janbaz, K. H., Saeed, S. A., & Gilani, A. H. (2002). Protective effect of rutin on paracetamol- and CCl4-induced hepatotoxicity in rodents. *Fitoterapia, 73*(7–8), 557-563.

Javed, H., Khan, M. M., Ahmad, A., Vaibhav, K., Ahmad, M. E., Khan, A., Ashafaq, M., Islam, F., Siddiqui, M. S., Safhi, M. M., & Islam, F. (2012). Rutin prevents cognitive impairments by ameliorating oxidative stress and neuroinflammation in rat model of sporadic dementia of Alzheimer type. *Neuroscience, 210*(0), 340-352.

Jeon, S.-M., Bok, S.-H., Jang, M.-K., Lee, M.-K., Nam, K.-T., Park, Y. B., Rhee, S.-J., & Choi, M.-S. (2001). Antioxidative activity of naringin and lovastatin in high cholesterol-fed rabbits. *Life Sciences, 69*(24), 2855-2866.

Jeon, S.-M., Park, Y. B., & Choi, M.-S. (2004). Antihypercholesterolemic property of naringin alters plasma and tissue lipids, cholesterol-regulating enzymes, fecal sterol and tissue morphology in rabbits. *Clinical Nutrition, 23*(5), 1025-1034.

Jin, G., & Yoshioka, H. (2005). Synthesis of lipophilic poly-lauroyl-(+)-catechins and radical-scavenging activity. *Bioscience, Biotechnology, and Biochemistry, 69*(3), 440-447.

Kamalakkannan, N., & Prince, P. S. M. (2006). Antihyperglycaemic and antioxidant effect of rutin, a polyphenolic flavonoid, in streptozotocin-induced diabetic wistar rats. *Basic & Clinical Pharmacology & Toxicology, 98*(1), 97-103.

Kang, W.-S., Chung, K.-H., Chung, J.-H., Lee, J.-Y., Park, J.-B., Zhang, Y.-H., Yoo, H.-S., & Yun, Y.-P. (2001). Antiplatelet activity of green tea catechins is mediated by inhibition of cytoplasmic calcium increase. *Journal of Cardiovascular Pharmacology, 38*(6), 875-884.

Katsoura, M. H., Polydera, A. C., Tsironis, L., Tselepis, A. D., & Stamatis, H. (2006). Use of ionic liquids as media for the biocatalytic preparation of flavonoid derivatives with antioxidant potency. *Journal of Biotechnology, 123*(4), 491-503.

Kazłowska, K., Hsu, T., Hou, C.-C., Yang, W.-C., & Tsai, G.-J. (2010). Anti-inflammatory properties of phenolic compounds and crude extract from *Porphyra dentata*. *Journal of Ethnopharmacology, 128*(1), 123-130.

Kim, D.-S., Ji, H. D., Rhee, M. H., Sung, Y.-Y., Yang, W.-K., Kim, S. H., & Kim, H.-K. (2014). Antiplatelet activity of *Morus alba* leaves extract, mediated *via* inhibiting granule secretion and blocking the phosphorylation of extracellular-signal-regulated kinase and akt. *Evidence-Based Complementary and Alternative Medicine, 2014.*

Kim, K. H., Lee, K. W., Kim, D. Y., Park, H. H., Kwon, I. B., & Lee, H. J. (2005). Optimal recovery of high-purity rutin crystals from the whole plant of *Fagopyrum esculentum* Moench (buckwheat) by extraction, fractionation, and recrystallization. *Bioresource Technology, 96*(15), 1709-1712.

Knekt, P., Kumpulainen, J., Järvinen, R., Rissanen, H., Heliövaara, M., Reunanen, A., Hakulinen, T., & Aromaa, A. (2002). Flavonoid intake and risk of chronic diseases. *The American Journal of Clinical Nutrition, 76*(3), 560-568.

Kobayashi, T., Adachi, S., & Matsuno, R. (2003). Kinetic analysis of the immobilized-lipase-catalyzed synthesis of octanoyl octyl glucoside in acetonitrile. *Biochemical Engineering Journal, 16*(3), 323-328.

Kontogianni, A., Skouridou, V., Sereti, V., Stamatis, H., & Kolisis, F. N. (2001). Regioselective acylation of flavonoids catalyzed by lipase in low toxicity media. *European Journal of Lipid Science and Technology, 103*(10), 655-660.

Kontogianni, A., Skouridou, V., Sereti, V., Stamatis, H., & Kolisis, F. N. (2003). Lipase-catalyzed esterification of rutin and naringin with fatty acids of medium carbon chain. *Journal of Molecular Catalysis B: Enzymatic, 21*, 59 - 62.

Koo, M. W. L., & Cho, C. H. (2004). Pharmacological effects of green tea on the gastrointestinal system. *European Journal of Pharmacology, 500*(1–3), 177-185.

Kreft, S., Štrukelj, B., Gaberščik, A., & Kreft, I. (2002). Rutin in buckwheat herbs grown at different UV-B radiation levels: comparison of two UV spectrophotometric and an HPLC method. *Journal of Experimental Biology, 53*(375), 1801-1804.

La Casa, C., Villegas, I., Alarcón de la Lastra, C., Motilva, V., & Martín Calero, M. J. (2000). Evidence for protective and antioxidant properties of rutin, a natural flavone, against ethanol induced gastric lesions. *Journal of Ethnopharmacology, 71*(1–2), 45-53.

Lambert, J. D., & Elias, R. J. (2010). The antioxidant and pro-oxidant activities of green tea polyphenols: a role in cancer prevention. *Archives of Biochemistry and Biophysics, 501*(1), 65-72.

Lee, C.-H., Jeong, T.-S., Choi, Y.-K., Hyun, B.-H., Oh, G.-T., Kim, E.-H., Kim, J.-R., Han, J.-I., & Bok, S.-H. (2001). Anti-atherogenic effect of citrus flavonoids, naringin and naringenin, associated with hepatic ACAT and aortic VCAM-1 and MCP-1 in high cholesterol-fed rabbits. *Biochemical and Biophysical Research Communications, 284*(3), 681-688.

Lee, W., Ku, S.-K., & Bae, J.-S. (2012). Barrier protective effects of rutin in LPS-induced inflammation *in vitro* and *in vivo*. *Food and Chemical Toxicology, 50*(9), 3048-3055.

Lin, J. P., Yang, J. S., Lin, J. J., Lai, K. C., Lu, H. F., Ma, C. Y., Sai-Chuen Wu, R., Wu, K. C., Chueh, F. S., & Gibson Wood, W. (2012). Rutin inhibits human leukemia tumor growth in a murine xenograft model *in vivo*. *Environmental Toxicology, 27*(8), 480-484.

Liu, Y., Gou, L., Fu, X., Li, S., Lan, N., & Yin, X. (2013). Protective effect of rutin against acute gastric mucosal lesions induced by ischemia-reperfusion. *Pharmaceutical Biology, 51*(7), 914-919.

Lotito, S. B., & Fraga, C. G. (2000). Catechins delay lipid oxidation and α-tocopherol and β-carotene depletion following ascorbate depletion in human plasma. *Experimental Biology and Medicine, 225*(1), 32-38.

Lue, B.-M., Guo, Z., Glasius, M., & Xu, X. (2010). Scalable preparation of high purity rutin fatty acid esters. *Journal of the American Oil Chemists' Society, 87*(1), 55-61.

Mahmoud, A. M. (2012). Influence of rutin on biochemical alterations in hyperammonemia in rats. *Experimental and Toxicologic Pathology, 64*(7–8), 783-789.

Mahmud, M. S., Safinski, T., Nelson, M. I., Sidhu, H. S., & Adesina, A. A. (2009). Kinetic analysis of oleic acid esterification using lipase as catalyst in a microaqueous environment. *Industrial & Engineering Chemistry Research, 49*(3), 1071-1078.

Manach, C., Scalbert, A., Morand, C., Rémésy, C., & Jiménez, L. (2004). Polyphenols: food sources and bioavailability. *The American Journal of Clinical Nutrition, 79*(5), 727-747.

Marangoni, A. G. (2003). *Enzyme kinetics: a modern approach*. USA: John Wiley & Sons Inc.

Martinelle, M., Holmquist, M., & Hult, K. (1995). On the interfacial activation of *Candida antarctica* lipase A and B as compared with *Humicola lanuginosa* lipase. *Biochimica et Biophysica Acta (BBA) - Lipids and Lipid Metabolism, 1258*(3), 272-276.

Martins, S., Mussatto, S. I., Martínez-Avila, G., Montañez-Saenz, J., Aguilar, C. N., & Teixeira, J. A. (2011). Bioactive phenolic compounds: Production and extraction by solid-state fermentation. A review. *Biotechnology Advances, 29*(3), 365-373.

Mattarei, A., Biasutto, L., Rastrelli, F., Garbisa, S., Marotta, E., Zoratti, M., & Paradisi, C. (2010). Regioselective *o*-derivatization of quercetin *via* ester intermediates. An improved synthesis of rhamnetin and development of a new mitochondriotropic derivative. *Molecules, 15*, 4722-4736.

Mellou, F., Lazari, D., Skaltsa, H., Tselepis, A., Kolisis, F., & Stamatis, H. (2005). Biocatalytic preparation of acylated derivatives of flavonoid glycosides enhances

their antioxidant and antimicrobial activity. *Journal of Biotechnology, 116,* 295 - 304.

Mellou, F., Loutrari, H., Stamatis, H., Roussos, C., & Kolisis, F. (2006). Enzymatic esterification of flavonoids with unsaturated fatty acids: Effect of the novel esters on vascular endothelial growth factor release from K562 cells. *Process Biochemistry, 41*(Suppl 9), 2029 - 2034.

Moussou, P., Falcimaigne, A., Ghoul, M., Danoux, L., & Pauly, G. (2007). Esters of flavonoids with ω-substituted C6-C22 fatty acids. Patent US 20070184098.

Nakajima, N., Ishihara, K., Itoh, T., Furuya, T., & Hamada, H. (1999). Lipase-catalyzed direct and regioselective acylation of flavonoid glucoside for mechanistic investigation of stable plant pigments. *Journal of Bioscience and Bioengineering, 87,* 105 – 107.

Naoe, K., Ohsa, T., Kawagoe, M., & Imai, M. (2001). Esterification by *Rhizopus delemar* lipase in organic solvent using sugar ester reverse micelles. *Biochemical Engineering Journal, 9*(1), 67-72.

Nichols, J. A., & Katiyar, S. K. (2010). Skin photoprotection by natural polyphenols: anti-inflammatory, antioxidant and DNA repair mechanisms. *Archives of Dermatological Research, 302*(2), 71-83.

Nie, Y. C., Wu, H., Li, P. B., Luo, Y. L., Long, K., Xie, L. M., Shen, J. G., & Su, W. W. (2012). Anti-inflammatory effects of naringin in chronic pulmonary neutrophilic inflammation in cigarette smoke-exposed rats. *Journal of Medicinal Food, 15*(10), 894-900.

Olennikov, D. N., & Partilkhaev, V. V. (2012). Isolation and densitometric HPTLC analysis of rutin, narcissin, nicotiflorin, and isoquercitrin in *Caragana spinosa* shoots. *JPC-Journal of Planar Chromatography-Modern TLC, 25*(1), 30-35.

Palombo, E. A. (2011). Traditional medicinal plant extracts and natural products with activity against oral bacteria: potential application in the prevention and treatment of oral diseases. *Evidence-Based Complementary and Alternative Medicine, 2011*.

Pandey, K. B., & Rizvi, S. I. (2009). Plant polyphenols as dietary antioxidants in human health and disease. *Oxidative Medicine and Cellular Longevity, 2*(5), 270-278.

Passicos, E., Santarelli, X., & Coulon, D. (2004). Regioselective acylation of flavonoids catalyzed by immobilized *Candida antarctica* lipase under reduced pressure. *Biotechnology Letters, 26*(Suppl 13), 1073 - 1076.

Patti, A., Piatelli, M., & Nicolosi, G. (2000). Use of *Mucor miehei* lipase in the preparation of long chain 3-*O*-acylcatechins. *Journal of Molecular Catalysis B: Enzymatic, 10*, 577 - 582.

Pencreac'h, G., & Baratti, J. C. (1996). Hydrolysis of p-nitrophenyl palmitate in n-heptane by the *Pseudomonas cepacia* lipase: A simple test for the determination of lipase activity in organic media. *Enzyme and Microbial Technology, 18*(6), 417-422.

Perrier, E., Mariotte, A.-M., Boumendjel, A., & Bresson-Rival, D. (2001). Flavonoid esters and their use notably in cosmetics. Patent US 6235294.

Pietta, P.-G. (2000). Flavonoids as antioxidants. *Journal of Natural Products, 63*(7), 1035-1042.

Real, H. J. V., Alfaia, A. J., Calado, A. R., & Ribeiro, M. H. (2007). High pressure-temperature effects on enzymatic activity: Naringin bioconversion. *Food Chemistry, 102*(3), 565-570.

Ribeiro, I. A. C., & Ribeiro, M. H. L. (2008). Kinetic modelling of naringin hydrolysis using a bitter sweet alfa-rhamnopyranosidase immobilized in *k*-carrageenan. *Journal of Molecular Catalysis B: Enzymatic, 51*(1–2), 10-18.

Riva, S., Danieli, B., & Luisetti, M. (1996). A two-step efficient chemoenzymatic synthesis of flavonoid glycoside malonates. *Journal of Natural Products, 59*(6), 618-621.

Riva, S. (2002). Enzymatic modification of the sugar moieties of natural glycosides. *Journal of Molecular Catalysis B: Enzymatic, 19-20*, 43 - 54.

Romero, M., Calvo, L., Alba, C., & Daneshfar, A. (2007). A kinetic study of isoamyl acetate synthesis by immobilized lipase-catalyzed acetylation in *n*-hexane. *Journal of Biotechnology, 127*(2), 269-277.

Šabeder, S., Habulin, M., & Knez, Ž. (2006). Lipase-catalyzed synthesis of fatty acid fructose esters. *Journal of Food Engineering, 77*(4), 880-886.

Salem, J. H., Humeau, C., Chevalot, I., Harscoat-Schiavo, C., Vanderesse, R., Blanchard, F., & Fick, M. (2010). Effect of acyl donor chain length on isoquercitrin acylation and biological activities of corresponding esters. *Process Biochemistry, 45*(3), 382-389.

Scalbert, A., Johnson, I. T., & Saltmarsh, M. (2005). Polyphenols: antioxidants and beyond. *The American Journal of Clinical Nutrition, 81*(1), 215S-217S.

Segel, I. H. (1975). *Enzyme kinetics: Behavior and analysis of rapid equilibrium and steady state enzyme systems*. USA: John Wiley & Sons, Inc.

Selloum, L., Bouriche, H., Tigrine, C., & Boudoukha, C. (2003). Anti-inflammatory effect of rutin on rat paw oedema, and on neutrophils chemotaxis and degranulation. *Experimental and Toxicologic Pathology, 54*(4), 313-318.

Shaik, N., Zbidah, M., & Lang, F. (2012). Inhibition of Ca^{2+} entry and suicidal erythrocyte death by naringin. *Cellular Physiology and Biochemistry, 30*(3), 678-686.

Shin, D. W., Kim, S. N., Lee, S. M., Lee, W., Song, M. J., Park, S. M., Lee, T. R., Baik, J.-H., Kim, H. K., Hong, J.-H., & Noh, M. (2009). (-)-Catechin promotes

adipocyte differentiation in human bone marrow mesenchymal stem cells through PPARγ transactivation. *Biochemical Pharmacology, 77*(1), 125-133.

Shintre, M. S., Ghadge, R. S., & Sawant, S. B. (2002). Kinetics of esterification of lauric acid with fatty alcohols by lipase: Effect of fatty alcohol. *Journal of Chemical Technology & Biotechnology, 77*(10), 1114-1121.

Silva, E., Souza, J., Rogez, H., Rees, J.-F., & Larondelle, Y. (2007). Antioxidant activities and polyphenolic contents of fifteen selected plant species from the Amazonian region. *Food Chemistry, 101*(3), 1012-1018.

Singh, D., Chander, V., & Chopra, K. (2004). Protective effect of naringin, a bioflavonoid on ferric nitrilotriacetate-induced oxidative renal damage in rat kidney. *Toxicology, 201*(1-3), 1-8.

Slimestad, R., & Verheul, M. (2011). Properties of chalconaringenin and rutin isolated from cherry tomatoes. *Journal of Agricultural and Food Chemistry, 59*(7), 3180-3185.

Spizzirri, U. G., Iemma, F., Puoci, F., Cirillo, G., Curcio, M., Parisi, O. I., & Picci, N. (2009). Synthesis of antioxidant polymers by grafting of gallic acid and catechin on gelatin. *Biomacromolecules, 10*(7), 1923-1930.

Stergiou, P.-Y., Foukis, A., Filippou, M., Koukouritaki, M., Parapouli, M., Theodorou, L. G., Hatziloukas, E., Afendra, A., Pandey, A., & Papamichael, E. M. (2013). Advances in lipase-catalyzed esterification reactions. *Biotechnology Advances, 31*(8), 1846-1859.

Stevenson, D. E., & Hurst, R. D. (2007). Polyphenolic phytochemicals – just antioxidants or much more? *Cellular and Molecular Life Sciences, 64*(22), 2900-2916.

Sun, S., Shan, L., Liu, Y., Jin, Q., Song, Y., & Wang, X. (2009). Solvent-free enzymatic synthesis of feruloylated diacylglycerols and kinetic study. *Journal of Molecular Catalysis B: Enzymatic, 57*(1–4), 104-108.

Swarts, J. W., Vossenberg, P., Meerman, M. H., Janssen, A. E. M., & Boom, R. M. (2008). Comparison of two-phase lipase-catalyzed esterification on micro and bench scale. *Biotechnology and Bioengineering, 99*(4), 855-861.

Tipoe, G. L., Leung, T.-M., Hung, M.-W., & Fung, M.-L. (2007). Green tea polyphenols as an anti-oxidant and anti-inflammatory agent for cardiovascular protection. *Cardiovascular & Haematological Disorders-Drug Targets (Formerly Current Drug Targets-Cardiovascular & Hematological Disorders), 7*(2), 135-144.

Tsao, R. (2010). Chemistry and biochemistry of dietary polyphenols. *Nutrients, 2*(12), 1231-1246.

Uesato, S., Kitagawa, Y., Hara, Y., Tokuda, H., Okuda, M., Mou, X. Y., Mukainaka, T., & Nishino, H. (2000). Antitumor promoting activities of 3-*O*-acyl-(-)-epigallocatechins. *Bioorganic & Medicinal Chemistry Letters, 10*(15), 1673-1675.

Uppenberg, J., Hansen, M. T., Patkar, S., & Jones, T. A. (1994). The sequence, crystal structure determination and refinement of two crystal forms of lipase B from *Candida antarctica*. *Structure, 2*(4), 293-308.

Urano, M., Kagawa, H., Harigaya, Y., Li, S., & Onda, M. (1991). Heterocycles. XXVI. A total synthesis of optically pure (+)-catechin pentaacetate. *Journal of Heterocyclic Chemistry, 28*(8), 1845-1847.

Vakhlu, J., & Kour, A. (2006). Yeast lipases: Enzyme purification, biochemical properties and gene cloning. *Electronic Journal of Biotechnology Advances, 9*, 1-17.

Velayutham, P., Babu, A., & Liu, D. (2008). Green tea catechins and cardiovascular health: An update. *Current Medicinal Chemistry*, *15*(18), 1840.

Viskupicova, J., Danihelova, M., Ondrejovic, M., Liptaj, T., & Sturdik, E. (2010). Lipophilic rutin derivatives for antioxidant protection of oil-based foods. *Food Chemistry*, *123*(Suppl 1), 45 - 50.

Viskupicova, J., Ondrejovic, M., & Maliar, T. (2012). Enzyme-mediated preparation of flavonoid esters and their applications. *INTECH Open Access Publisher*.

Wei, M., Yang, Z., Li, P., Zhang, Y., & Sse, W. C. (2007). Anti-osteoporosis activity of naringin in the retinoic acid-induced osteoporosis model. *The American Journal of Chinese Medicine, 35*(04), 663-667.

Wirth, C., Buchholz, H., & Carola, C. (2008). Tiliroside or derivative, drugs, foods; ultraviolet radiation filters; aging and oxidation resistance; free radical scavengers; antiinflammatory, anticarcinogenic, and antiallergen agents; plant extracts; topically applied. Patent US 20080199414.

Wu, C.-H., Lin, M.-C., Wang, H.-C., Yang, M.-Y., Jou, M.-J., & Wang, C.-J. (2011). Rutin inhibits oleic acid induced lipid accumulation *via* reducing lipogenesis and oxidative stress in hepatocarcinoma cells. *Journal of Food Science, 76*(2), T65-T72.

Wu, J.-B., Fong, Y.-C., Tsai, H.-Y., Chen, Y.-F., Tsuzuki, M., & Tang, C.-H. (2008). Naringin-induced bone morphogenetic protein-2 expression *via* PI3K, Akt, c-Fos/c-Jun and AP-1 pathway in osteoblasts. *European Journal of Pharmacology*, *588*(2–3), 333-341.

Wu, P., Ma, G., Li, N., Deng, Q., Yin, Y., & Huang, R. (2015). Investigation of *in vitro* and *in vivo* antioxidant activities of flavonoids rich extract from the berries of *Rhodomyrtus tomentosa* (Ait.) Hassk. *Food Chemistry, 173*, 194-202.

Yadav, G. D., & Trivedi, A. H. (2003). Kinetic modeling of immobilized lipase-catalyzed transesterification of *n*-octanol with vinyl acetate in non-aqueous media. *Enzyme and Microbial Technology, 32*(7), 783-789.

Yang, J., Guo, J., & Yuan, J. (2008). *In vitro* antioxidant properties of rutin. *LWT-Food Science and Technology, 41*(6), 1060-1066.

Yeum, C.-H., & Choi, J.-S. (2006). Effect of naringin pretreatment on bioavailability of verapamil in rabbits. *Archives of Pharmacal Research, 29*(1), 102-107.

Yilmaz, Y., & Toledo, R. T. (2004). Major flavonoids in grape seeds and skins: antioxidant capacity of catechin, epicatechin, and gallic acid. *Journal of Agricultural and Food Chemistry, 52*(2), 255-260.

Yoshida, Y., Kimura, Y., Kadota, M., Tsuno, T., & Adachi, S. (2006). Continuous synthesis of alkyl ferulate by immobilized *Candida antarctica* lipase at high temperature. *Biotechnology Letters, 28*(18), 1471-1474.

Yu, J., Zhang, J., Zhao, A., & Ma, X. (2008). Study of glucose ester synthesis by immobilized lipase from *Candida* sp. *Catalysis Communications, 9*(6), 1369-1374.

Zaidi, A., Gainer, J., Carta, G., Mrani, A., Kadiri, T., Belarbi, Y., & Mir, A. (2002). Esterification of fatty acids using nylon-immobilized lipase in *n*-hexane: kinetic parameters and chain-length effects. *Journal of Biotechnology, 93*(3), 209-216.

Zhang, J., Zhang, P., Liu, T., Zhou, L., Zhang, L., Lin, R., Yang, G., Wang, W., & Li, Y. (2015). Solubility of naringin in ethanol and water mixtures from 283.15 to 318.15 K. *Journal of Molecular Liquids, 203*(0), 98-103.

Zhang, S., Yang, X., & Morris, M. E. (2004). Flavonoids are inhibitors of breast cancer resistance protein (ABCG2)-mediated transport. *Molecular Pharmacology, 65*(5), 1208-1216.

LIST OF PUBLICATION & CONFERENCE

1. Razak, N.N.A, & Annuar, M.S.M. (2015). Enzymatic synthesis of flavonoid ester: elucidation of its kinetic mechanism and equilibrium thermodynamic behavior. *Industrial & Engineering Chemistry Research*, 54(21): 5604-5612.
2. Razak, N.N.A, & Annuar, M.S.M. (2014). Kinetics and Equilibrium Thermodynamic of Lipase-catalyzed Synthesis of Rutin Aliphatic Esters. Paper presented at the International Conference on Pharmaceutical, Medical & Environmental Health, 17 to 18th September 2014, Batu Ferringhi, Penang, Malaysia, (International).

I&EC research
Industrial & Engineering Chemistry Research

Article

pubs.acs.org/IECR

Enzymatic Synthesis of Flavonoid Ester: Elucidation of Its Kinetic Mechanism and Equilibrium Thermodynamic Behavior

N. N. A. Razak[†] and M. S. M. Annuar*[,†,‡]

[†]Institute of Biological Sciences, Faculty of Science, and [‡]Centre for Research in Biotechnology for Agriculture (CEBAR), University of Malaya, 50603 Kuala Lumpur, Malaysia

ABSTRACT: In this study, flavonoid rutin was acylated with lauric acid in acetone catalyzed by an immobilized lipase from *Candida antarctica*. In addition to the reaction not being well studied, the esterification also involves two immiscible substrates, which posed a significant challenge. Analysis indicated that the lipase-mediated esterification exhibits a ping-pong bi−bi mechanism with no apparent inhibition by the two substrates. The activation energy, E_a, for the esterification was calculated as ∼37 kJ mol^{-1}. The esterification process was found to be endothermic, with enthalpy (ΔH) and entropy (ΔS) values of approximately +50 kJ mol^{-1} and +110 J mol^{-1} K^{-1}, respectively. Based on the value of the Gibbs free energy change (ΔG), the esterification reaction under the conditions studied was predicted to be nonspontaneous below 175 °C but spontaneous at higher temperatures. The study also confirmed, through ^{13}C NMR analysis, the exact location of rutin esterification. The investigated esterification biochemistry highlighted important behavior concerning the enzyme-mediated synthesis of functionalized flavonoid.

1. INTRODUCTION

Because of the beneficial biological activities of flavonoids, researchers are continuously searching for natural antioxidants as an alternative to synthetic ones for use in food and cosmetic products.[1] However, the use of these antioxidants is strongly limited because of their hydrophilic nature, which reduces their solubility and stability in lipophilic environments. Therefore, the preparation of lipophilic flavonoids by acylation is a promising method for modifying these compounds. It is proposed that, by selectively modifying flavonoids, improved properties such as penetration through the cell membrane and novel bioactivities could be obtained.[2,3]

To circumvent the disadvantages of the conventional chemical process, enzyme-mediated catalysis in a nonaqueous medium has opened up new routes for obtaining products derived from natural antioxidants with high added value.[3−8] Lipase is preferred because of its high regioselectivity and mild reaction conditions that avoid substrate alteration. The use of enzymes makes it possible to develop a significantly simple approach for the preparation of flavonoid esters.[9−12] However, the acylation of flavonoids is limited by their solubility in organic solvents.

Most enzyme kinetic studies are related to reactions of soluble substrates, whereas the literature on esterification kinetics between immiscible substrates is clearly lacking. Most of these studies have focused on the esterification of sugar with acids/esters.[13−16] The only kinetic data available on flavonoid esterification by lipase were reported by Céliz et al.[17]

Therefore, it is of great importance to investigate the prominent aspects of this ill-studied and difficult reaction. The present investigation was focused on the kinetics of lipase-catalyzed esterification of flavonoids with acyl donors. The most significant challenge of this study is that the reaction is limited by the solubility of the flavonoids. Generally, Michaelis−Menten kinetics describes well reactions that take place in a homogeneous phase. A working kinetic model plays an important role in the elucidation of the reaction mechanism. In addition, the equilibrium thermodynamics of flavonoid esterification was also studied. Understanding these fundamental aspects is essential for the rational design of synthesis reactions/reactors for flavonoid esters, which constitute important ingredients in the food, pharmaceutical, and cosmetic industries.

2. MATERIALS AND METHODS

2.1. Materials. Lipase from *Candida antarctica* immobilized on acrylic resin (CAL-B), molecular sieve 4 Å, and the acyl acceptor rutin were purchased from Sigma-Aldrich Chemical Co. The acyl donor lauric acid (dodecanoic acid), acetone, ammonium formate, methanol, acetic acid, and deuterated dimethyl sulfoxide (DMSO-d_6) were supplied by Merck. Analytical-grade solvents and reagents were used throughout this study.

2.2. Enzymatic Synthesis of Rutin Ester. The enzymatic synthesis of rutin ester was carried out at various initial concentrations of rutin (0.003−0.012 M) with different initial concentrations of lauric acid (0.05−0.55 M) in acetone. Because of its low solubility, 1 g of rutin stock was dissolved in 25 mL of acetone that was previously dried with 4 Å molecular sieves and filtered using a Buchner funnel. The rutin filtrate was collected, and the actual concentration of soluble rutin was assayed by high-performance liquid chromatography (HPLC). The solubility of the rutin stock solution in acetone was determined to be 1.48×10^{-2} g (g of solvent)$^{-1}$ (molality = 2.42×10^{-2} mol kg^{-1}) at 25 ± 1 °C and 1 atm. The rutin residue was dried at 55 °C, kept at −4 °C, and reused for other

Received: March 16, 2015
Revised: May 13, 2015
Accepted: May 13, 2015
Published: May 13, 2015

DOI: 10.1021/acs.iecr.5b00996
Ind. Eng. Chem. Res. 2015, 54, 5604−5612

esterification processes. The batch esterification process was performed in screw-capped glass tubes shaken horizontally at 200 rpm. The reaction was initiated by adding 0.15 g of lipase to 15.0 mL of the reaction medium. A constant reaction temperature within the range 20−55 °C was applied during each experimental run. To monitor the progress of the reaction, samples (0.2 mL aliquot each) for analysis were withdrawn at regular intervals until 120 h. Each sample was dried at 70 °C, resuspended in 1.0 mL of methanol, and filtered through a 0.22-μm polytetrafluoroethylene (PTFE) filter for subsequent analysis by HPLC. Three independent replicates were performed for each experiment conducted. Control experiments (without catalyst) were also conducted in parallel.

2.3. Analytical Methods. *2.3.1. High-Performance Liquid Chromatography (HPLC).* Quantitative analysis of rutin and rutin ester were performed on an HPLC (Jasco, Tokyo, Japan) system equipped with a degasser (DG 980 50), a binary pump (PU 980), an autosampler (AS 950), a column oven (CO 965), and an ultraviolet (UV) detector (UV 975). The detector was operated for ultraviolet wavelength detection at 280 nm. A Chromolith HR RP-18^e column (4.6 × 10 mm, 2 μm, Merck) fitted with an analytical guard column (4.6 × 10 mm × 2 μm) was used for chromatographic separation. The temperature of the column was maintained at 35 °C with a flow rate of 1 mL min^{-1}. An injection volume of 20 μL was used. The separation of the different components of the reaction medium was performed using a gradient (A/B) of methanol (A) and water with 0.1% acetic acid (B) as follows: 0.1 min, 30/70; 5.0 min, 100/0; 10.0 min, 100/0; 11.0 min, 30/70; 15.0 min, 30/70. Data acquisition was performed using ChromNav software (Jasco, Tokyo, Japan). The conversion yield was calculated between the molar concentration of acylated flavonoid (rutin) and its initial molar concentration

$$\text{conversion yield (\%)} = \frac{[\text{F}]_{\text{initial}} - [\text{F}]_{\text{residual}}}{[\text{F}]_{\text{initial}}} \times 100 \quad (1)$$

where $[\text{F}]_{\text{initial}}$ is the initial rutin concentration and $[\text{F}]_{\text{residual}}$ is the rutin concentration remaining after the reaction. The calibration curve for rutin was obtained using standards dissolved in methanol. Rutin ester was collected from the HPLC eluate, and the external linear calibration was plotted using purified samples.

2.3.2. Liquid Chromatography/Tandem Mass Spectrometry (LC/MS/MS). Molecular-weight analyses for rutin and rutin laurate were performed by liquid chromatography (LC). A liquid chromatograph (Shimadzu, LC 20 AD, binary pump) interfaced to an AB Sciex 3200 QTrap LC/MS/MS system with a Perkin-Elmer FX 15 uHPLC system was used for the integration, calibration, and collection of LC-MS spectra, as well as data processing for qualitative and quantitative analyses. The stationary phase was a Phenomenex Aqua C18 reverse-phase column (50 mm × 20 mm, 5 μm of particle size). Separation of the reaction components was achieved at a constant flow rate of 0.25 mL min^{-1} using different gradients (A/B) of 0.1% formic acid and 5 mM ammonium formate in water (A) and acetonitrile with 0.1% formic acid and 5 mM ammonium formate (B) as follows: 0.01 min, 90/10; 8.00 min, 10/90; 11.00 min, 10/90; 11.10 min, 90/10; 15.00 min, 90/10. The column oven temperature was operated at 40 °C, and the injection volume was 20 μL with a total running time of 15 min. The mass spectrometer was operated in negative electrospray ionization (ESI), mode and the electrospray source parameters were fixed as follows: electrospray capillary voltage, 3.5 kV; source temperature, 500 °C. Nitrogen was used in the electrospray ionization source. The desolvation gas and source gas flow rates were 40 psi. The declustering potential and entrance potential were set at 40 and 10 V, respectively.

2.3.3. NMR Analysis. The chemical structure of the purified rutin laurate was authenticated by ^{1}H NMR and ^{13}C NMR analysis in DMSO-d_6 using a Bruker AC 600 MHz spectrometer.

2.4. Kinetic Parameters. *2.4.1. Initial Esterification Rate.* The esterification rate was determined from the polynomial regression plot of the apparent product concentration as a function of time. A tangent was drawn from the origin on the polynomial regression. Thus, in the case of rutin ester, the initial rate (v, M h^{-1}) was calculated using the equation

$$v = \frac{\Delta C}{\Delta t} \quad (2)$$

where ΔC (M) refers to the change in the rutin ester concentration within the time interval Δt (Δt = 0−1 h).

The reaction rate can be described using the ping-pong bi−bi kinetic model, assuming no inhibition from either the substrate or the product. The model for the reaction rate is given by Segel[18] as

$$v = \frac{V_{\max}[\text{LA}][\text{F}]}{K_{\text{m}}^{\text{F}}[\text{LA}] + K_{\text{m}}^{\text{LA}}[\text{F}] + [\text{LA}][\text{F}]} \quad (3)$$

where v is the initial reaction rate; $V_{\max}$ is the maximum reaction rate (M h^{-1}); and K_{m}^{LA} and K_{m}^{F} are the binding constants (Michaelis constants) for the substrate lauric acid (LA) and the flavonoid rutin (F), respectively. The reaction rates obtained at various lauric acid and rutin concentrations were fitted to this model using nonlinear regression (Polymath 6.0 software).

2.4.2. Activation Energy. The activation energy (E_a, J mol^{-1}) for the esterification process was calculated using the linearized Arrhenius equation

$$\ln k_1' = \ln A - \frac{E_a}{RT} \quad (4)$$

where A is the frequency factor, R is the gas constant (8.3145 J mol^{-1} K^{-1}), and T is the absolute temperature (K). To calculate k_1', the volumetric rate of rutin esterification was plotted against different initial fatty acid concentrations for each temperature tested (20−55 °C). The rate constant k_1' was obtained from the slope of the resulting linear plot.

2.5. Thermodynamic Parameters. The esterification reaction was assumed to be at equilibrium when the formation of rutin ester in acetone showed no further changes in concentration over time at a particular temperature. The transition of rutin to rutin ester was also considered as a one-step process; thus, the apparent equilibrium constant K_{eq} was calculated as

$$K_{\text{eq}} = \frac{[\text{FE}]_{\text{eq}}[\text{W}]_{\text{eq}}}{[\text{F}]_{\text{eq}}[\text{LA}]_{\text{eq}}} \quad (5)$$

where K_{eq} is the apparent equilibrium constant, $[\text{FE}]_{\text{eq}}$ and $[\text{W}]_{\text{eq}}$ are the flavonoid ester (rutin ester) and water concentrations (in molarity), respectively, at equilibrium. $[\text{F}]_{\text{eq}}$ and $[\text{LA}]_{\text{eq}}$ are the respective concentrations (in molarity) of residual rutin and lauric acid at equilibrium. $[\text{FE}]_{\text{eq}}$ and $[\text{F}]_{\text{eq}}$

DOI: 10.1021/acs.iecr.5b00996
Ind. Eng. Chem. Res. 2015, 54, 5604−5612

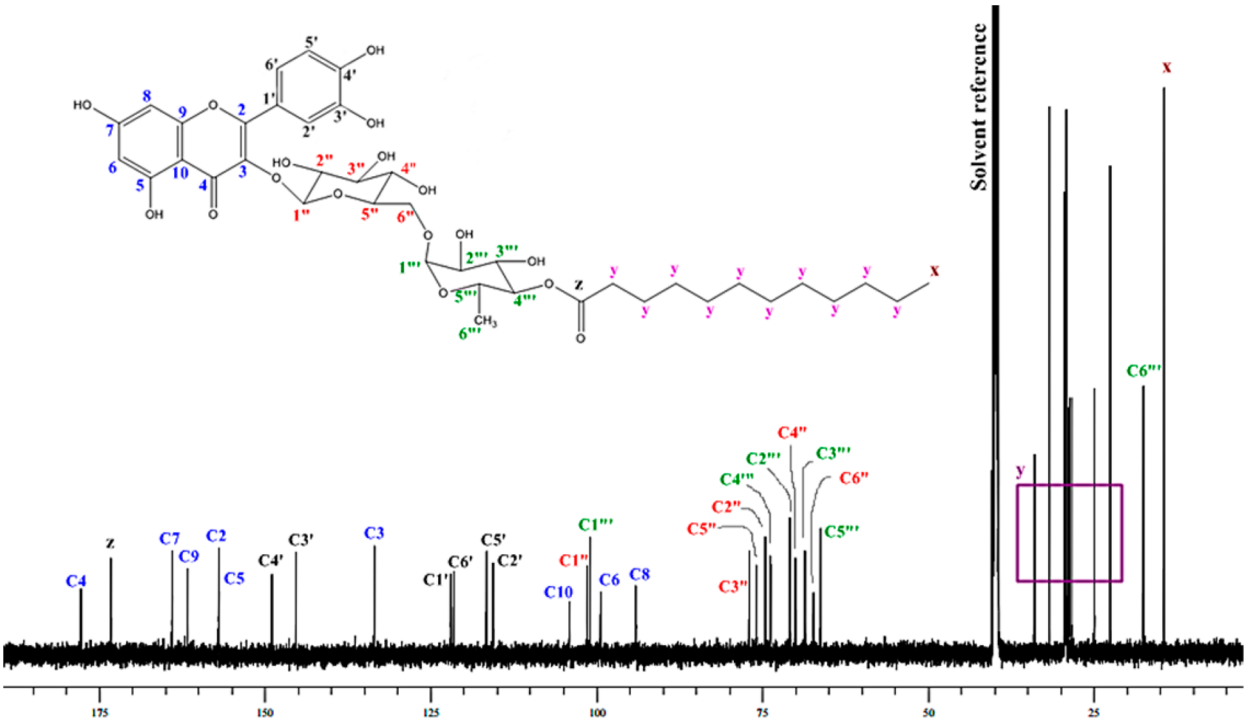

Figure 1. ^{13}C NMR spectrum of rutin laurate.

were determined from the plotted external linear calibration. Meanwhile, $[W]_{eq}$ was calculated from the stoichiometry of ester synthesis, where 1 mol of water is produced per mole of ester synthesized. Based on the same stoichiometry, 1 mol of lauric acid is used per mole of ester synthesized; therefore, $[LA]_{eq}$ was calculated from the difference between the initial lauric acid concentration and $[FE]_{eq}$.

K_{eq} was measured at various temperatures. The temperature dependence of K_{eq} is expressed according to van't Hoff equation as

$$\ln K_{eq} = -\frac{\Delta H}{RT} + \frac{\Delta S}{R} \tag{6}$$

where ΔH is the van't Hoff enthalpy change (J mol^{-1}) and ΔS is the entropy change (J mol^{-1} K^{-1}).

At constant pressure and temperature, the Gibbs free energy change (ΔG, J mol^{-1}) for the reaction under nonstandard conditions was calculated using the equation

$$\Delta G = \Delta H - T\Delta S \tag{7}$$

The energy surplus or deficit arising from the difference between Gibbs free energy change under nonstandard conditions (ΔG, J mol^{-1}) and the Gibbs free energy change at certain defined standard conditions (ΔG°, J mol^{-1}) was calculated as

$$\Delta G - \Delta G^{\circ} = RT \ln K_{eq} \tag{8}$$

where K_{eq} is the apparent equilibrium constant under nonstandard conditions, R is the gas constant (8.3145 J mol^{-1} K^{-1}), and T is the absolute temperature (K).

3. RESULTS AND DISCUSSION

3.1. Product Authentication by LC/MS/MS and NMR Analyses. From the m/z values and fragmentation pattern following LC/MS/MS analysis, rutin showed principal fragments at m/z 300 and m/z 609. In the case of an acylated rutin, an additional strong signal was presence at m/z 792 (t_R = 9.54 min), indicating that a single lauric acid moecule was acylated to a molecule of rutin (viz. rutin laurate).

Rutin (quercetin-3-*O*-rutinoside) is a flavonoid glycoside made up of one molecule of quercetin as aglycon and disaccharide rutinose as glycon. Up to this point, the exact acylation position on the rutin molecule is still being debated.[3,19−21] Nevertheless, previous findings generally agreed that the acylation occurs on the hydroxyl groups of the glycoside moiety of the rutin structure.

The chemical structure of the purified product was further confirmed by NMR spectroscopy. For the ^{1}H NMR spectrum, only a downfield peak at 4.65 ppm was observed for rutin laurate. The terminal methyl (CH_3) protons of the ester occurred at 0.75 ppm, and the chemical shift due to methylene (CH_2) protons in the fatty acid moiety of the rutin ester occurred at 1.85−1.23 ppm. The exact position of esterification was subsequently deduced using ^{13}C NMR analysis (Figure 1).

The occurrence of peaks from 33.9 to 22.5 ppm suggests the formation of an ester with an aliphatic chain, with the terminal methyl protons (CH_3) appearing at 14.4 ppm. The peak at 173.2 ppm is associated with the methylene protons linked directly to the carbonyl (C═O) group of the ester. It was found that the signal of the C4‴ position (Rha, C4‴) for the rhamnose moiety shifted by 1.5 ppm (from 72.3 to 73.7 ppm). Hence, based on these observations, we suggest that the acylation takes place specifically on the secondary 4‴-OH group of the rhamnose moiety. This finding provides experimental evidence in the confirmation of the exact location of rutin esterification proposed by earlier reports.[3,10,20]

^{1}H NMR chemical shifts for rutin laurate (DMSO-d_6): δ (ppm) 12.59 (1H, s, C5—OH), 7.55 (1H, dd, J = 2.5, 8.5 Hz, C6′—H), 7.53 (1H, d, J = 2.5 Hz, C2′—H), 6.84 (1H, d, J = 8.5 Hz, C5′—H), 6.39 (1H, d, J = 1.2 Hz, C8—H), 6.20 (1H, d, J = 1.2 Hz, C6—H), 5.35 (1H, d, J = 7.5 Hz, C1″—H), 4.65

DOI: 10.1021/acs.iecr.5b00996
Ind. Eng. Chem. Res. 2015, 54, 5604−5612

(1H, t, J = 9.8 Hz, C4‴—$H_{acylated}$), 4.39 (1H, s, C1‴—H), 3.06−3.72 (12H, m, sugar H), 1.85 (2H, m, CH_2 fatty chain), 1.45 (2H, m, CH_2 fatty chain), 1.23 (24H, m, CH_2 fatty chain), 0.85 (3H, d, J = 6.0 Hz, C6‴—H), 0.75 (3H, t, CH_3 fatty chain).

^{13}C NMR chemical shifts for rutin laurate (DMSO-d_6): δ (ppm) 177.7 (C4), 173.2 (C═O), 164.3 (C7), 161.7 (C9), 156.9 (C2), 156.8 (C5), 148.9 (C3′), 145.3 (C4′), 133.5 (C3), 121.9 (C1′), 121.5 (C6′), 116.6 (C5′), 115.6 (C2′), 104.1 (C10), 101.4 (C1″), 100.9 (C1‴), 99.3 (C6), 94.1 (C8), 76.9 (C3″), 75.9 (C5″), 74.5 (C2″), 73.7 (C4‴), 70.8 (C2‴), 70.0 (C4″), 68.6 (C3‴), 67.3 (C6″), 66.2 (C5‴), 33.9 (aliphatic chain), 31.7 (aliphatic chain), 29.4 (aliphatic chain), 29.3 (aliphatic chain), 29.2 (aliphatic chain), 29.1 (aliphatic chain), 28.8 (aliphatic chain), 24.9 (aliphatic chain), 22.5 (aliphatic chain), 17.5 (C6‴), 14.4 (CH_3 aliphatic chain).

3.2. Initial Esterification Rate. To determine the initial rate of esterification, different initial quantities of rutin were reacted with different initial quantities of lauric acid while the amounts of organic solvent (acetone) and enzyme were held constant. Lauric acid, which showed a relatively higher solubility in acetone than rutin, was provided in an excess of 10−110 times (mole/mole) to rutin so that a high initial rate of esterification and yield of rutin laurate could be achieved. From the initial slope of each graph, the initial rate of esterification was calculated using eq 2. Figure 2 shows the variation of the initial esterification rate as a function of substrate concentration.

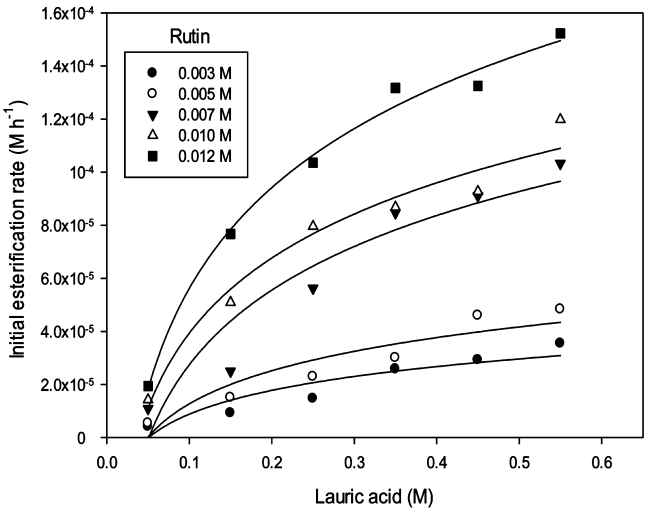

Figure 2. Initial esterification rate as a function of lauric acid and rutin concentrations performed at 55 °C and 200 rpm with 0.15 g of enzyme. (Standard deviation of the triplicate measurements was <5%.)

According to Figure 2, an increase in the concentrations of the substrates (i.e., rutin and lauric acid) led to a rapid increase in the initial rate of the reaction and in the concentration of rutin laurate. Assuming that the mass-transfer limitation of immobilized catalyst (CAL-B) was negligible based on reported studies,[22−24] the effects of these substrates and enzyme were in accordance with those expected for Michaelis−Menten kinetics in a homogeneous, single-phase solution.[25] The maximum initial rate of 1.5 × 10^{-4} M h^{-1} was achieved for 0.55 M of lauric acid and 0.012 M of rutin. These results were in agreement with those of other studies concerning the optimal flavonoid/acyl donor molar ratio to achieve the highest possible yield.[19,20,26,27]

The reaction was also carried out at various temperatures ranging from 293 to 328 K, and at a fixed rutin concentration of 0.005 M. Based on the results obtained, the initial rate of esterification and the conversion yield at equilibrium increased with increasing initial concentration of lauric acid (acyl donor) and temperature (Table 1). However, the maximum conversion

Table 1. Percentage Conversion Yields (%) at Various Temperatures for 0.005 M Rutin[a]

	temperature (K)				
concentration of lauric acid (×10^{-2} M)	293	303	313	318	328
5	21	24	20	23	20
15	28	30	30	37	27
25	28	37	43	46	47
35	30	43	47	48	49
45	36	48	49	51	52
55	36	49	55	54	56

[a]Standard deviation of the triplicate measurements was <5%.

became relatively constant at 54−56% for the highest initial lauric acid concentration tested (55 × 10^{-2} M) and the temperature range of 313−328 K. It is hypothesized that the accumulation of excess water byproduct within the reaction environment under these conditions would be unfavorable for further conversion.[26]

The maximum conversion yield was found to be lower than for other reported rutin esterifications,[20,28,29] which was attributed to the presence of molecular sieve in the current reaction system. Molecular sieve 4 Å is the most commonly used desiccant in the esterification reaction. From Table 2, the

Table 2. Effect of Addition of Molecular Sieve 4 Å (0.05 g g^{-1}) on the Rutin Concentration Dissolved in 5.0 mL of Acetone after 24 h

	concentration of filtered rutin (×10^{-3} M)	
rutin concentration (M)	before addition	after addition
0.01	3.5 ± 1.3	1.3 ± 0.9
0.02	6.3 ± 1.0	3.5 ± 1.4
0.03	7.7 ± 1.2	3.6 ± 0.8
0.04	8.1 ± 1.5	3.8 ± 1.2
0.05	9.2 ± 0.7	3.9 ± 1.3

absorption of rutin by molecular sieve 4 Å increased with increasing rutin concentration. After the addition of molecular sieves, at least a 2-fold reduction of the rutin concentration was observed. Application of molecular sieves to remove excess water byproduct from the esterification reaction should be reconsidered for this reason. In addition, it is also impractical because the regeneration of the desiccant is an energy-intensive process. Based on this consideration, molecular sieve was not included in the subsequent reaction mixture as it has strong affinity to adsorb rutin molecules, resulting in less rutin available for esterification.

As can be seen in Figure 3, the initial esterification rate was directly proportional to the lauric acid concentration (0.05−0.55 M) at any given temperature (293−328 K). The magnitude of product formation also increased at higher temperature. This can be explained by the fact that, in addition to improving the wriggling motion of enzyme molecules at

DOI: 10.1021/acs.iecr.5b00996
Ind. Eng. Chem. Res. 2015, 54, 5604−5612

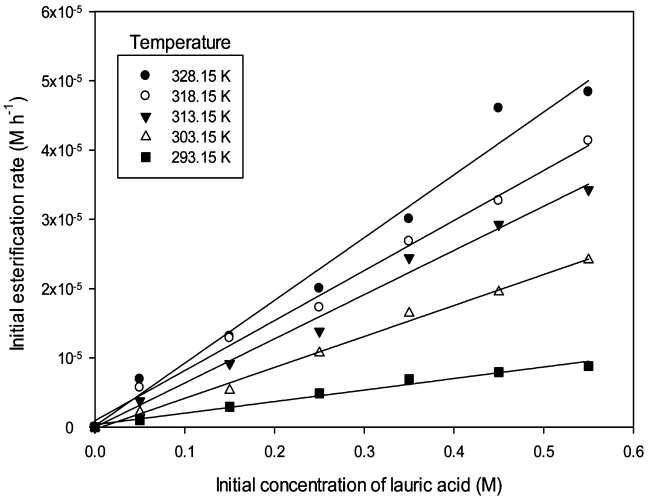

Figure 3. Initial esterification rate (M h^{-1}) as a function of the initial concentration of lauric acid (M) and temperature. Reaction conditions: rutin, 0.005 M; enzyme, 0.15 g; mixing rate, 200 rpm. (Standard deviation of the triplicate measurements was <5%.)

higher temperature, substrates diffuse faster, thus concurrently increasing the chances of their successfully binding to the active site of the enzyme.

3.3. Kinetic Model. To verify the kinetic mechanism of the present reaction, double-reciprocal plots were applied. The reciprocal initial reaction rate (v^{-1}) was plotted as a function of the reciprocal lauric acid concentration (S^{-1}) for several initial rutin concentrations, and vice versa. As shown in Figure 4, the lines in the double-reciprocal plot helped to verify that the reaction followed a ping-pong bi−bi mechanism. A similar mechanism has also been proposed for other lipase-catalyzed esterification, as reported elsewhere in the literature.[30−33]

In this reaction mechanism (Figure 5), lauric acid (acyl donor) first binds to the hydroxyl group of serine in the active site of lipase by a nucleophilic attack, forming an enzyme−lauric acid complex. The enzyme−lauric acid complex is then transformed into an enzyme−acyl intermediate with the concomitant release of the first product, water. This is followed by an attack of the second substrate, rutin, on this intermediate to form an enzyme−acyl−rutin complex. Later, this complex dissociates into rutin laurate, and the enzyme returns to its initial catalytic state ready for the next cycle of catalysis.

In addition, no apparent inhibition was exerted by either of the substrates, as no upward curvature was observed in either plot (Figure 4). The present study contrasts the observations of other reported esterification kinetics by lipase, which indicated inhibition at high concentrations of substrate.[22,24,30] These reports, however, considered alcohols and medium- or long-chain carboxylic acids. To date, the only kinetic data available on flavonoid ester reaction are on the esterification of prunin 6″-*O*-laurate.[17] Similarly to the current findings, the authors found no inhibition pattern for either substrate (i.e., prunin or vinyl laurate), even at the high concentrations of vinyl laurate (4000 mM) used in the reaction.

Because the reaction conforms to a ping-pong bi−bi mechanism with no substrate inhibition, the kinetic parameters of eq 3 were calculated using multiple regression fitting of the experimental values. The final kinetic equation that best fitted the enzymatic synthesis of rutin laurate using rutin and lauric acid was found to be

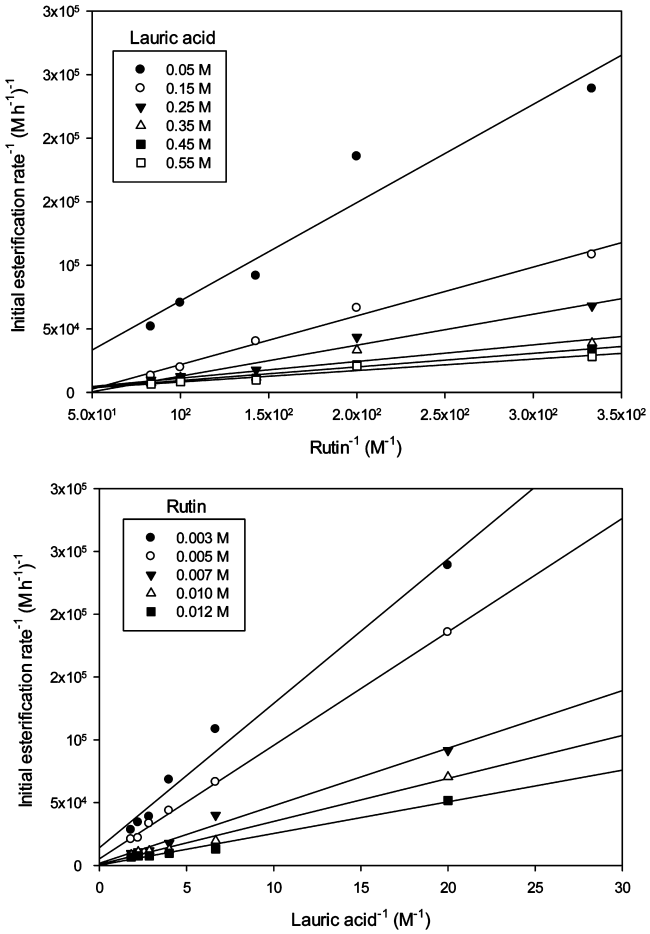

Figure 4. Double-reciprocal plots of initial reaction rate against (a) rutin concentration at a fixed lauric acid concentration and (b) lauric acid concentration at a fixed rutin concentration. Reaction conditions: 0.15 g of enzyme, 55 °C, and 200 rpm.

$$v = \frac{7.49 \times 10^{-4}[\mathrm{LA}][\mathrm{F}]}{0.044[\mathrm{LA}] + 0.99[\mathrm{F}] + [\mathrm{LA}][\mathrm{F}]} \quad (9)$$

where V_{max} = 7.45 × 10^{-4} (M h^{-1}), K_m^F = 0.044 M, and K_m^{LA} = 0.99 M. The verification of the experimental data fitted with eq 9 is shown in Figure 6. It was found that the experimental initial rates agreed very well with the calculated values, with R^2 = 0.99, which supports the observation that the kinetic model fit the experimental data well. Based on the kinetic parameters determined, it is clearly shown that the affinity of the enzyme toward rutin flavonoid was higher than that toward lauric acid, as K_m^F was lower than K_m^{LA}.

3.4. Apparent First-Order Rate Constant, k_1'. Based on the initial esterification rate as a function of the initial concentration of lauric acid, a k_1' value was calculated from the slope of each graph (Figure 3). As shown in Table 3, the apparent kinetics of the esterification reaction was found to exhibit a first-order behavior. With the increase in temperature, the slope of the line became steeper, reflecting a linear increase in k_1'. A higher k_1' value implies a faster esterification reaction. First-order esterification kinetics was also observed for the esterification of fatty acid lauric alcohol by *Lipolase* lipase[34] and the interesterification of triolein and caprylic acid by *Rhizomucor miehei* lipase.[35]

3.5. Apparent Activation Energy of Esterification (E_a). Based on the k_1' values obtained at different temperatures

DOI: 10.1021/acs.iecr.5b00996
Ind. Eng. Chem. Res. 2015, 54, 5604−5612

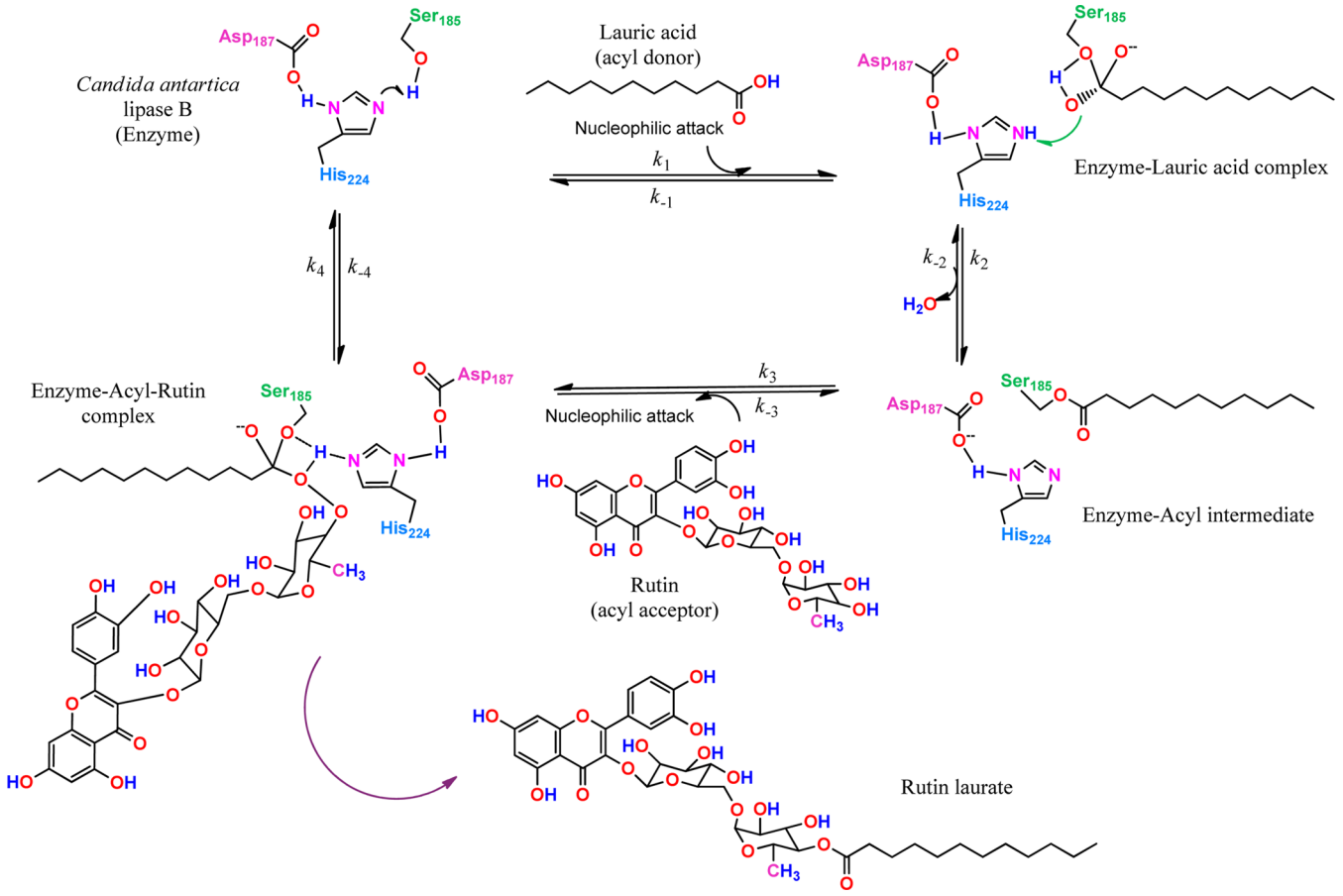

Figure 5. Schematic representation of lipase-catalyzed esterification of rutin and lauric acid by the ping-pong bi−bi mechanism.

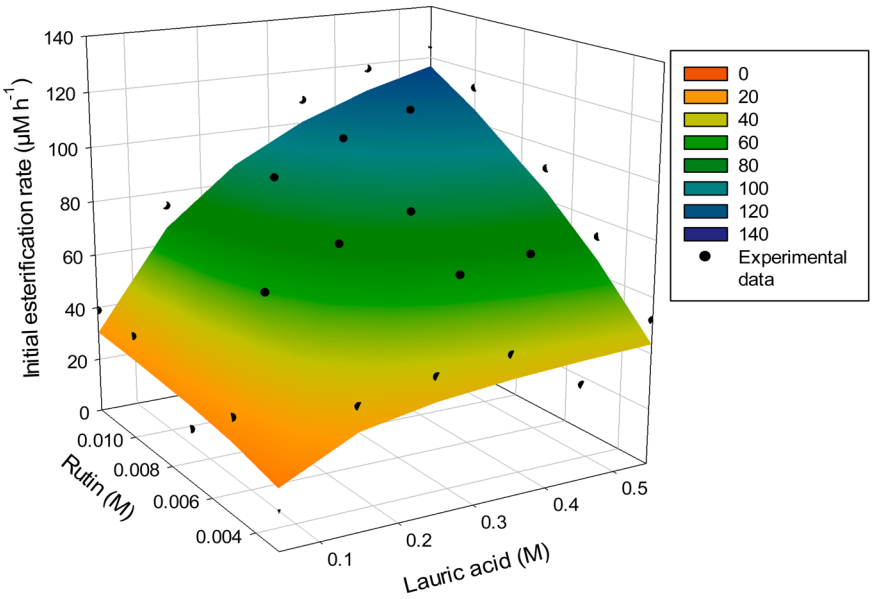

Figure 6. Agreement between calculation and experiment for the ping-pong bi−bi model.

(Table 3), the apparent activation energy (E_a) for the esterification was estimated using an Arrhenius plot. A plot of ln k_1' versus reciprocal temperature was obtained with a regression coefficient (R^2) of 0.9211 (Figure 7).

From the slope of the line, E_a was calculated to be ~37 kJ mol^{-1}, which is consistent with activation energy of enzyme-catalyzed reactions (i.e., 25−83 kJ mol^{-1}).[36] At present, no published data are available on the activation energy of the lipase-catalyzed synthesis of flavonoid ester. Because the acylation of rutin takes place at the hydroxyl group of its sugar moiety,[3,19,20,28] other comparable activation energies for lipase-catalyzed synthesis of glucose esters are 19 kJ mol^{-1} for the esterification of glucose with stearic acid,[37] 50 kJ mol^{-1} (12

DOI: 10.1021/acs.iecr.5b00996
Ind. Eng. Chem. Res. 2015, 54, 5604−5612

Table 3. Initial Rates of Esterification Reaction ($\times 10^{-6}$ M h^{-1}) at Different Concentrations of Lauric Acid and Apparent First-Order Rate Constants, k_1', at Various Temperatures[a]

	concentration of lauric acid ($\times 10^{-2}$ M)						
temperature (K)	5	15	25	35	45	55	apparent first-order rate constant, k_1' ($\times 10^{-6}$ h^{-1})
293	1.0	2.9	4.9	6.9	7.9	8.8	17.6
303	2.2	5.3	10.7	16.4	20.0	24.1	43.9
313	3.8	9.2	13.8	24.4	29.3	34.3	63.8
318	5.7	12.8	17.3	26.8	32.7	41.3	74.6
328	6.9	13.1	20.0	30.0	46.0	48.4	91.1

[a]Standard deviation of the triplicate measurements was <5%

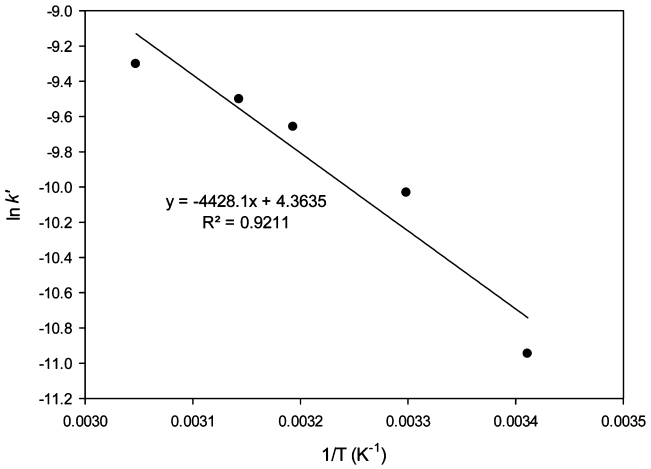

Figure 7. Arrhenius plot for the esterification of rutin with lauric acid.

kcal mol^{-1}) for glucose ester synthesized in acetone,[13] and 67 kJ mol^{-1} for the synthesis of 6-*O*-glucosyldecanoate.[16]

3.6. Thermodynamics of Esterification. Employing the van't Hoff equation, we determined the apparent changes in the enthalpy (ΔH) and entropy (ΔS) from the slope and y intercept, respectively, of the straight line (Figure 8). A plot of ln K_{eq} versus reciprocal temperature was fit by a straight line with a regression coefficient (R^2) of 0.984.

K_{eq} refers to the apparent equilibrium constant for the esterification process, which was calculated for the highest lauric acid concentration (i.e., 0.55 M) at each temperature tested (Table 4). The K_{eq} value increased with increasing temperature, a consequence of intensified successful collisions with the active site of the enzyme at high temperature.

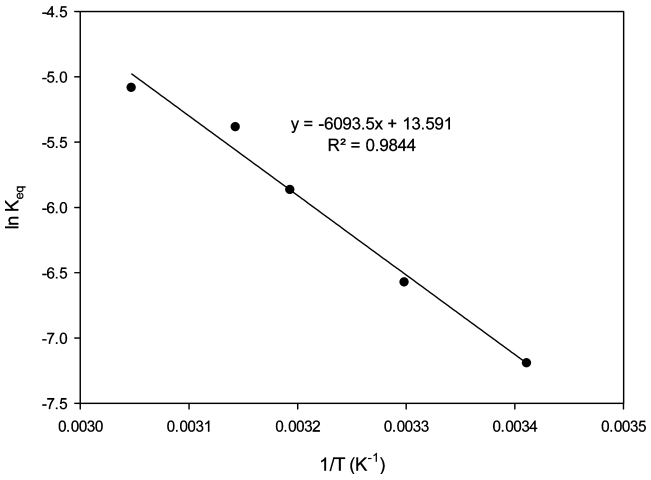

Figure 8. van't Hoff plot for the esterification of rutin with lauric acid.

From this work, the changes in enthalpy (ΔH) and entropy (ΔS) were calculated as approximately +50 kJ mol^{-1} and approximately +110 J mol^{-1} K^{-1}, respectively. The positive value of the enthalpy change (ΔH) for the process implies the endothermic nature of the esterification system, whereas the positive value of the entropy change (ΔS) reflects an esterification system that is becoming increasingly disordered as the temperature increases. The disorder in the system can be attributed primarily to the dispersal of excess byproduct water molecules. Because the reaction is endothermic, as shown by the positive value of ΔH, an increase in temperature is expected to favor the direction of product formation.[18]

The values obtained for the enthalpy and entropy changes were subsequently used in the calculation of the Gibbs free energy change, ΔG, using eq 7. The ΔG value indicates the degree of spontaneity of the esterification process. A strong positive value reflects an energetically unfavorable process. As shown in Table 4, the esterification reaction is nonspontaneous for the temperature range studied, namely, 293−328 K. Therefore, the esterification of rutin to rutin laurate is an energetically unfavorable process and, hence, nonspontaneous in nature. However, as more energy in the form of heat is supplied to the system, the tendency of the system to move toward spontaneous reaction increases, as shown by the decrease in the positive value of ΔG. This can be explained as follows: As the temperature increases, more heat is absorbed (ΔH) during the process, resulting in an increase in the thermal energy of the system. This results in an energetically favorable path to overcome the activation energy barrier for rutin laurate formation. In addition, thermal effects through convective processes also help to increase the probability of successful collision between the two substrates (rutin and lauric acid) and the catalyst (lipase) to form rutin laurate as a final product. This eventually results in a high probability for successful esterification.

According to Table 4, the differences between the energy change for the reaction under the conditions applied in this study and the energy change for the reaction under certain defined standard conditions ($\Delta G - \Delta G^{\circ}$) exhibited a significant deficit of energy for the temperature range studied. This further supports the endothermic nature of the esterification and the energy investment required to push the reaction forward in the absence of a biocatalyst such as CAL-B.

A plot of the Gibbs free energy change (ΔG) for the esterification reaction as a function of temperature is shown in Figure 9. The temperature dependence of ΔG is evident. The ΔG values were calculated with the assumption that the ΔH and ΔS values calculated earlier were constant within the temperature range examined. The plot also shows that $\Delta G = 0$

DOI: 10.1021/acs.iecr.5b00996
Ind. Eng. Chem. Res. 2015, 54, 5604−5612

Table 4. Values of Apparent K_{eq}, ΔG, and $\Delta G - \Delta G^{\circ}$ as Functions of Temperature[a]

absolute temperature, T (K)	T^{-1} ($\times 10^{-3}$ K^{-1})	apparent K_{eq} ($\times 10^{-3}$)	ln K_{eq}	ΔG (kJ mol^{-1})	$\Delta G - \Delta G^{\circ}$ (kJ mol^{-1})
293	3.41	0.8	−7.2	+18	−18
303	3.30	1.4	−6.6	+16	−17
313	3.19	2.8	−5.9	+15	−15
318	3.14	4.6	−5.4	+14	−14
328	3.05	6.2	−5.1	+13	−13

[a]At 0.55 M lauric acid.

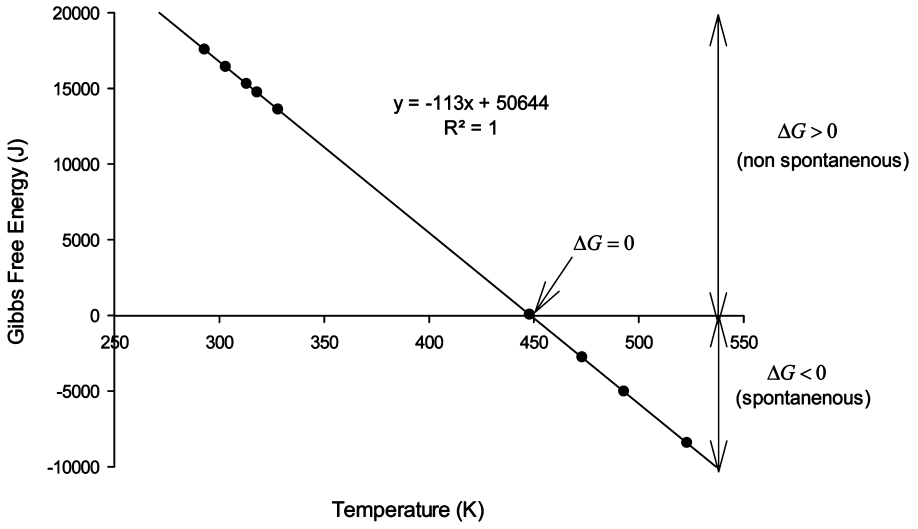

Figure 9. Gibbs free energy change for the esterification reaction as a function of temperature.

at approximately 448 K (or 175 °C), which means that, at this temperature, the energy of the products and reactants is at equilibrium.

According to Figure 9, the values of ΔG are positive from 293 to 328 K, indicating that the esterification process is not favored in this temperature range. The extrapolation of the graph shows that the reaction is spontaneous (i.e., ΔG is negative) above 175 °C (448 K). The increase in temperature amplifies the influence of the positive value of ΔS so that the entropic effect can overcome the effect of an endothermic process, that is, $T\Delta S > \Delta H$.

4. CONCLUSIONS

The findings reported in this article show the general applicability of an enzyme-mediated process for the biosynthesis of flavonoid esters. This work represents an important investigation of key strictures that could affect the synthesis of a flavonoid ester with pharmaceutical, food, cosmetic and health importance. The acylation yield and efficiency in the enzyme process can be manipulated by changes in simple parameters such the acyl donor concentration, reaction temperature, and biocatalyst loading. The process itself is specific and uncomplicated by other competing, unwanted side reaction(s), as shown in this study, where the enzymatic acylation of rutin with lauric acid takes place specifically on the secondary 4‴-OH of the rhamnose moiety. The thermal energy investment is minimal, limited by the enzyme stability and solvent boiling point, alongside the advantages outlined previously. The energy input is primarily to push the endothermic reaction forward, improve the solubility and mass transfer of the immiscible substrates, and concomitantly increase the rate of product formation. It is expected that other related and/or similar enzyme-mediated flavonoid esterification might also follow a ping-pong bi−bi mechanism as shown in this study. The analytical route outlined in this study provides crucial, fundamental information for the development of the stated process.

AUTHOR INFORMATION

Corresponding Author

*E-mail: suffian_annuar@um.edu.my. Tel.: +60379674003. Fax: +60379677182.

Notes

The authors declare no competing financial interest.

ACKNOWLEDGMENTS

The authors acknowledge University of Malaya for providing research grants PG033-2013A and RG330-15AFR.

REFERENCES

(1) Havsteen, B. H. The biochemistry and medical significance of the flavonoids. *Pharmacol. Ther.* **2002**, *96* (2), 67−202.

(2) Mellou, F.; Lazari, D.; Skaltsa, H.; Tselepis, A.; Kolisis, F.; Stamatis, H. Biocatalytic preparation of acylated derivatives of flavonoid glycosides enhances their antioxidant and antimicrobial activity. *J. Biotechnol.* **2005**, *116*, 295−304.

(3) Viskupicova, J.; Danihelova, M.; Ondrejovic, M.; Liptaj, T.; Sturdik, E. Lipophilic rutin derivatives for antioxidant protection of oil-based foods. *Food Chem.* **2010**, *123* (Suppl 1), 45−50.

(4) Passicos, E.; Santarelli, X.; Coulon, D. Regioselective acylation of flavonoids catalyzed by immobilized *Candida antarctica* lipase under reduced pressure. *Biotechnol. Lett.* **2004**, *26* (Suppl 13), 1073−1076.

(5) Patti, A.; Piatelli, M.; Nicolosi, G. Use of *Mucor miehei* lipase in the preparation of long chain 3-*O*-acylcatechins. *J. Mol. Catal. B: Enzym.* **2000**, *10*, 577−582.

DOI: 10.1021/acs.iecr.5b00996
Ind. Eng. Chem. Res. 2015, 54, 5604−5612

(6) Riva, S. Enzymatic modification of the sugar moieties of natural glycosides. *J. Mol. Catal. B: Enzym.* **2002**, *19*−*20*, 43−54.
(7) Zhang, D.-H.; Lv, Y.-Q.; Zhi, G.-Y.; Yuwen, L.-X. Kinetic biosynthesis of L-ascorbyl acetate by immobilized *Thermomyces lanuginosus* lipase (Lipozyme TLIM). *Bioprocess Biosyst. Eng.* **2011**, *34* (9), 1163−1168.
(8) Zhang, D.-H.; Li, C.; Zhi, G.-Y. Kinetic and thermodynamic investigation of enzymatic L-ascorbyl acetate synthesis. *J. Biotechnol.* **2013**, *168* (4), 416−420.
(9) Gao, C.; Mayon, P.; MacManus, D.; Vulfson, E. Novel enzymatic approach to the synthesis of flavonoid glycosides and their esters. *Biotechnol. Bioeng.* **2001**, *71* (Suppl 3), 235−243.
(10) Ardhaoui, M.; Falcimaigne, A.; Ognier, S.; Engasser, J. M.; Moussou, P.; Pauly, G.; Ghoul, M. Effect of acyl donor chain length and substitutions pattern on the enzymatic acylation of flavonoids. *J. Biotechnol.* **2004**, *110* (3), 265−272.
(11) Almeida, V.; Branco, C.; Assis, S.; Vieira, I.; Braz-Filho, R.; Branco, A. Synthesis of naringin 6″-ricinoleate using immobilized lipase. *Chem. Cent. J.* **2012**, *6* (1), 41.
(12) Bridson, J. H.; Grigsby, W. J.; Main, L. Synthesis and characterization of flavonoid laurate esters by transesterification. *J. Appl. Polym. Sci.* **2013**, *129* (1), 181−186.
(13) Acros, J. A.; Hill, C. G.; Otero, C. Kinetics of the lipase-catalyzed synthesis of glucose esters in acetone. *Biotechnol. Bioeng.* **2001**, *73* (2), 104−110.
(14) Naoe, K.; Ohsa, T.; Kawagoe, M.; Imai, M. Esterification by *Rhizopus delemar* lipase in organic solvent using sugar ester reverse micelles. *Biochem. Eng. J.* **2001**, *9* (1), 67−72.
(15) Flores, M. V.; Halling, P. J. Full model for reversible kinetics of lipase-catalyzed sugar−ester synthesis in 2-methyl 2-butanol. *Biotechnol. Bioeng.* **2002**, *78* (7), 795−801.
(16) Gumel, A. M.; Annuar, M. S. M.; Heidelberg, T.; Chisti, Y. Thermo-kinetics of lipase-catalyzed synthesis of 6-*O*-glucosyldecanoate. *Bioresour. Technol.* **2011**, *102* (19), 8727−8732.
(17) Céliz, G.; Martearena, M. R.; Scaroni, E.; Daz, M. Kinetic study of the alkyl flavonoid ester prunin 6″-*O*-laurate synthesis in acetone catalysed by immobilised *Candida antarctica* lipase B. *Biochem. Eng. J.* **2012**, *69*, 69−74.
(18) Segel, I. H. *Enzyme Kinetics: Behavior and Analysis of Rapid Equilibrium and Steady State Enzyme Systems*; John Wiley and Sons: New York, 1975.
(19) Ishihara, K.; Nishimura, Y.; Kubo, T.; Okada, C.; Hamada, H.; Nakajima, N. Enzyme-catalyzed acylation of plant polyphenols for interpretation of their functions. *Plant Biotechnol.* **2002**, *19* (3), 211−214.
(20) Mellou, F.; Loutrari, H.; Stamatis, H.; Roussos, C.; Kolisis, F. Enzymatic esterification of flavonoids with unsaturated fatty acids: Effect of the novel esters on vascular endothelial growth factor release from K562 cells. *Process Biochem.* **2006**, *41* (Suppl 9), 2029−2034.
(21) Nakajima, N.; Ishihara, K.; Itoh, T.; Furuya, T.; Hamada, H. Lipase-catalyzed direct and regioselective acylation of flavonoid glucoside for mechanistic investigation of stable plant pigments. *J. Biosci. Bioeng.* **1999**, *87*, 105−107.
(22) Hari Krishna, S.; Karanth, N. G. Lipase-catalyzed synthesis of isoamyl butyrate: A kinetic study. *Biochim. Biophys. Acta* **2001**, *1547* (2), 262−267.
(23) Mahmud, M. S.; Safinski, T.; Nelson, M. I.; Sidhu, H. S.; Adesina, A. A. Kinetic analysis of oleic acid esterification using lipase as catalyst in a microaqueous environment. *Ind. Eng. Chem. Res.* **2009**, *49* (3), 1071−1078.
(24) Romero, M.; Calvo, L.; Alba, C.; Daneshfar, A. A kinetic study of isoamyl acetate synthesis by immobilized lipase-catalyzed acetylation in *n*-hexane. *J. Biotechnol.* **2007**, *127* (2), 269−277.
(25) Doran, P. M. *Bioprocess Engineering Principles*; Academic Press Ltd.: London, 1995.
(26) Gayot, S.; Santarelli, D.; Coulon, D. Modification of flavonoid using lipase in non-conventional media: Effect of the water content. *J. Biotechnol.* **2003**, *101*, 29−36.
(27) Kontogianni, A.; Skouridou, V.; Sereti, V.; Stamatis, H.; Kolisis, F. N. Lipase-catalyzed esterification of rutin and naringin with fatty acids of medium carbon chain. *J. Mol. Catal. B: Enzym.* **2003**, *21*, 59−62.
(28) Lue, B.-M.; Guo, Z.; Glasius, M.; Xu, X. Scalable preparation of high purity rutin fatty acid esters. *J. Am. Oil Chem. Soc.* **2010**, *87* (1), 55−61.
(29) Zheng, M.-M.; Wang, L.; Huang, F.-H.; Guo, P.-M.; Wei, F.; Deng, Q.-C.; Zheng, C.; Wan, C.-Y. Ultrasound irradiation promoted lipase-catalyzed synthesis of flavonoid esters with unsaturated fatty acids. *J. Mol. Catal. B: Enzym.* **2013**, *95*, 82−88.
(30) Chowdary, G.; Prapulla, S. Kinetic study on lipase-catalyzed esterification in organic solvents. *Indian J. Chem.* **2005**, *44* (11), 2322−2327.
(31) Prlainović, N. Ž.; Bezbradica, D. I.; Knežević-Jugović, Z. D.; Kozlowska, R. T.; Mijin, D. Ž. A kinetic study of *Candida rugosa* lipase-catalyzed synthesis of 4,6-dimethyl-3-cyano-2-pyridone. *J. Braz. Chem. Soc.* **2010**, *21* (12), 2285−2293.
(32) Stamatis, H.; Xenakis, A.; Menge, U.; Kolisis, F. N. Kinetic study of lipase catalyzed esterification reactions in water-in-oil microemulsions. *Biotechnol. Bioeng.* **1993**, *42* (8), 931−937.
(33) Zaidi, A.; Gainer, J.; Carta, G.; Mrani, A.; Kadiri, T.; Belarbi, Y.; Mir, A. Esterification of fatty acids using nylon-immobilized lipase in *n*-hexane: Kinetic parameters and chain-length effects. *J. Biotechnol.* **2002**, *93* (3), 209−216.
(34) Shintre, M. S.; Ghadge, R. S.; Sawant, S. B. Kinetics of esterification of lauric acid with fatty alcohols by lipase: Effect of fatty alcohol. *J. Chem. Technol. Biotechnol.* **2002**, *77* (10), 1114−1121.
(35) Camacho Paez, B.; Robles Medina, A.; Camacho Rubio, F.; Esteban Cerdán, L.; Molina Grima, E. Kinetics of lipase-catalysed interesterification of triolein and caprylic acid to produce structured lipids. *J. Chem. Technol. Biotechnol.* **2003**, *78* (4), 461−470.
(36) Dixon, M.; Webb, E. C. *Enzymes*, 3rd ed.; Longman Group Ltd.: London, 1979.
(37) Yu, J.; Zhang, J.; Zhao, A.; Ma, X. Study of glucose ester synthesis by immobilized lipase from *Candida* sp. *Catal. Commun.* **2008**, *9* (6), 1369−1374.

DOI: 10.1021/acs.iecr.5b00996
Ind. Eng. Chem. Res. 2015, 54, 5604−5612